1.0

1.1

1.25 1.4 1.6

2.8 2.5

2.2
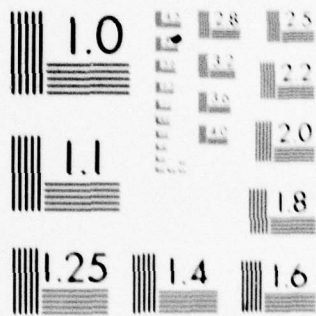
2.0

1.8

MICROCOPY RESOLUTION TEST CHART
NATIONAL BUREAU OF STANDARDS-1963-A

AFGL-TR-78-0262

LEVEL

MOLECULAR REACTION RATES

by

Chun C. Lin

Sunggi Chung

University of Wisconsin-Madison

Madison, Wisconsin 53706

FINAL REPORT

Period Covered: 1 August 1973 through 30 September 1978

30 October 1978

AIR FORCE GEOPHYSICS LABORATORY
AIR FORCE SYSTEMS COMMAND
UNITED STATES AIR FORCE
HANSCOM AFB, MASSACHUSETTS 01731

REPORT DOCUMENTATION PAGE		READ INSTRUCTIONS BEFORE COMPLETING FORM
1. REPORT NUMBER AFGL-TR-78-0262	2. GOVT ACCESSION NO.	3. RECIPIENT'S CATALOG NUMBER
4. TITLE (and Subtitle) MOLECULAR REACTION RATES		5. TYPE OF REPORT & PERIOD COVERED Final rept. 1 August 1973-30 September 1978
		6. PERFORMING ORG. REPORT NUMBER
7. AUTHOR(s) Chun C. Lin Sunggi Chung		8. CONTRACT OR GRANT NUMBER(s) F19628-73-C-0274
9. PERFORMING ORGANIZATION NAME AND ADDRESS Department of Physics University of Wisconsin-Madison Madison, Wisconsin 53706		10. PROGRAM ELEMENT, PROJECT, TASK AREA & WORK UNIT NUMBERS 61102F 2310G4AB
11. CONTROLLING OFFICE NAME AND ADDRESS Air Force Geophysics Laboratory Hanscom AFB, Massachusetts 01731 Monitor/Edward T. P. Lee/OPR		12. REPORT DATE 30 October 1978
		13. NUMBER OF PAGES 116
14. MONITORING AGENCY NAME & ADDRESS(if different from Controlling Office)		15. SECURITY CLASS. (of this report) Unclassified
		15a. DECLASSIFICATION/DOWNGRADING SCHEDULE

16. DISTRIBUTION STATEMENT (of this Report)

Approved for public release; distribution unlimited.

17. DISTRIBUTION STATEMENT (of the abstract entered in Block 20, if different from Report)

19. KEY WORDS (Continue on reverse side if necessary and identify by block number)

Electron excitation; Electron-molecule collision; Excitation of Molecules; Dissociation of Molecules; Born Approximation; Method of Close-coupling Multiconfiguration Wave Functions.

20. ABSTRACT (Continue on reverse side if necessary and identify by block number)

Theoretical excitation/dissociation cross sections of H_2 molecule by electron impact have been calculated by Born approximation and by the method of close-coupling. The ab initio calculations have been facilitated by using the Gaussian-type orbital technique. In the case of dissociation of O_2 via the Schumann-Runge system, the theoretical calculations are based on the multi-configuration self-consistent-field wave functions.

DD FORM 1473 EDITION OF 1 NOV 65 IS OBSOLETE
1 JAN 73

Preface

Although research activities in atomic and molecular collision processes have flourished over the last two decades, theoretical calculations of molecular reaction rates remain a very difficult subject. In this report we describe some of our efforts to treat electron-molecule collision problems in a first-principle manner.

One can roughly divide the problem into two parts, i.e., (a) calculation of the interaction and coupling potential, and (b) solution of the scattering equations. A common practice is to use single-configuration self-consistent-field target molecular wave functions to obtain the interaction and coupling potentials. With these potentials one may solve the scattering by means of the Born approximation. This is done for the case of electron impact on hydrogen molecules in Part I. The Born approximation has the advantage of computational simplicity, but is not always reliable in the low-energy region. For more accurate work we resort to the method of close coupling. In Part II we report the first close-coupling calculation for excitation of electronic states (and dissociation) of the molecules by electron impact with full allowance of projectile-target electron exchange. In some cases, notably those in which the target molecule has an open-shell structure in the ground electronic state, the use of single-configuration self-consistent-field target wave functions (for calculating interaction and coupling potentials) is not adequate. A multi-configuration self-consistent-field computational scheme is developed and applied to the oxygen molecule as described in Part III.

PART I
DISSOCIATION OF HYDROGEN MOLECULE
BY ELECTRON IMPACT

I. INTRODUCTION

Electron-impact dissociation of molecules is an important basic process for atmospheric physics[1] and laser work.[2] A molecule can be dissociated by electron impact when it is excited to the continuum "vibrational" levels of an electronic state. Such an excited electronic state may be a purely repulsive state or a bound state with discrete vibrational levels in addition to continuum levels. The atomic species of dissociation products are dictated by the dissociation limit to which the potential-energy curve is joined. Here, we report theoretical studies of two electron-impact dissociation processes of the H_2 molecule

$$H_2 \xrightarrow{e} H_2^* \to H(1s) + H(1s) , \tag{1}$$

$$H_2 \xrightarrow{e} H_2^* \to H(1s) + H(2s) . \tag{2}$$

The only excited state H_2^* in (1) is the $b^3\Sigma_u^+$ state. However, since the $b^3\Sigma_u^+$ state is also the lowest triplet state, excitation to the discrete levels of the higher triplet states will contribute to process (1) via cascade to $b^3\Sigma_u^+$ as well as direct excitation of the repulsive $b^3\Sigma_u^+$ state. The excited state H_2^* in (2) may be any one of the four states,[3] $B'^1\Sigma_u^+$, $e^3\Sigma_u^+$, $E^1\Sigma_g^+$, and $a^3\Sigma_g^+$, all of which are bound states. Therefore, dissociation results from excitation only to the continuum levels of these states, i.e. excitation to these states above the dissociation limit. In Fig. 1 these two processes are illustrated.

Although the theory of electron-impact dissociation can be formulated under the same general framework as that of electron-molecule inelastic collisions, ab initio calculation of cross sections is complicated by the multicenter integrals in the transition amplitudes as well as the unbound (repulsive) nature of the dissociating states. However, in the case of

excitation to bound electronic states, the technique of Gaussian-type orbitals (GTO) has furnished a very efficient means of calculating cross sections.[4] We now extend the method of GTO to the case of dissociative collisions, and cross sections of electron-impact dissociation of H_2 are reported.

Several theoretical studies[5-8] related to process (1) have been reported, but we have found no first-principle calculation published for process (2). Among the previously published theoretical treatments of electron-impact dissociation of the H_2 molecule [process (1)], the most recent and complete one to our knowledge is that of Cartwright and Kuppermann,[5] based on the Born approximation with Rudge's[9] and Ochkur's[10] treatment for exchange. In their paper the molecular electronic wave functions were expressed in terms of the Slater-type orbitals (STO) and a considerable amount of numerical work was needed to evaluate a typical three-center integral. The "delta-function" approximation was adopted there,[5] resulting in a significant reduction of computation. However, the method of Gaussian orbitals makes the evaluation of the electronic transition moment (due to electron impact) a rather simple task and the Born integrals can be readily performed without invoking the delta-function approximation or the closely related Franck-Condon-factor (FC) approximation. In this work the continuum vibrational wave functions of the excited electronic state are determined at various energies (above dissociation limit), and the Born integrals are evaluated exactly with full allowance for variation of the electronic transition moment with respect to the internuclear distance. In order to account for the cascade contributions to process (1), we have also computed the excitation cross sections to the discrete levels of the $a^3\Sigma_g^+$, $c^3\Pi_u$, $d^3\Pi_u$, and $e^3\Sigma_u^+$ states.

Like the work of Cartwright and Kuppermann[5] and the earlier works,[6,7] the Born approximation with Rudge's[9] and Ochkur's[10] modification for treating

the exchange amplitude is adopted here. The incident electron energy is varied to as high as 1000 eV for excitation of the singlet states. Although we present the singlet excitation cross sections down to the threshold, the emphasis should be placed on the high-energy region because of the use of the Born approximation. In the high-energy region (say above 100 eV) the effect of the electron exchange is quite negligible. Nevertheless, the electron exchange in this case is taken into account by Ochkur's scheme. For the singlet-triplet excitation processes, cross sections have been computed from the threshold to 150 eV. Since the singlet-triplet cross sections decrease very rapidly with increasing energy, the interest lies mainly in the low-energy region. Although the plane-wave approximation inherent in the Born approximation is justified only at high-incident energies, the improvement resulted from the modifications introduced by Rudge and by Ochkur may make these modifications applicable to much lower energies than the original Born-Oppenheimer approximation. Indeed the excitation cross sections calculated by the Rudge scheme are in quite satisfactory agreement with the experimental data for the $C^3\Pi_u$ state of N_2.[4]

II. METHOD OF COMPUTATION

A. Formulation

The general theoretical formulation for the dissociation of diatomic molecules via excitation to repulsive states is similar to that developed previously for excitation of discrete states.[4] Here we are mainly concerned with the calculation of excitation to a continuum vibrational state of an excited electronic state by means of the Born approximation with Rudge's and Ochkur's modification. The rotational motion of the molecule will not

be included explicitly in the formulation, but such an effect will be taken into account by averaging the cross sections over the orientation of the molecular axis in space.

Denoting the electronic coordinates of the H_2 molecule as $\vec{r}_1$, $\vec{r}_2$ and the internuclear separation as $\vec{R}$, we write the wave functions of the ground electronic-vibrational (00) state and of the final state (nW) as

$$\Psi_{00}(\vec{r}_1,\vec{r}_2,\vec{R}) = \psi_0(\vec{r}_1,\vec{r}_2,\vec{R})\chi_{00}(R) \ , \tag{3}$$

$$\Psi_{nW}(\vec{r}_1,\vec{r}_2,\vec{R}) = \psi_n(\vec{r}_1,\vec{r}_2,\vec{R})\chi_{nW}(R) \ , \tag{4}$$

where ψ_0 and ψ_n are the electronic wave functions of the ground (0) and excited (n) states, and χ_{00} is the discrete (v=0) vibrational function of the ground state, whereas χ_{nW} is the unbound "vibrational" function of the upper state characterized by energy W above the dissociation limit (see Fig. 1). Since we do not consider the spin-orbit interactions, the spin functions can be factored out; we assume that this has been done in Eqs.(3) and (4). The spatial part of electronic functions ψ_0 and ψ_n is written as the products of one-electron orbitals, viz.,

$$\psi_0(\vec{r}_1,\vec{r}_2,\vec{R}) = \phi_{1\sigma_g}(\vec{r}_1,\vec{R})\phi_{1\sigma_g}(\vec{r}_2,\vec{R}) \ , \tag{5}$$

$$\psi_n(\vec{r}_1,\vec{r}_2,\vec{R}) = \sqrt{\tfrac{1}{2}}\,[\phi_{1\sigma_g'}(\vec{r}_1,\vec{R})\phi_{ex}(\vec{r}_2,\vec{R}) \pm \phi_{1\sigma_g'}(\vec{r}_2,\vec{R})\phi_{ex}(\vec{r}_1,\vec{R})], \tag{6}$$

where the + and - signs refer to a singlet and triplet excited-state function respectively, and distinction is made of the $1\sigma_g$ orbitals in Eqs. (5) and (6). The collision process is characterized by the wave vectors of the incident and scattered electron ($\vec{k}_{00}$ and $\vec{k}_{nW}$), their difference being designated by $\vec{K}$. It is convenient to introduce the electronic transition amplitude defined as

$$\mathcal{E}_{on}(K,R,\Theta,\phi) = -\int \psi_n^*(\vec{r}_1,\vec{r}_2,\vec{R})(e^{i\vec{k}\cdot\vec{r}_1} + e^{i\vec{k}\cdot\vec{r}_2})\psi_0(\vec{r}_1,\vec{r}_2,\vec{R})d\vec{r}_1 d\vec{r}_2, \quad (7)$$

where Θ and ϕ specify the relative orientation between $\vec{R}$ and $\vec{K}$. Analogous to the case of excitation to discrete vibrational levels, the differential cross sections for excitation to a unit energy range about W of a singlet and a triplet state (above the dissociation limit) are

$$I_{nW}^{S}(\theta\phi) = (\omega_n k_{nW}/4\pi k_{00})\int |\chi_{nW}^*(R)\chi_{00}(R)(2K^{-2}-T^{-2})$$

$$\times \mathcal{E}_{on}(K,R,\Theta,\phi)|^2 R^2 dR \sin\Theta \, d\Theta \, d\phi \, , \quad (8)$$

$$I_{nW}^{T}(\theta\phi) = (3\omega_n k_{nW}/4\pi k_{00})\int |\chi_{nW}^*(R)\chi_{00}(R)T^{-2}\mathcal{E}_{on}(K,R,\Theta,\phi)|^2$$

$$\times R^2 dR \sin\Theta \, d\Theta \, d\phi \, , \quad (9)$$

respectively where ω_n is the degeneracy of the excited state and T^2 is equal to k_{00}^2 and $[k_{nW} - i(2\epsilon)^{\frac{1}{2}}]^2$ for the Ochkur and Rudge modification respectively with ϵ being the ionization energy in a.u. of the initial state.

Integration of Eqs. (8) and (9) over the scattered angle θ and ϕ gives the cross section $Q(n,W)$ of exciting to a unit energy range about W of the upper state,

$$Q(nW) = \int I_{nW}(\theta\phi) \sin\theta d\theta d\phi \, . \quad (10)$$

Then the total dissociation cross section through excitation of an electronic state is

$$Q(n) = \int_0^\infty Q(nW)dW \, . \quad (11)$$

Eq. (9) [or (8)] may be simplified if the Franck-Condon-factor approximation is invoked to suppress the R-dependence of $\mathcal{E}_{on}$, viz.,

$$I_{nW}^T \simeq (3\omega_n k_{nW} q_{nW}/4\pi k_{00}) \int |T^{-2} \mathcal{C}_{on}(K,R_o,\Theta,\phi)|^2 \sin\Theta d\Theta d\phi , \tag{12}$$

where R_o is usually taken as the equilibrium bond length of the ground state, and the Franck-Condon factor q_{nW} is

$$q_{nW} = |\int \chi_{nW}^*(R) \chi_{00}(R) R^2 dR|^2 . \tag{13}$$

Although our calculations are not based on the Franck-Condon-factor approximation, this concept serves a useful purpose, as the cross sections are now simply proportional to q_{nW}. For the purpose of later discussion we define the sum of the Franck-Condon factors of the discrete levels (S_d) and of the continuum levels (S_c) as

$$S_d(n) = \Sigma_{v(discrete)} q_{nv} = \Sigma_{v(discrete)} |\int \chi_{nv}^*(R) \chi_{00}(R) R^2 dR|^2 , \tag{14}$$

$$S_c(n) = \int_{(continuum)} dW \, q_{nW} = \int dW |\int \chi_{nW}^*(R) \chi_{00}(R) R^2 dR|^2 , \tag{15}$$

where in Eq. (14) χ_{nv} is the v-th discrete vibrational function of an excited electronic state (n). The quantities $S_d(n)$ and $S_c(n)$ provide us with an estimate of relative excitation cross sections to discrete levels and to continuum levels of a given electronic state (n). Finally, it is noted that S_d and S_c would add up to unity.

B. Details of computation

The electronic wave functions of the H_2 molecule are determined by the self-consistent-field method with a basis set consisting of six s-type and four p-type GTO's for seven different values of internuclear distances, R = 0.5, 0.6, 0.7, 0.74, 0.8, 0.9, and 1.0 $\overset{o}{A}$. With these wave functions we have computed $\mathcal{C}_{on}(K,R,\Theta,\phi)$ for 32 values of K. The vibrational wave functions χ_{00} and χ_{nW} are computed numerically in tabular form.

The potential-energy curves used are due to Kolos and Wolniewicz[11] for the $X^1\Sigma_g^+$, $b^3\Sigma_u^+$, $E^1\Sigma_g^+$, and $a^3\Sigma_g^+$ states; due to Spindler[12] for the $B'^1\Sigma_u^+$ state; and due to Sharp[3] for the $e^3\Sigma_u^+$ state. Numerical integration of Eqs. (8) and (9) then gives the differential cross sections. The cross sections Q(nW) of Eq. (10) are computed for continuum energy W from 2 to 10 eV for the $b^3\Sigma_u^+$ state, and 0 to 4 eV for the other states. In addition, the cross sections to the discrete vibrational levels of the $a^3\Sigma_g^+$, $c^3\Pi_u$, $d^3\Pi_u$, and $e^3\Sigma_u^+$ states are also computed by the procedure described previously.[4]

III. $H_2 \overset{e}{\leftrightarrows} H(1s) + H(1s)$

As described in Sec. I, the H_2 molecule may dissociate into two H(1s) atoms through direct excitation to the $b^3\Sigma_u^+$ state or excitation to higher triplet states followed by radiative cascades to the $b^3\Sigma_u^+$ state. Calculations for excitation via these two different mechanisms are described separately in the following subsections.

A. Excitation to the $b^3\Sigma_u^+$ state

The cross sections of the $b^3\Sigma_u^+$ state are calculated by using Rudge's treatment of exchange amplitude and presented in Table I and Fig. 2. In obtaining the total cross sections we have taken the limits of integration for

Eq. (11) as 2 to 10 eV. This is seen to be quite sufficient as we find $S_c(b^3\Sigma_u^+)$ of Eq. (15) to be 0.998 using the same limits of integration. A similar calculation with Ochkur's exchange gives considerably larger cross sections than those shown in Table I, especially at energies below 40 eV. It has been suggested[4] that Rudge's scheme is preferable to Ochkur's for the singlet-triplet excitation; hence only cross sections by Rudge's scheme are presented for the triplet states.

In order to see how the computed cross sections depend on the accuracy of the wave functions, we have repeated the calculation by using the wave function of Phillipson and Mulliken (PM)[13] for the $b^3\Sigma_u^+$ state and that of McLean, Weiss, and Yoshimine (MWY)[14] for the ground state. The latter wave function is made of five different electronic configurations so that a good deal of electron correlation is believed to be accounted for. To facilitate the numerical procedure, the STO basis functions of the above wave functions are curve-fitted into the GTO form. The substitution of the PM function for our Gaussian-basis SCF wave function of the $b^3\Sigma_u^+$ state produces virtually no change in the cross sections, whereas the use of the MWY function for the ground state gives results which are about 7% smaller than those in Table I.

B. Excitation to the discrete vibrational levels of the $a^3\Sigma_g^+$, $c^3\Pi_u$, $d^3\Pi_u$, and $e^3\Sigma_u^+$ states

In order to account for the cascade contributions to dissociation into two H(1s) atoms, we have computed the cross sections for excitation to the discrete levels of the $a^3\Sigma_g^+$, $c^3\Pi_u$, $d^3\Pi_u$, and $e^3\Sigma_u^+$ states, and the results are included in Table I. There is very little overlap between the ground electronic-vibrational state and continuum level of these excited states except the $e^3\Sigma_u^+$ state, for which S_d and S_c of Eqs. (14) and (15) are

respectively 0.80 and 0.20. The cross sections of the $e^3\Sigma_u^+$ state in Table I refer to excitation of <u>discrete levels only</u>.

As shown in Table I about one-half of the dissociation cross sections comes from excitation of the higher triplet states and subsequent cascades. We see that the major part of such contribution comes from the two lowest triplet states, i.e., $c^3\Pi_u$ (20%) and $a^3\Sigma_g^+$ (16%), and much smaller amount from the $e^3\Sigma_u^+$ (6%) and $d^3\Pi_u$ (5%) states. In view of the trend of diminishing cross sections, the cascade contributions from still higher states are expected to be small and will not be considered here.

C. Comparison with other theoretical calculations

Cartwright and Kuppermann[5] have calculated the excitation cross sections of the $b^3\Sigma_u^+$ state by means of the Born approximation with the "delta-function approximation"for treating the continuum vibrational functions. Their results obtained by means of the Rudge modification of the Born approximation are included in Fig. 2 and are seen to be about 20% larger than ours. In order to better understand this difference, we repeated our calculation with the delta-function approximation (also known as the "reflection approximation"). The error in the total cross sections [Eq. (11)] introduced by the use of this approximation is only about 3%, although the distribution of cross sections $Q(nW)$ [Eq. (10)] with respect to W is shifted by about 0.2 eV toward high W. Therefore we believe that a large part of the difference must be attributed to the difference in the electronic wave functions used in their and our calculations, and to the different means of evaluating the electronic transition moment. Their ground-state function was taken to be the two-parameter wave function of Weinbaum which may give cross sections appreciably different from those resulted from our SCF wave functions. Khare and Moiseiwitsch[6] have

reported calculation of excitation cross sections of the $b^3\Sigma_u^+$ state using
the Ochkur exchange. These authors introduced a separate-atoms approximation
to simplify the computational work. The vibrational wave functions were not
taken into account in their work and the $b^3\Sigma_u^+$ excited electronic state was
regarded as a single level at 11 eV above the ground state. Nevertheless,
their peak cross section of 1.2 πa_o^2 is in reasonable agreement with our
peak value of 1.01 πa_o^2 when the Ochkur exchange is used. Khare[7] has sub-
sequently re-calculated the $b^3\Sigma_u^+$ cross sections using one-center wave functions
so that the separate-atoms approximation could be discarded and the excitation
energy of the $b^3\Sigma_u^+$ state was taken as 10.6 eV with the vibrational part of the
wave function neglected. The peak cross section[15] for $b^3\Sigma_u^+$ of Khare's
calculation with Ochkur's exchange as presented in Fig. 7 of the paper of
Cartwright and Kuppermann is only a few percent below our value of 1.01 πa_o^2.
This agreement, however, should be regarded as fortuitous in view of the
difference between Khare's approach and ours. We have performed some test
calculations and found that the Franck-Condon-factor approximation gives a
reasonably good estimate of cross sections (typically within 10%), which may
be explained by the fact that the R-dependence of the transition moment in
Eqs. (8) and (9) is nearly linear so that the value of the transition moment
at the equilibrium separation (R_o) is close to the averaged value over R.

Edelstein[8] used a variational method to calculate the dissociation cross
sections. In his work the molecular vibration is not explicitly included.
His cross sections show a special feature of peaking at two different incident
energies which is not found in the results of Cartwright and Kuppermann or
of ours. We are not able to find enough details of the computational pro-
cedure in Ref. 8 to analyze the reasons for this discrepancy.

Cartwright and Kuppermann[5] have also computed excitation cross sections

of the bound $a^3\Sigma_g^+$ state by using Rudge's exchange. Their cross sections are about 20% larger than our results. We believe this difference is mainly due to the different wave functions used in the calculations as in the case of the $b^3\Sigma_u^+$ state. Theoretical cross sections of the $c^3\Pi_u$ and $a^3\Sigma_g^+$ states computed by using Ochkur's exchange have been given in Ref. 7. Because of the difference in approach between Khare's work and ours, no comparison between the two sets of results will be made.

D. Comparison with experiments

Corrigan[16] investigated the electron-impact dissociation of the H_2 molecule by monitoring the rate of pressure decrease in a closed system as the dissociation products are removed. Because of the nature of his experiment, the measured cross sections include contributions not only from excitation to electronic states, but also from ionization of molecular hydrogen. By subtracting the latter contribution, he obtained the dissociation cross sections via the excited states of the neutral H_2 molecule. These reported cross sections still cover the cross sections for producing excited-state $H(n\ell)$ atoms as no distinction is made of the atomic species. In order to make Corrigan's experimental data compatible with the present theoretical cross sections for producing ground-state $H(1s)$ atoms only, it is necessary to subtract from Corrigan's data the experimental cross sections for the production of the excited-state atoms. Mumma and Zipf[17] measured the Lyman-alpha radiation of atomic hydrogen resulting from electron-impact dissociation of molecular hydrogen from the threshold to 350 eV. We have used these cross sections to correct for $H(2p)$. Although we have computed the cross sections for electron-impact dissociation into $H(1s)$ + $H(2s)$, because of competing mechanisms such as predissociation (see Sec. IV) which we have not dealt with

here, we decided to use the published experimental cross sections to account for the production of H(2s). The experimental data of Vroom and de Heer[18] show that the ratio of emission cross section for formation of H(2s) to the cross section for H(2p) by electron impact is 0.485 and constant in the entire impact-energy range (0.05-6 keV) of their experiment. Assuming that this ratio (0.485) remains substantially unchanged below 50 eV, we have also corrected for H(2s). It should be pointed out that these H(2p) and H(2s) cross sections include cascades from higher excited states as well as direct formation of H(2p) and H(2s) from dissociation. Vroom and de Heer[18] further found that the cross sections for formation of H(np) atoms for $n \geq 3$ are quite small. Therefore, we believe that the correction for H(2p) and H(2s) as outlined above should account for nearly all of H(nℓ) production (nℓ≠1s).

In Fig. 3 is shown a comparison of our theoretical dissociation cross sections (sum of the contributions from the b,a,c,e,d states as listed in Table I) with the experimental data of Corrigan corrected for the production of excited-state atoms as described in the preceding paragraph. The overall agreement is seen to be quite good. As mentioned in Sec. III-B, population of the $b^3\Sigma_u^+$ state by means of excitation to the very high triplet states (such as those above $d^3\Pi_u$) with subsequent cascade has been neglected in our calculations and inclusion of these contributions may somewhat increase the theoretical cross sections. Also at the high-energy end the cross sections reported by Corrigan may be subject to appreciable uncertainties introduced by his subtraction of the effects of ionization.

Cross sections obtained from energy-loss experiment have been reported by Ramien[19] in 1931. His cross sections, however, are smaller than Corrigan's by about a factor two. Comparison between Corrigan's data with the cross sections of Ramien[19] and of Engelhardt and Phelps[20] has been discussed in Ref. 16.

IV. $H_2 \overset{e}{\leftrightarrows} H(1s) + H(2s)$

Dissociation of H_2 into $H(1s) + H(2s)$ is complicated by the possibility of predissociation. Formation of $H(1s)$ and $H(2s)$ by electron impact may result from (i) direct excitation to the continuum portion of the $B'^1\Sigma_u^+$, $e^3\Sigma_u^+$, $E^1\Sigma_g^+$, and $a^3\Sigma_g^+$ states, (ii) excitation to some other excited electronic states which cross (or nearly cross) with the B', a, E and e states in such a manner as to produce predissociation, (iii) excitation to the higher excited states followed by dissociative cascade to the four states leading to $H(1s) + H(2s)$. An ab initio calculation of electron-impact predissociation requires very accurate knowledge of the potential curves of numerous excited states which is beyond the scope of this work. Also the lack of detailed information, concerning the branching ratios among many available cascade channels from any given higher excited state, makes it difficult to obtain a quantitative estimate of process (iii). Thus in the present work we will confine ourselves to process (i).

A. Dissociation via the $B'^1\Sigma_u^+$, $e^3\Sigma_u^+$, and $E^1\Sigma_g^+$

The dissociative excitation cross sections of the $B'^1\Sigma_u^+$, $e^3\Sigma_u^+$, and $E^1\Sigma_g^+$ states are presented in Table II and the sum of cross sections (of B', e, and E states) is shown in Fig. 4. Because the potential-energy curve of the $a^3\Sigma_g^+$ state is so unfavorable for dissociative excitation [$S_c(a^3\Sigma_g^+)$ of Eq. (15) is only 0.0026] that we omit this state from consideration. However, one can estimate the dissociative excitation cross sections of the $a^3\Sigma_g^+$ state by using the Franck-Condon-factor approximation along with $S_c = 0.0026$ and the cross sections of the $a^3\Sigma_g^+$ state (discrete levels) in Table I. It is seen that they are indeed much smaller than the contributions from the other three states.

From Table II we see that the $B'^1\Sigma_u^+$ state account for more than 95% of this dissociation process above 60 eV. Near the threshold excitation of the $e^3\Sigma_u^+$ state is shown to be an important contributor. It should be pointed out that due to the variation of the transition moment with R, the ratio of cross sections $(e^3\Sigma_u^+)$ of discrete levels to those of continuum levels differ from the corresponding ratio $S_d(e^3\Sigma_u^+)/S_c(e^3\Sigma_u^+)$, which is 0.8/0.2.

B. Comparison with experiment

Vroom and de Heer[18] measured the cross sections for the electron-impact production of H(2s) atoms in the energy range of 50 to 6000 eV. More recently, the standard[21] used for normalization of experimental cross sections was re-examined, and as a result Mumma and Zipf[17] suggested a factor of 0.8 by which the previously reported experimental cross sections should be multiplied. Therefore, the cross sections of Vroom and de Heer have been corrected accordingly and are shown in Fig. 4. It appears that the present theoretical cross sections account for 61-67% of the experimental values. The difference (33-39% of experimental data) may well be due to other competing processes leading to formation of H(2s) atoms. First, predissociation into H(1s) + H(2s) through excitation to the states of Π_u symmetry is shown to be an important process by experiments.[22] Second, consideration should be given to the possibility of excitation of the higher excited states with subsequent cascades to the dissociating states. However, not all of the highly excited H_2 molecule will decay to the dissociating states $(B'^1\Sigma_u^+, E^1\Sigma_g^+,$ and $e^3\Sigma_u^+)$ since there are lower states (such as $B^1\Sigma_u^+, X^1\Sigma_g^+,$ and $b^3\Sigma_u^+$) which offer competing cascade paths. Moreover, the $B'^1\Sigma_u^+, E^1\Sigma_g^+,$ and $e^3\Sigma_u^+$ are bound states, unlike the $b^3\Sigma_u^+$ state, so that only the fraction of cascades to the continuum portion of these states

will contribute to the formation of H(2s) atoms. Because of these competitions
we believe that the cascade contribution to formation of H(2s) atoms is not
likely to be very substantial. Finally the experimental data of Vroom and
de Heer may contain, in addition to process (2), contribution from excitation
through doubly excited states, i.e.,

$$H_2 \overset{e}{\leftrightarrow} H(2s) + H(n\ell), \quad n\ell \neq 1s$$
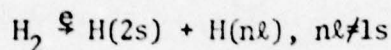
(at energies above the appropriate thresholds) which have been excluded in our
theoretical consideration. In the experiment of electron-impact dissociation
of H_2 described in Ref. 22, some of the H(2s) atoms produced exhibit a threshold
of incident electron energy in the neighborhood of 29 eV, indeed suggesting a
possible dissociative mechanism such as

$$H_2 \overset{e}{\leftrightarrow} H(2s) + H(2p) ,$$
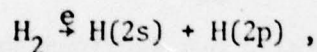
although no determination of the absolute cross sections for this process was
reported. In the experimental condition of Ref. 18, the measured cross
sections represent the sum of contributions from the processes discussed above.
Therefore one would expect our theoretical cross sections to be smaller than
the experimental values.

The energy-dependence of the experimental cross sections[18] shows that the
dissociating state is an optically allowed one. Our results are in agreement
with the experiment in this regard as the major contributor is found to be
the $B'^1\Sigma_u^+$ state. This characteristic energy-dependence will remain unchanged
when predissociation of the $^{1,3}\Pi_u$ states is considered. To summarize, our
calculation indicates that the dissociative excitation of the $B'^1\Sigma_u^+$, $e^3\Sigma_u^+$,
and $E^1\Sigma_g^+$ states accounts for as much as two-thirds of measured cross sections
for production of H(2s) atoms. The remainder is very likely due to pre-
dissociation of $^{1,3}\Pi_u$ states and to the excitation of doubly excited states.

V. CONCLUSION

The mechanism of electron-impact dissociation of molecules may be sub-
divided into (i) direct excitation of repulsive states (including excitation
of bound states above the dissociation limits), (ii) excitation of discrete
levels of bound states followed by cascades to a dissociating state, and
(iii) excitation of bound states which are predissociative (i.e., mixed with
dissociating states). The method of Gaussian-type orbitals has been proven
to be a very efficient means of dealing with excitation of discrete levels
of molecules. As the computation of continuum functions poses no difficulty,
the method of GTO can be readily extended to ab initio calculations of
processes (i) and (ii). In order to make reliable calculation of pre-
dissociation [process (iii)], accurate electronic wave functions and detailed
knowledge of potential-curve crossing are required. Once this information
is available, the Gaussian technique can be applied to treat the problem of
excitation to the predissociative states.

In this report we have presented the results of the electron-impact dissoc-
iation of the H_2 molecule into $H(1s) + H(1s)$, and into $H(1s) + H(2s)$ computed
within the framework of the Born approximation. In the former case we find
that the total dissociation cross sections receive about equal contributions
from the direct excitation of the repulsive $b^3\Sigma_u^+$ state and from the excitation
of higher triplet states with subsequent cascade to $b^3\Sigma_u^+$. The present
theoretical cross sections are in a reasonably good agreement with the experi-
mental values of Corrigan when the latter are made compatible so as to represent
the process leading to $H(1s) + H(1s)$ only.

As to the process of $H(1s) + H(2s)$, the excitation of the $B'^1\Sigma_u^+$, $e^3\Sigma_u^+$,
and $E^1\Sigma_g^+$ states (above the dissociation limit) may account for almost two-
thirds of the measured cross sections of Vroom and de Heer. Among these

dissociating states the $B'^1\Sigma_u^+$ state is by far (95% or more) the most important contributor at incident energies above 60 eV. At lower energies the $e^3\Sigma_u^+$ becomes important, particularly near the threshold. The balance (about one-third) is expected (but not independently verified) to come from excitation of the $^{1,3}\Pi_u$ states which are predissociated by the $B'^1\Sigma_u^+$ and $e^3\Sigma_u^+$ states. It is also likely that some contribution comes from excitation of some doubly excited states. Although our results are consistent with the experimental data, further studies concerning predissociation and the nature of some of the doubly excited states are necessary in order to have a more complete understanding of dissociation of H_2 into $H(1s) + H(2s)$.

REFERENCES

1. K. Takayanagi and Y. Itikawa, Space Science Review $\underline{11}$, 380 (1970).

2. A. V. Phelps, in Proceedings of the Workshop on Dissociative Excitation of Simple Molecules edited by L. J. Kieffer (JILA Information Center Report No. 12, Boulder, Colorado).

3. T. E. Sharp, Atomic Data $\underline{2}$, 119 (1971).

4. S. Chung and C. C. Lin, Phys. Rev. A $\underline{6}$, 988 (1972) and the references therein.

5. D. C. Cartwright and A. Kuppermann, Phys. Rev. $\underline{163}$, 86 (1967).

6. S. P. Khare and B. L. Moiseiwitsch, Proc. Phys. Soc. (London) $\underline{88}$, 605 (1966).

7. S. P. Khare, Phys. Rev. $\underline{157}$, 107 (1967).

8. L. A. Edelstein, Nature $\underline{182}$, 932 (1958).

9. M. R. H. Rudge, Proc. Phys. Soc. (London) $\underline{85}$, 607 (1965); $\underline{86}$, 763 (1965); D. J. T. Morrison and M. R. H. Rudge, ibid. $\underline{91}$, 565 (1967).

10. V. I. Ochkur, Zh. Eksp. Teor. Fiz. $\underline{45}$, 734 (1963) [Sov. Phys.-JETP $\underline{48}$, 503 (1964)].

11. W. Kolos and L. Wolniewicz, J. Chem Phys. $\underline{43}$, 2429 (1965); $\underline{50}$, 3228 (1969); $\underline{48}$, 3672 (1968).

12. R. J. Spindler Jr., J. Quant. Spectrosc. Radiat. Trans. $\underline{9}$, 627 (1969).

13. P. E. Phillipson and R. S. Mulliken, J. Chem. Phys. $\underline{28}$, 1248 (1958).

14. A. D. McLean, A. Weiss, and M. Yoshimine, Rev. Mod. Phys. $\underline{32}$, 211 (1960).

15. We find it difficult to read the cross sections of Khare's work directly from Fig. 1 of Ref. 7 since the peak cross section lies between two markers of the vertical axis labelled as $0.08 \, \pi a_o^2$ and $1.2 \, \pi a_o^2$. Thus we use the value attributed to Khare as reproduced in Fig. 7 of Ref. 5.

16. S. J. B. Corrigan, J. Chem. Phys. $\underline{43}$, 4381 (1965).

17. M. J. Mumma and E. C. Zipf, J. Chem. Phys. $\underline{55}$, 1661 (1971).

18. D. A. Vroom and F. J. de Heer, J. Chem. Phys. <u>50</u>, 580 (1969).

19. H. Ramien, Z. Physik <u>70</u>, 353 (1931).

20. A. G. Engelhardt and A. V. Phelps, Phys. Rev. <u>131</u>, 2115 (1963).

21. W. L. Fite and R. T. Brackmann, Phys. Rev. <u>112</u>, 1151 (1958).

22. M. Misakian and J. C. Zorn, Phys. Rev. A <u>6</u>, 2181 (1972); and references therein.

Table I. Dissociation cross sections for production of $H(1s) + H(1s)$ via excitation of the $b^3\Sigma_u^+$ state (repulsive) and the $a^3\Sigma_g^+$, $e^3\Sigma_u^+$, $c^3\Pi_u$, and $d^3\Pi_u$ states (bound) in units of 10^{-17} cm^2.

Energy (eV)	Cross sections				
	$b^3\Sigma_u^+$	$a^3\Sigma_g^+$	$c^3\Pi_u$	$e^3\Sigma_u^+$ [a]	$d^3\Pi_u$
10	1.76				
13	4.47	1.07	1.96		
15	4.18	1.22	1.98	0.334	0.408
20	2.69	0.854	1.19	0.286	0.311
30	1.10	0.342	0.433	0.122	0.120
40	0.525	0.160	0.196	0.0574	0.0532
50	0.287	0.0857	0.104	0.0309	0.0278
70	0.112	0.0328	0.0396	0.118	0.0103
100	0.0401	0.0116	0.0140	0.0041	0.0036
150	0.0123	0.0035	0.0042	0.0012	0.0011

[a] Excitation to discrete vibrational levels only.

Table II. Dissociation cross sections for production of H(1s) + H(2s) via excitation[a] of the $B'^1\Sigma_u^+$, $E^1\Sigma_g^+$, and $e^3\Sigma_u^+$ states in units of $10^{-18}\,cm^2$.

Energy (eV)	Cross Sections		
	$B'^1\Sigma_u^+$	$E^1\Sigma_g^+$	$e^3\Sigma_u^+$
15	0.0623	0.0290	0.151
18	1.33	0.113	0.860
20	1.98	0.141	0.800
40	3.91	0.166	0.163
60	3.75	0.133	0.0509
80	3.41	0.108	0.0217
100	3.09	0.0910	0.0112
150	2.50	0.0645	0.0033
200	2.10	0.0498	
500	1.13	0.0219	
1000	0.674	0.0108	

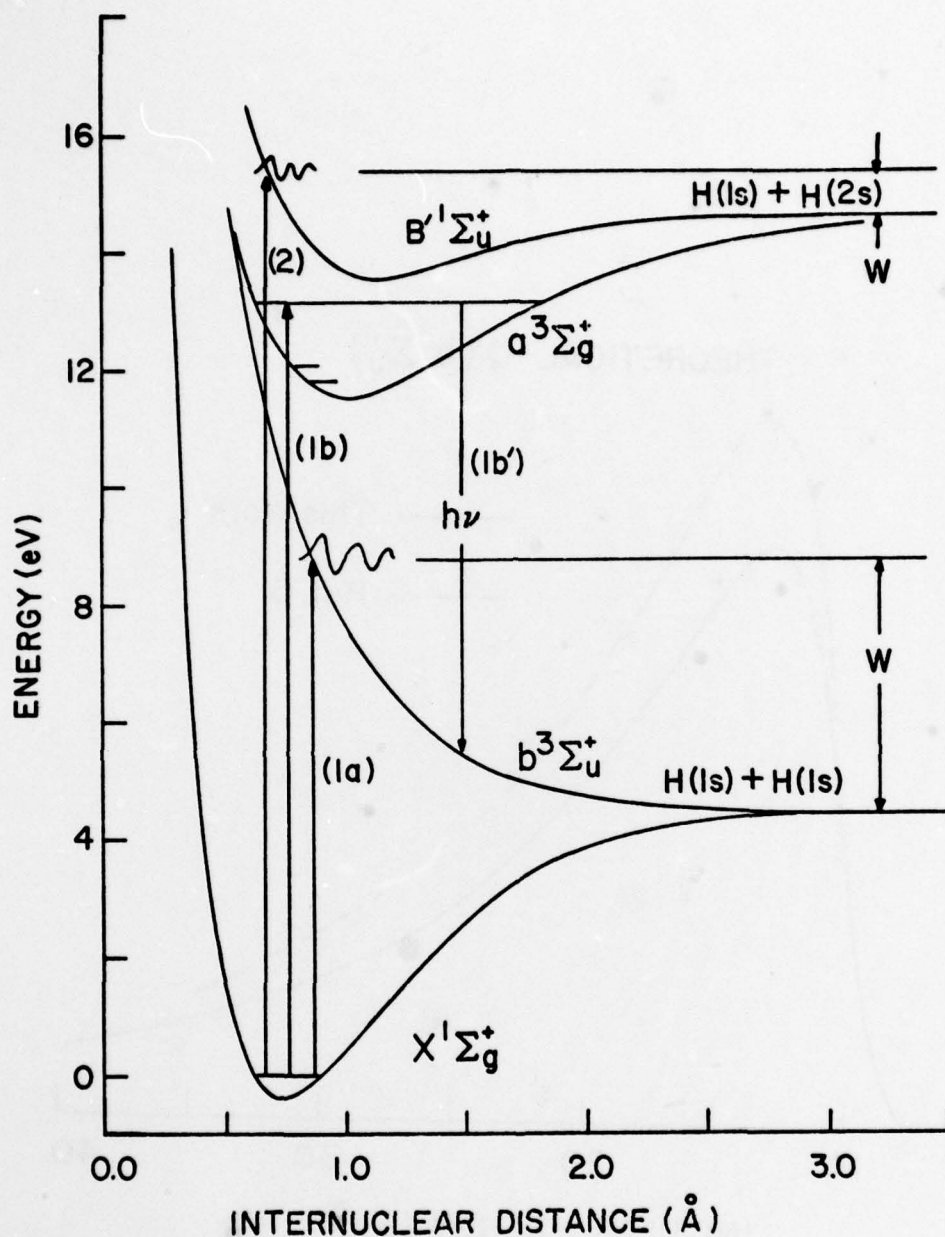[a] Excitation to these states above the dissociation limit only.

Fig. 1. Potential-energy curves of the H_2 molecule illustrating different mechanisms of dissociation by electron impact. Dissociation into H(1s) + H(1s) results from direct excitation of the repulsive $b^3\Sigma_u^+$ state (1a), and also from excitation of higher triplet states such as $a^3\Sigma_g^+$ state (1b) followed by radiative cascade to the $b^3\Sigma_u^+$ state (1b'). Dissociation into H(1s) + H(2s) results from excitation of the $B'^1\Sigma_u^+$ state (also $E^1\Sigma_g^+$, $e^3\Sigma_u^+$, and $a^3\Sigma_g^+$ states) above the dissociation limit (2).
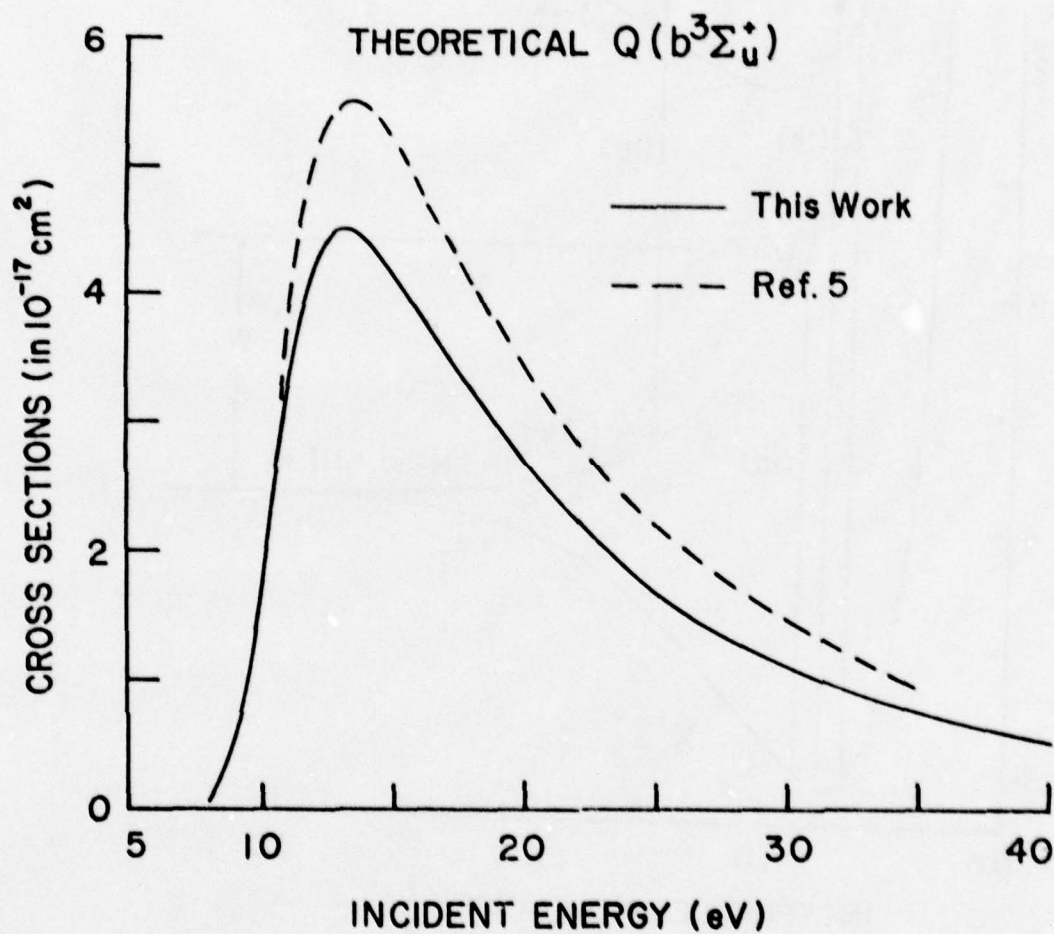
Fig. 2. Excitation cross sections of the $b^3\Sigma_u^+$ state calculated by the Born-Rudge scheme. The results of this work are represented by the solid curve, and those of Ref. 5 by the dashed curve.
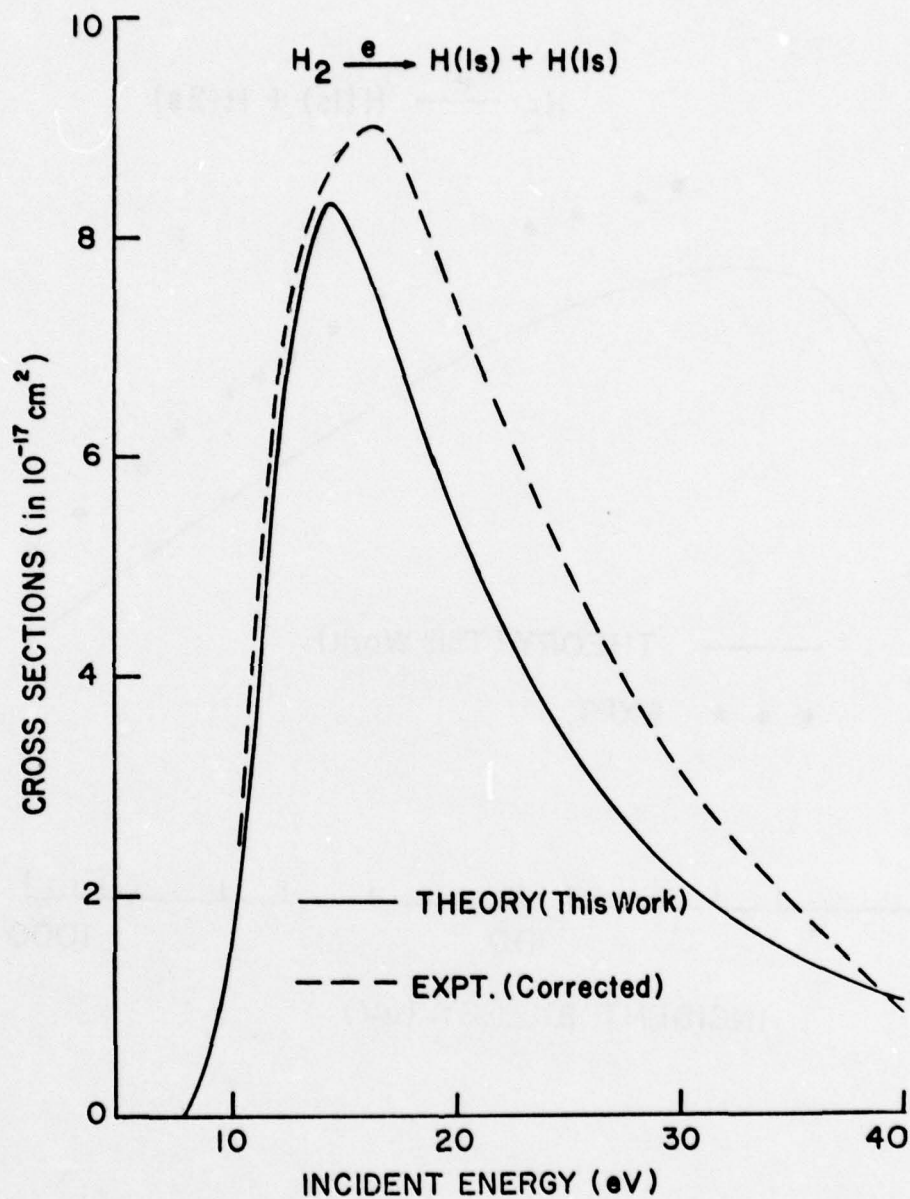
Fig. 3. Theoretical cross sections of this work (solid curve) for the dissociation process $H_2 \xrightarrow{e} H(1s) + H(1s)$ as compared with the experimental values of Ref. 17 (corrected to represent the production of H(1s) atoms only as described in Sec. IIID (dashed curve).
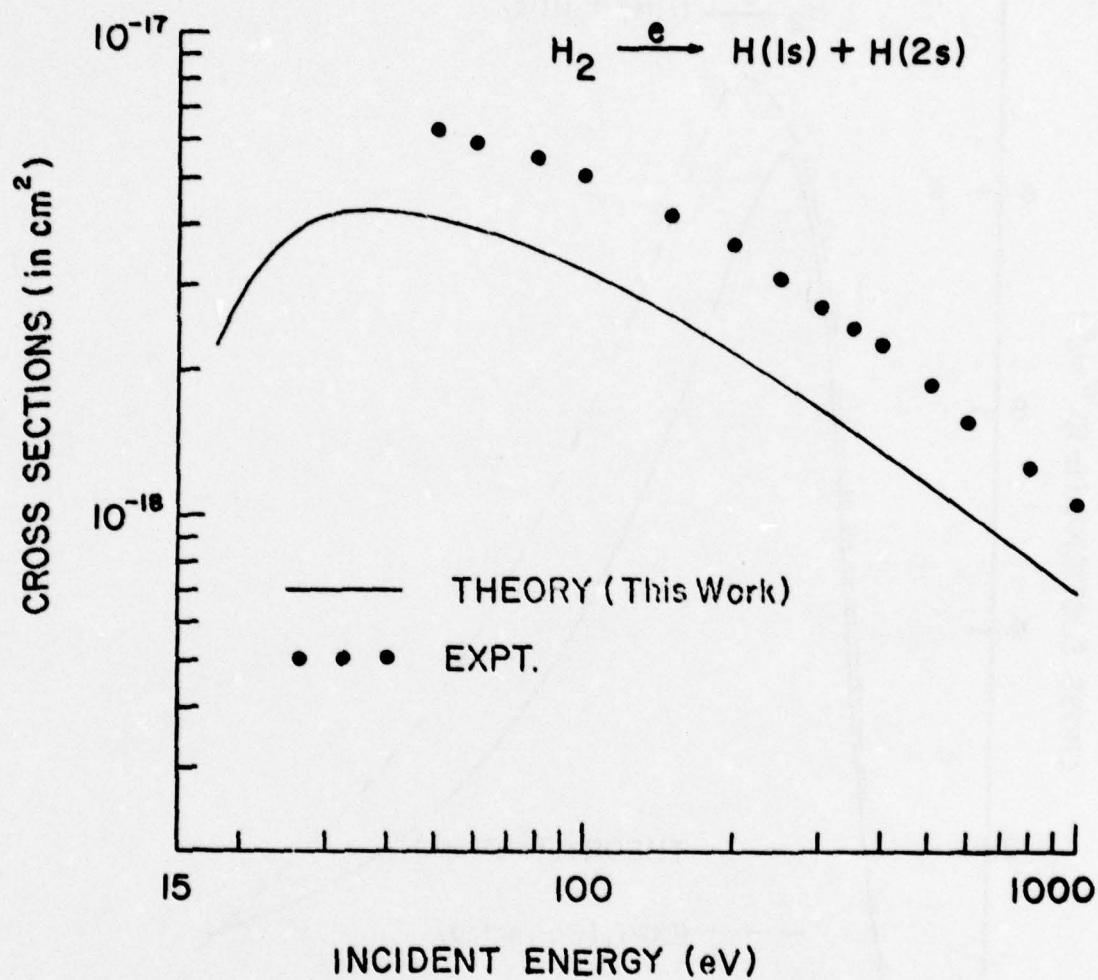
Fig. 4. Theoretical cross sections of this work (solid curve) for the dissociation process $H_2 \xrightarrow{e} H(1s) + H(2s)$ via excitation of the $B'^1\Sigma_u^+$, $E^1\Sigma_g^+$, and $e^3\Sigma_u^+$ states. The experimental cross sections of Ref. 20 are multiplied by a factor of 0.8 as suggested by Ref. 19. The experimental cross sections are for the rate of production of H(2s) atoms, thus they also include other modes of dissociation (see Sec. IV B).

PART II

APPLICATION OF THE CLOSE-COUPLING METHOD TO EXCITATION OF

ELECTRONIC STATES AND DISSOCIATION OF H_2 BY ELECTRON IMPACT

I. INTRODUCTION

Excitation of the electronic states of molecule by electron impact is one of the simplest basic processes in molecular collision phenomena. The importance of such excitation processes in many areas of studies has stimulated considerable experimental efforts in recent years. However, the progress in the theoretical aspects of the problem has been much slower. In fact the status of the theory of electron-impact excitation of the electronic states of diatomic molecules is in a rather primitive stage in comparison with the corresponding electron-atom processes. For a few diatomic molecules (H_2, N_2, CO), systematic studies[1-8] of the excitation cross sections for a number of singlet and triplet states have been made by means of the Born approximation and/or the modified versions of it. The modifications of the Born approximation as introduced by Ochkur[9] and by Rudge[10] enable one to handle the exchange interaction between the colliding and the target electrons in a simple way. Excitation from a singlet to another singlet state can be treated either by the first Born approximation (referred to as the Born approximation in this paper), or by one of the modified versions when the exchange effect is included. On the other hand one must resort to the Born-Ochkur or the Born-Rudge approximation for excitation to triplet states. In Refs. 1 and 2, it is suggested that Born-Ochkur approximation be used for singlet-singlet excitation, but the Born-Rudge scheme is recommended for singlet-triplet processes. Comparison with experiments shows satisfactory agreement for a few states, but rather large discrepancy is found for some others. Viewed as a whole, one can only regard the Born-type calculation as a means of providing theoretical estimates but not always cross sections of precise quantitative significance. In the cases of singlet-triplet processes, the excitation functions generally

peak at a few eV above the threshold and decrease steeply with increasing energy. For many applications, the major interest in triplet excitation lies in the near-threshold region where the cross sections are large, but this is also the region in which the validity of the Born approximation becomes questionable. Recently a calculation based on "the first-order many-body formula" (a form of distorted-wave approximation) was advanced[11], which is yet to be tested against more rigorous theory. Like the Born-Ochkur and Born-Rudge approximations before it, this method, too, takes advantage of relative simplicity in computation but also falls short of serious theoretical justification. Collectively, these efforts are a testimony that while the need for theoretical cross sections is great, the means of obtaining them is restricted - no doubt, due to the computational complexity involved in the molecular problems.

The most rigorous and systematic formalism commonly applied to the electron-atom collision processes is the method of close coupling.[12-17] About ten years ago a very ambitious effort of applying the close-coupling method to electron-H_2 excitation was undertaken by Fajen.[18] He calculated the excitation cross sections of the $B^1\Sigma_u^+$, $C^1\Pi_u$, and $E^1\Sigma_g^+$ states of H_2 by a multi-state close coupling scheme. To make the problem tractable, Fajen neglected the exchange interaction between the colliding and target electrons. The emphasis of his work is mainly focused on the problem of singlet-singlet excitation in the high and intermediate energies, particularly the effect of multi-state indirect coupling on the cross sections of the $E^1\Sigma_g^+$ state. Black and Lane[19,20] also calculated the cross sections of the $B^1\Sigma_u^+$ state by the close-coupling method. The electron-exchange was approximated as an effective exchange potential by the scaled Slater-Hartree-Fock form to simplify the computation.[20] The latter work was primarily concerned with the resonant excitation of the $B^1\Sigma_u^+$ state at low incident-electron energies (11-13 eV).

In this report we apply the method of close coupling to the electron-H_2 problem with the projectile-target electron exchange included, and calculate excitation cross sections for several triplet states as well as the $B^1\Sigma_u^+$ state. The theoretical formulation and the computational procedures parallel closely those of the atomic cases with two notable differences coming from the axial symmetry of molecule and the two-center nature of (homonuclear diatomic) molecular wave functions. From the computational standpoint, these differences translate into one additional truncation of an infinite sum beyond the atomic calculation. In our calculations this truncation is fully justified with a demonstrated convergence. Aside from this point, all computations are carried out to the same degree of refinement as the corresponding electron-atom problems.

II. GENERAL THEORY

The development of the close-coupling theory dates back to the 1950's.[12] Since then this method has been applied with increasing frequency to electron-atom problems,[13-17] so that the general theory of the close-coupling method is rather well known now. Nevertheless, for the purpose of later discussions, we specialize it to electron-diatomic molecule collision processes which result in an excitation of electronic states. The formulation here parallels closely to those already published in conjunction with electron-atom case, particularly, the work by Smith, Henry, and Burke.[14]

In the field of electron-molecule collision, when an excitation is made from one electronic state to another, we are interested in the excitation cross sections that are averaged over the initial rotational substates, and summed over the final rotational substates. In order to compute such cross sections, it is possible — in fact desirable from the computational point of view — to formulate the problem in the molecule-fixed frame of reference,[21,22] thereby ignoring the rotational structure completely. However, in its stead, we average the direction of the incident electron with respect to the orientation of molecule. Only assumption needed here is that the energy of scattered electrons be much greater than energy-spacings of the rotational states.

As to the treatment of the vibrational motion, it is a common practice to use the Franck-Condon-factor (FC) approximation, by which electronic states of molecules are considered "vibrationless." This simplifies the calculation, since the vibrational wave functions now enter the computation only through FC factors so that the scattering equations can be solved without the knowledge of vibrational motion. The validity of this approximation has been examined.[3] In this report we will focus our attention to the electronic motion and ignore the

dependency of electronic functions on the internuclear distance. Thus, in what follows, all electronic functions are those corresponding to the equilibrium separation of a ground state.

An electronic state of a diatomic molecule is defined by the angular momentum along the molecular axis λ, and the spin (sm). We use n to distinguish different states which have the same quantum numbers (λsm). Thus, we write an N-electron electronic wave function as

$$\Phi(n\lambda sm|\vec{x}_1,\ldots,\vec{x}_N),\tag{1}$$

where $\vec{x}_i$ represents the spatial ($\vec{r}_i$) and spin (σ_i) coordinates of the i-th electron. Φ's are fully antisymmetrized products consisting of one-electron molecular orbitals $\phi_j(n_j\lambda_j|\vec{r})$ with α- or β-spin, and they are assumed to satisfy the Schroedinger equation exactly,

$$H_{mol}\Phi(n\lambda sm) = E_{n\lambda}\Phi(n\lambda sm),\tag{2}$$

$$H_{mol} = -\sum_{i=1}^{N}[\tfrac{1}{2}\nabla_i^2 + Z(|\vec{r}_A-\vec{r}_i|^{-1} + |\vec{r}_B-\vec{r}_i|^{-1})]$$

$$+ \sum_{i=1}^{N-1}\sum_{j=i+1}^{N} |\vec{r}_i-\vec{r}_j|^{-1},\tag{3}$$

where Z is the nuclear charge, and $\vec{r}_A$ and $\vec{r}_B$ are the position vectors of the two nuclei. The scattered-electron wave is characterized by angular momenta ($\ell m'$) and spin (s=$\tfrac{1}{2}$, m=$\pm\tfrac{1}{2}$).

The essence of the close-coupling method consists of expanding the total (N+1)-electron function of the collision system in terms of a suitable set of basis functions. Due to the axially symmetric field in which these (N+1) electrons move, the total angular momentum projected on the molecular axis $\Lambda=\lambda+m'$ is a constant of the collision process.

As we deal only with spin-independent Hamiltonians, the total spin (SM) are good quantum numbers. In fact the cross sections are independent of M.

Accordingly, we adopt a basis set which are eigenfunctions of (SMΛ), i.e.,

$$\psi_\mu^{SM\Lambda}(X^{-i}) \equiv \psi_{n\lambda\ell s}^{SM\Lambda}(\vec{x}_1,\ldots,\hat{r}_i\sigma_i,\ldots,\vec{x}_{N+1})$$

$$= \Sigma_m\, C(s,\tfrac{1}{2},m,M\text{-}m|SM)Y_{\ell,\Lambda-\lambda}(\hat{r}_i)\xi(\tfrac{1}{2},M\text{-}m|\sigma_i)$$

$$\times\, \Phi(n\lambda sm|\vec{x}_1,\ldots,\vec{x}_{i-1},\vec{x}_{i+1},\ldots,\vec{x}_{N+1}), \tag{4}$$

where $C(j_1 j_2 m_1 m_2|JM)$ is the Clebsch-Gordan coefficient, $Y_{\ell m}$ is the spherical harmonic, and ξ is α- or β-spin function. We also used two short-hand notations; X^{-i} indicates that r_i-coordinate is missing in the basis function as shown and the channel index $\mu \equiv (n\lambda\ell)$.[23] The total (N+1)-electron wave function is now expanded in an explicitly antisymmetrized form as

$$\psi^T(\vec{x}_1,\ldots,\vec{x}_{N+1}) = \Sigma_{SM\Lambda\mu}\psi_\mu^{SM\Lambda}(\vec{x}_1,\ldots,\vec{x}_{N+1}), \tag{5}$$

and

$$\psi_\mu^{SM\Lambda}(\vec{x}_1,\ldots,\vec{x}_{N+1}) = \sum_{i=1}^{N+1} \Sigma_{\mu'}\, (N+1)^{-\frac{1}{2}}(-1)^{i-1}r_i^{-1}F_{\mu'\mu}(r_i)\psi_{\mu'}^{SM\Lambda}(X^{-i}), \tag{6}$$

where $r^{-1}F_{\mu'\mu}(r)$ are to be determined by solving the scattering equation In this paper we will not consider the bound (N+1)-electron states in the expansion of Eq. (5). Inclusion of such bound states allows for the possibility of electron-capture into the target molecule,[24] and would be essential in the studies of resonance behaviors of excitation functions such as in Ref. 20. We seek the solution of the Schroedinger equation,

$$(H\text{-}E)\psi^T(\vec{x}_1,\ldots,\vec{x}_{N+1}) = 0, \tag{7}$$

where the (N+1)-electron Hamiltonian H is

$$H = H_{mol} - \tfrac{1}{2}\nabla^2_{N+1} + V(\vec{r}_1,\ldots,\vec{r}_{N+1}) \tag{8}$$

$$V(\vec{r}_1,\ldots,\vec{r}_{N+1}) = -Z \left(|\vec{r}_A - \vec{r}_{N+1}|^{-1} + |\vec{r}_B - \vec{r}_{N+1}|^{-1} \right)$$

$$+ \sum_{i=1}^{N} |\vec{r}_i - \vec{r}_{N+1}|^{-1}. \tag{9}$$

In lieu of Eq. (7) we apply the variational principle to the integral (a standard prescription here),

$$\delta \int d\vec{x}_1 \ldots d\vec{x}_{N+1} \; \psi_\mu^{SM\Lambda *}(\vec{x}_1,\ldots,\vec{x}_{N+1}) [H-E] \psi^T(\vec{x}_1,\ldots\vec{x}_{N+1}) = 0, \tag{10}$$

with a subsidiary condition that the scattered-electron functions be orthogonal to all the relevant target one-electron orbitals ϕ_j. (Imposition of this orthogonality condition precludes the possibility of electron capture into those orbitals.) For electron-atom problems, because of the spherical symmetry of the target, this is equivalent to requiring orthogonality between the scattered radial functions $r^{-1}F_{\mu'\mu}$ and the target orbitals of the same ℓ. This orthogonality relation offers a great deal of simplification to the scattering equations. For molecular systems, the requirement of $r^{-1}F_{\mu'\mu}$ being orthogonal to the relevant molecular orbitals would certainly ensure the orthogonality of the colliding-electron wave function to the target states, but the former is somewhat more stringent than the latter. However, in this work we adopt the former version in order to take advantage of the simplification in handling the exchange terms in the scattering equation, i.e.,[25]

$$\int \phi_j^*(n_j\lambda_j|\vec{r}) [Y_{\ell',\Lambda-\lambda'}(\hat{r}) r^{-1} F_{n'\lambda'\ell'}(r)] d\vec{r} = 0. \tag{11}$$

Upon expanding

$$\phi_j(n_j\lambda_j|\vec{r}) = \sum_\ell Y_{\ell\lambda_j}(\hat{r}) \phi_{j,\ell}(n_j\lambda_j|r) , \tag{12}$$

Eq. (11) becomes

$$\Sigma_\ell \, \delta_{\ell,\ell'} \, \delta_{\lambda_j,\Lambda-\lambda'} \int \phi_{j,\ell}(n_j\lambda_j|r) \, r^{-1}F_{n'\lambda'\ell'}(r)r^2dr = 0, \tag{13}$$

for all molecular orbitals $\phi_j(n_j\lambda_j|r)$. This orthogonality condition may be treated by means of the Lagrangian undetermined multiplier $M_{n_j\lambda_j\ell}$, which amounts to adding to Eq.(10), the following equation

$$\delta\!\int\!\Sigma_j\Sigma_\ell \, \delta_{\ell,\ell'} \, \delta_{\lambda_j,(\Lambda-\lambda')} \, M_{n_j\lambda_j\ell} \, \phi_{j,\ell}(n_j\lambda_j|r)$$
$$\times \, r^{-1}F_{n'\lambda'\ell'}(r)r^2dr = 0. \tag{14}$$

From Eqs. (10) and (14), we obtain the familiar set of integro-differential equations,

$$[\frac{d^2}{dr^2} - \frac{\ell'(\ell'+1)}{r^2} + k'^2]F_{\mu'\mu}(r) = 2\,\Sigma_{\mu''}[U_{\mu'\mu''}(r) + W_{\mu'\mu''}(r)]F_{\mu''\mu}(r)$$
$$+ \Sigma_j\Sigma_\ell\delta_{\ell\ell'}\delta_{\lambda_j,(\Lambda-\lambda')}M_{n_j\lambda_j\ell}\phi_{j,\ell}(n_j\lambda_j|r), \tag{15}$$

where the direct (U) and exchange (W) potentials are

$$U_{\mu'\mu''}(r_{N+1}) = \int \psi_{\mu'}^{SM\Lambda*}(X^{-(N+1)}) \, V(\vec{r}_1,\ldots,\vec{r}_{N+1})$$
$$\times \, \psi_{\mu''}^{SM\Lambda}(X^{-(N+1)}) \, d\vec{r}_1\ldots d\vec{r}_N d\hat{r}_{N+1}, \tag{16}$$

$$W_{\mu'\mu''}(r_{N+1}) F_{\mu''\mu}(r_{N+1}) = -N \int \psi_{\mu'}^{SM\Lambda*}(X^{-N}) \, r_N^{-1}F_{\mu''\mu}(r_N)$$
$$\times \, |\vec{r}_N-\vec{r}_{N+1}|^{-1} \psi_{\mu''}^{SM\Lambda}(X^{-(N+1)})d\vec{r}_1\ldots d\vec{r}_N d\hat{r}_{N+1}, \tag{17}$$

and

$$k'^2 = 2(E-E_{n'\lambda'}). \tag{18}$$

We will not attempt to simplify Eqs. (16) and (17) until we come to a specific application. However, we point out here that these coupling potentials vanish between channels of differing parity.[26] Parity of a channel $(n\lambda\ell)$ associated with $(n\lambda)$ electronic state may be defined as $(-1)^\ell$ for "gerade"

states ($\Sigma_g, \Pi_g, \ldots$), and $(-1)^{\ell+1}$ for "ungerade" states ($\Sigma_u, \Pi_u, \ldots$). As a result, the scattering equations separate into two sets according to even or odd parity just as in an electron-atom collision problem. The solutions $F_{\mu'\mu}(r)$ are subject to the boundary conditions,

$$F_{\mu'\mu}(r) \to 0, \text{ as } r \to 0$$

$$F_{\mu'\mu}(r) \sim \frac{1}{k'^{\frac{1}{2}}} [\delta_{\mu'\mu} e^{-i(k'r - \frac{1}{2}\ell'\pi)} - e^{i(k'r - \frac{1}{2}\ell'\pi)} S_{\mu'\mu}^{SM\Lambda}], \text{ as } r \to \infty, \tag{19}$$

where $S_{\mu'\mu}$ is the scattering matrix. Following a similar analysis of Blatt and Biedenharn,[12] the scattering amplitude is

$$f^{SM\Lambda}(n\lambda\ell s \to n'\lambda'\ell's' | \hat{k}, \hat{r}) = \frac{2\pi}{(kk')^{\frac{1}{2}}} i^{\ell-\ell'} Y_{\ell,\Lambda-\lambda}^{*}(\hat{k})$$

$$\times Y_{\ell',\Lambda-\lambda'}(\hat{r}) T_{\mu'\mu}^{SM\Lambda}, \tag{20}$$

where the transition matrix T is

$$T_{\mu'\mu}^{SM\Lambda} = \delta_{\mu'\mu} - S_{\mu'\mu}^{SM\Lambda}. \tag{21}$$

The differential cross section in $\hat{r}$-direction is

$$I(n\lambda s \to n'\lambda's' | \hat{k}, \hat{r})$$

$$= \frac{4\pi^2}{k^2} \Sigma_S \frac{(2S+1)}{2(2s+1)} \Sigma_{\Lambda\ell\ell'} | Y_{\ell,\Lambda-\lambda}(\hat{k}) Y_{\ell',\Lambda-\lambda'}(\hat{r}) T_{n'\lambda'\ell',n\lambda\ell}^{SM\Lambda} |^2. \tag{22}$$

Integration over the scattered angle yields a total cross section for a given incident direction $(\hat{k})$. As stated before, we are to average the cross sections with respect to $\hat{k}$, i.e.,

$$Q(n\lambda s \to n'\lambda's') = \frac{1}{4\pi} \int d\hat{k} \, d\hat{r} \, I(n\lambda s \to n'\lambda's' | \hat{k}, \hat{r})$$

$$= \frac{\pi}{k^2} \Sigma_S \frac{(2S+1)}{2(2s+1)} \Sigma_{\Lambda\ell\ell'} | T_{n'\lambda'\ell',n\lambda\ell}^{SM\Lambda} |^2. \tag{23}$$

For the purpose of later discussions, it is convenient to have cross sections expressed as

$$Q(n\lambda s \rightarrow n'\lambda's') = \Sigma_S \frac{(2S+1)}{2(2s+1)} \sum_{\Lambda=-\infty}^{\infty} \sum_{\ell=|\Lambda-\lambda|}^{\infty} \sum_{\ell'=|\Lambda-\lambda'|}^{\infty} Q^{SM\Lambda}(n\lambda s\ell \rightarrow n'\lambda's'\ell'), \quad (24)$$

with

$$Q^{SM\Lambda}(n\lambda s\ell \rightarrow n'\lambda's'\ell') = \frac{\pi}{k^2} \ |T^{SM\Lambda}_{n'\lambda'\ell',n\lambda\ell}|^2 \ . \tag{25}$$

In accordance with the FC approximation, Eq. (23) is viewed as the cross section from any <u>one</u> vibrational level of $(n\lambda s)$ to <u>all</u> vibrational levels of $(n'\lambda's')$ state. Therefore, cross sections between a pair of vibrational levels are to be scaled by the appropriate Franck-Condon factor $q_{nv,n'v'}$, i.e.,

$$Q(n\lambda sv \rightarrow n'\lambda's'v') = q_{nv,n'v'}Q(n\lambda s \rightarrow n'\lambda's'),$$

$$\tag{26}$$

$$q_{nv,n'v'} = |\int \chi^*_{n'v'}(R) \ \chi_{nv}(R)R^2 dR|^2,$$

where $\chi_{nv}(R)$ is the vibrational wave function of (nv) state.

It is worthwhile to draw the contrast between the electron-atom and electron-molecule systems. An obvious difference is that the electronic wave functions of a diatomic molecule are centered around two nuclei. This causes difficulty in computing the coupling potentials, which will be discussed in Sec. IV-A. The other point of practical interest is the following. In an electron-atom collision, the scattering equations are diagonal in $\vec{L} = \vec{\ell}_a + \vec{\ell}$ and M_L ($\vec{\ell}_a$ and $\vec{\ell}$ being the angular momenta of the atom and scattered electron respectively), and the cross sections are independent of M_L. Accordingly, the cross sections corresponding to Eq. (24) are (apart from the parity consideration) given by

$$Q^{atom}(n\ell_a s \rightarrow n'\ell'_a s') = \Sigma_S \frac{(2S+1)}{2(2s+1)} \sum_{L=0}^{\infty} \frac{(2L+1)}{(2\ell_a+1)} \sum_{\ell=|L-\ell_a|}^{L+\ell_a}$$

$$\sum_{\ell'=|L-\ell'_a|}^{L+\ell'_a} Q^{LS}(n\ell_a\ell s \rightarrow n'\ell'_a\ell's'). \tag{27}$$

Thus, once the number of target states $(n\ell_a)$ are decided on, one set of scattering equations corresponding to a given pair of L, M_L are solved at a time, yielding partial cross sections Q^{LS}. Further, for a given L, ℓ and ℓ' are restricted to a finite number of values as shown in Eq. (27). Strictly speaking, L runs from 0 to ∞. In practice, since the partial cross sections Q^{LS} diminish with increasing L for large L, the series in Eq. (27) may be terminated after summing a finite number of Q^{LS} for $L=0,1,\ldots L_{max}$. The point we like to emphasize here is that L_{max} is chosen - and may be increased later - according to the knowledge of partial cross sections Q^{LS} already calculated for $L \leq L_{max}$.

However, for the electron-excitation of molecule considered in this paper, only Λ is a good quantum number.[27] Thus, the scattering equations for a given Λ would in principle contain infinite number of channels corresponding to $\ell = |\Lambda-\lambda|, |\Lambda-\lambda|+2,\ldots$etc. as shown in Eq. (24). Again, truncation of channels (with respect to ℓ) is inevitable. However, in this case the truncation must be made before the scattering equations are solved. In other words, whether or not a sufficient number of channels were included in a calculation can be ascertained only after the calculation had already been completed. This is an additional burden in the calculation of molecular excitation. We will discuss this further in Sec. III.

III. APPLICATION TO ELECTRON-H_2 COLLISION

Within the theoretical framework outlined in the previous section, we made a series of two-state close-coupling calculations by including the ground state $X^1\Sigma_g^+$ and each of the $B^1\Sigma_u^+$, $a^3\Sigma_g^+$, $b^3\Sigma_u^+$, $c^3\Pi_u$, and $e^3\Sigma_u^+$ states. With the number of electronic states thus limited to two, we must still decide how many partial waves ($\ell\ell'$) are to be included in a calculation, as pointed out at the end of Sec. II. After some test calculations we found that for the singlet-triplet excitation it is quite adequate to include three partial waves or less per electronic state in the energy-range (up to 40 eV) of incident electrons considered here. However, in the case of excitation to the singlet state ($B^1\Sigma_u^+$), it appears that a very large number of partial waves would be required. Therefore, we adopt the following practical scheme[18] to carry out the close-coupling calculations with a limited number of partial waves while maintaining sufficient degree of accuracy.

A. Special Treatment for Singlet-Singlet Excitation

Let us denote the close-coupling (CC) cross section of $(X^1\Sigma_g^+ \rightarrow B^1\Sigma_u^+)$ excitation by

$$Q^{(CC)}(B1\Sigma_u^+) = \Sigma_{\ell\ell'}, \Sigma_\Lambda \, Q^{(CC)\Lambda}(\ell,\ell'). \tag{28}$$

This is a short-hand version of Eq. (24) with $S=M=\frac{1}{2}$ and $s=s'=0$. We assert here that for sufficiently large $(\ell,\ell'>L)$, $Q^{(CC)\Lambda}(\ell,\ell')$ approach the corresponding partial cross sections $Q^{(Born)\Lambda}(\ell,\ell')$ by the Born approximation. Barnes, Lane, and Lin[16] verify this in their work on electron-Na collision with a qualitative physical reason behind it. Therefore, we may calculate $Q^{(CC)\Lambda}(\ell,\ell')$ for $(\ell,\ell')\leq L$, and substitute $Q^{(Born)\Lambda}(\ell,\ell')$ for $Q^{(CC)\Lambda}(\ell,\ell')$ for $(\ell,\ell')>L$, viz.,

$$Q^{(CC)}(B^1\Sigma_u^+) \simeq \overset{L}{\underset{\ell\ell'}{\Sigma}}\Sigma_\Lambda \; Q^{(CC)\Lambda}(\ell,\ell') + \Sigma_{\ell\ell'>L}\Sigma_\Lambda \; Q^{(Born)\Lambda}(\ell,\ell')$$

$$= \overset{(Born)}{Q(total)} + \overset{L}{\underset{\ell\ell'}{\Sigma}}\{\Sigma_\Lambda[Q^{(CC)\Lambda}(\ell,\ell') - Q^{(Born)\Lambda}(\ell,\ell')]\} \tag{29}$$

We will substantiate this claim later.

B. Coupling Potentials

The electronic wave functions used in this work are as follows:

$$\Phi(X^1\Sigma_g^+; \; s=m=o) = [1\sigma_g\alpha(1) \; 1\sigma_g\beta(2)] \; ,$$

$$\Phi(B^1\Sigma_u^+; \; s=m=o) = \sqrt{\tfrac{1}{2}} \; \{1\sigma_g\alpha(1) \; 1\sigma_u\beta(2)] - [1\sigma_g\beta(1) \; 1\sigma_u\alpha(2)]\},$$

$$\Phi(a^3\Sigma_g^+; \; s=1,m=o) = \sqrt{\tfrac{1}{2}}\{[1\sigma_g\alpha(1) \; 2\sigma_g\beta(2)] + [1\sigma_g\beta(1) \; 2\sigma_g\alpha(2)]\}, \tag{30}$$

$$\Phi(a^3\Sigma_g^+; \; s=m=1) = [1\sigma_g\alpha(1) \; 2\sigma_g\alpha(2)] \; ,$$

and similarly for $b^3\Sigma_u^+$, $e^3\Sigma_u^+$, and $c^3\Pi_u$ ($\lambda=\pm1$) states with $2\sigma_g$ replaced respectively by $1\sigma_u$, $2\sigma_u$, and $1\pi_u$ ($\lambda=\pm1$) orbitals. Here, we used the brackets to represent the normalized determinants. The detailed form of the molecular orbitals will be given later. The threshold energies of these states are listed in Table I, which should be viewed in the context of FC approximation. Let us consider a process in which an incident electron ($s=m_s=\frac{1}{2}$) impinges upon an H_2 molecule in the ground state ($s=m_s=o$). Consistent with this, we construct basis functions as in Eq. (4), which are spin-eigenfunctions of $S=M=\frac{1}{2}$ with $N=2$. For example, with the $X^1\Sigma_g^+$ state we have

$$\psi_{X\lambda\ell s}^{SM\Lambda}(X^{-3}) = Y_{\ell,\Lambda-\lambda}(\hat{r}_3)\alpha(3)\Phi(X^1\Sigma_g^+; \; s=m=o), \tag{31}$$

and likewise for the $B^1\Sigma_u^+$ state. In the case of $a^3\Sigma_g^+$ we write

$$\psi_{a\lambda\ell S}^{SM\Lambda}(X^{-3}) = Y_{\ell,\Lambda-\lambda}(\hat{r}_3) \{\sqrt{\tfrac{2}{3}}\,\beta(3)\phi(a^3\Sigma_g^+;\ s=m=1)$$

$$-\sqrt{\tfrac{1}{3}}\alpha(3)\phi(a^3\Sigma_g^+;\ s=1,\ m=o)\}. \tag{32}$$

The basis functions associated with other triplet states are obtained similarly. With these explicit expressions [Eqs. (30)-(32)], the potentials [Eqs. (16), (17)] may be reduced to the following:

$$U_{\mu\mu'}(r) = \delta_{s,s'}[V_{n\lambda\ell s,n'\lambda'\ell's'}^N(r) + V_{n\lambda\ell s,n'\lambda'\ell's'}^e(r)], \tag{33}$$

where

$$V_{n\lambda\ell s,n'\lambda'\ell's'}^N(r) = -\delta_{(n\lambda),(n'\lambda')} \int d\hat{r}\, Y_{\ell,\Lambda-\lambda}^*(\hat{r})\, Y_{\ell',\Lambda-\lambda'}(\hat{r})$$

$$\times \{|\vec{r}_A-\vec{r}|^{-1} + |\vec{r}_B-\vec{r}|^{-1}\}, \tag{34}$$

and

$$V_{n\lambda\ell s,n'\lambda'\ell's'}^e(r) = \int d\hat{r}\, Y_{\ell,\Lambda-\lambda}^*(\hat{r})\, Y_{\ell',\Lambda-\lambda'}(\hat{r})$$

$$\times \Sigma_j\, f_j\, \int \phi_j^*(\vec{r}')\, |\vec{r}-\vec{r}'|^{-1}\phi_j'(\vec{r}')\, d\vec{r}'. \tag{35}$$

The Kronecker delta in Eq. (33) restricts the direct-coupling potentials to those between channels belonging to electronic states of same spin, with the obvious consequence that a singlet-to-triplet excitation is achieved only through electron-exchange. The potential due to the nuclear charge V^N is diagonal in electronic states as shown in Eq. (34). The part due to the molecular electrons V^e is a sum of integrals involving one-electron molecular orbitals (MO) ϕ_j, ϕ_j' with numerical factors f_j. Analogous to this, we find

$$W_{\mu\mu'}(r)F_{\mu'\mu''}(r) = -\Sigma_j \, g_j \int \phi_j^*(\vec{r}')Y_{\ell',\Lambda-\lambda'}(\hat{r}') \, |\vec{r}-\vec{r}'|^{-1}$$

$$\times \, \phi_j^!(\vec{r}) \, Y_{\ell,\Lambda-\lambda}^*(\hat{r}) \, (rr')^{-1}F_{\mu'\mu''}(r') \, d\hat{r} \, d\vec{r}' \; . \tag{36}$$

For convenience we use short-hand notations

$$(\phi_j^! \, , \phi_j) \equiv \int \phi_j^*(\vec{r}') \, |\vec{r}-\vec{r}'|^{-1}\phi_j^!(\vec{r}')d\vec{r}' \; , \tag{37}$$

$$\{\phi_j^! \, , \phi_j\} \equiv \int \phi_j^*(\vec{r}') \, Y_{\ell',\Lambda-\lambda'}(\hat{r}') \, |\vec{r}-\vec{r}'|^{-1}$$

$$\times \, \phi_j^!(\vec{r}) \, Y_{\ell,\Lambda-\lambda}^*(\hat{r}) \, (rr')^{-1}F_{\mu'\mu''}(r') \, d\hat{r} \, d\vec{r}' \; . \tag{38}$$

We display in Tables II-IV the coupling potentials between channels with respect to the electronic states to which they belong.

In order to express these potentials more explicitly we use the following well-known expansions, with the origin of the coordinate system chosen at the center of homonuclear diatomic molecule as shown in Fig. 1. That is,

$$|\vec{r}_A-\vec{r}|^{-1} = \frac{1}{R_>} \, \Sigma_K (\frac{4\pi}{2K+1})^{\frac{1}{2}}(\frac{R_<}{R_>})^K \, Y_{K,0}(\hat{r}) \; , \tag{39}$$

$$|\vec{r}_B-\vec{r}|^{-1} = \frac{1}{R_>} \, \Sigma_K (-1)^K \, (\frac{4\pi}{2K+1})^{\frac{1}{2}}(\frac{R_<}{R_>})^K \, Y_{K,0}(\hat{r}) \; , \tag{40}$$

$$|\vec{r}-\vec{r}'|^{-1} = \frac{1}{r_>} \, \Sigma_K \, (\frac{4\pi}{2K+1}) \, (\frac{r_<}{r_>})^K \, \Sigma_m \, Y_{K,m}^*(\hat{r}')Y_{K,m}(\hat{r}), \tag{41}$$

where $R_>$ and $R_<$ stand for the greater or lesser of r and (R/2), and $r_>$ and $r_<$ for greater or lesser of r and r'. With these expansions we find

$$V_{n\lambda\ell s,n'\lambda'\ell's'}^N(r) = -\delta_{(n\lambda),(n'\lambda')}(\frac{2}{R_>}) \, \sum_{K=|\ell-\ell'|}^{\ell+\ell'} \, {}^{(K=even)}$$

$$\times \, c^K(\ell'\Lambda-\lambda',\ell\Lambda-\lambda) \, (\frac{R_<}{R_>})^K \; , \tag{42}$$

$$V^e_{n\lambda\ell s,n'\ell'\ell's'}(r) = \Sigma_j \, f_j \sum_{K=|\ell-\ell'|}^{\ell+\ell'} c^K(\ell'\Lambda-\lambda', \ell\Lambda-\lambda)$$

$$\times \, y_K(\phi_j,\phi_j'|r),$$

(43)

where we used the notation of Condon and Shortley,[28] i.e.,

$$c^K(\ell'm'\ell m) = [\frac{4\pi}{2K+1}]^{\frac{1}{2}} \int d\hat{r} \, Y^*_{\ell m}(r) Y_{K,\bar{m}-m'}(r) Y_{\ell'm'}(\hat{r}),$$

(44)

and the y_K function is

$$y_K(\phi_j,\phi_j'|r) = (-1)^{\lambda_j'-\lambda_j} [\frac{4\pi}{2K+1}]^{\frac{1}{2}} \int \phi_j^*(n_j\lambda_j|\vec{r}')$$

$$\times \, Y_{K,\lambda_j-\lambda_j'}(\hat{r}) \, (\frac{1}{r_>})(\frac{r_<}{r_>})^K \phi_j' \, (n_j' \, \lambda_j' \, |\vec{r}')d\vec{r}'$$

$$= (-1)^{\lambda_j'-\lambda_j}[\frac{4\pi}{2K+1}]^{\frac{1}{2}}[\{r^{-K-1}\int_0^r r'^K r'^2 dr' + r^K \int_r^\infty r'^{-K-1}r'^2 dr'\}$$

$$\times \, \{\int d\hat{r}' \, \phi_j^*(n_j\lambda_j|\vec{r}') \, Y_{K,\lambda_j-\lambda_j'}(\hat{r}')\phi_j' \, (n_j' \, \lambda_j' \, |\vec{r}')\}],$$

(45)

where λ_j is the angular momentum along the molecular axis of a <u>molecular orbital</u> ϕ_j. Similarly,

$$W_{\mu\mu'}(r) \, F_{\mu'\mu''}(r) = -\Sigma_j g_j \, \Sigma_{K,g} \, (\frac{4\pi}{2K+1}) \, r \int d\hat{r} \, Y^*_{Kg}(\hat{r}) \, Y^*_{\ell,\Lambda-\lambda} \, (\hat{r})$$

$$\times \, \phi_j'(\vec{r})[\{r^{-K-1} \int_0^r r'^K \, F_{\mu'\mu''}(r') \, dr' + r^K \int_r^\infty r'^{-K-1}F_{\mu'\mu''}(r')dr'\}$$

$$\times \, r' \int d\hat{r}' \, Y_{Kg}(\hat{r}') \, Y_{\ell',\Lambda-\lambda}(\hat{r}')\phi_j^*(\vec{r}') \,].$$

(46)

To simplify this we use the relation

$$Y_{\ell_1 m_1}(\hat{r})Y_{\ell_2 m_2}(\hat{r}) = \sum_{L=|\ell_1-\ell_2|}^{\ell_1+\ell_2} [\frac{(2\ell_1+1)(2\ell_2+1)}{4\pi(2L+1)}]^{\frac{1}{2}} C(\ell_1\ell_2 m_1 m_2|L \, M=m_1+m_2)$$

$$\times \, C(\ell_1\ell_2 00|L0) \, Y_{LM}(\hat{r}),$$

(47)

and define a function Z_K, viz.,

$$Z_K(\phi_j \ell m | r) = \left[\frac{4\pi}{2K+1}\right]^{\frac{1}{2}} r \int d\hat{r} \, Y_{Kg}(\hat{r}) \, Y_{\ell m}(\hat{r}) \phi_j^*(\vec{r})$$

$$= r \sum_{L=|K-\ell|}^{K+\ell} \left[\frac{2\ell+1}{2L+1}\right]^{\frac{1}{2}} C(K\ell g m | LM) \, C(K\ell 00 | L0)$$

$$\times \int d\hat{r} \, Y_{LM}(\hat{r}) \phi_j^*(n_j \lambda_j | \vec{r}) \, . \tag{48}$$

The last integral in the above equation restricts $M = \lambda_j$, which in turn sets $g = \lambda_j - m$ so that the summation over g is merely formal in Eq. (46). Combining Eqs. (47) and (48) into (46), we find

$$W_{\mu\mu'}(r) F_{\mu'\mu''}(r) = -\Sigma_j g_j \, \Sigma_K \, Z_K^*(\phi_j' \ell \, \Lambda - \lambda \, | r)$$

$$\times [\{r^{-K-1} \int_0^r r'^K F_{\mu'\mu''}(r') dr' + r^K \int_r^\infty r'^{-K-1} F_{\mu'\mu''}(r') dr'\}$$

$$\times Z_K(\phi_j \ell' \Lambda - \lambda' | r')] . \tag{49}$$

We note that the parameter K in Eqs. (42) and (43) and L in Eq. (48) are limited to a finite number of values so that those series [Eqs. (42), (43), and (48)] can be summed without any omission as indeed done in this work. The exception to this occurs in Eq. (49) with regard to K, where K has no upper limit. As a practical matter this infinite series must be truncated, and we found it sufficient to retain the three leading terms in this work.

IV. METHOD OF COMPUTATION

In the usual approach of expressing the molecular orbitals (MO) by linear combinations of atomic orbitals (LCAO), the molecular wave functions are centered around the two nuclei. The greatest (if not the only) difficulty with an electron-molecule calculation arises from this two-center nature of molecular function, the consequence of which needs no elaboration here. In this section we develop a computational technique suitable for the potentials by exploiting the advantages offered by the Gaussian-type orbitals (GTO).

To begin with, we define Gaussian functions centered at A and B with exponents a, b, (see Fig. 2),

$$G(a,A) \equiv \exp\{-a[(x-A_x)^2 + (y-A_y)^2 + (z-A_z)^2]\}$$

$$= \exp\{-a(\frac{R^2}{4} + r^2 + Rr\cos\theta)\} \tag{50}$$

$$G(b,B) = \exp\{-b(\frac{R^2}{4} + r^2 - Rr\cos\theta)\}, \tag{51}$$

The Gaussians shown above are known as s-type, from which p_z-, p_x-, and p_y-type GTO can be derived, i.e.,

$$G_{p_z}(a,A) = (z-A_z) G(a,A) = (r\cos\theta - \frac{R}{2}) G(a,A),$$

$$G_{p_x}(a,A) = (x-A_x) G(a,A) = r\sin\theta\cos\phi \, G(a,A), \text{ etc.} \tag{52}$$

Crucial to our computational procedure is the fact that the exponent in Eq. (50) is _rational_; in contrast, for the Slater-type orbitals (STO) the exponent would be _irrational_. In terms of these Gaussian functions, the one-electron molecular orbitals appearing in Eq. (30) are expressed as

$$\phi_{\sigma_g, \sigma_u} = \sum_{i=1}^{6} c_i \{G(a_i, A) \pm G(a_i, B)\}$$

$$+ \sum_{j=7}^{10} c_i \{(r\cos\theta - \frac{R}{2})G(a_j, A) \mp (r\cos\theta + \frac{R}{2}) G(a_j, B)\}, \tag{53}$$

with σ_g and σ_u taking the upper and lower signs respectively, and

$$\phi_{\pi_u} = e^{\pm i\phi} \sum_{j=7}^{10} c_j \, r\sin\theta \, \{G(a_j, A) + G(a_j, B)\}. \tag{54}$$

The expansion coefficients c's are determined by the self-consistent-field (SCF) calculations for each of the $X^1\Sigma_g^+$, $B^1\Sigma_u^+$, $a^3\Sigma_g^+$, $b^3\Sigma_u^+$, $c^3\Pi_u$, and $e^3\Sigma_u^+$ states at $R = 0.74$ Å corresponding to the equilibrium separation of the ground state $(X^1\Sigma_g^+)$. These coefficients are listed in Table V along with the corresponding exponents of six s-type and four p-type Gaussians.[29] The general procedure of SCF calculation is discussed in the literature.[30] In case of $(1\sigma_g)(2\sigma_u)e^3\Sigma_u^+$ which is the second lowest state of this symmetry, the SCF procedure is applied to the second lowest root of the secular equation; the $2\sigma_u$ orbital so obtained is found to be orthogonal to the $1\sigma_u$ orbital of the $(1\sigma_g)(1\sigma_u)b^3\Sigma_u^+$ state. In all cases the orbital coefficients are converged within 10^{-5}.

A. Coupling Potentials

With a substitution of Eqs. (53) and (54), reduction of the last integral in Eq. (48) becomes possible. For example, we have

$$\int d\hat{r}\, Y_{LM}(\hat{r}) \phi_{\pi_u}^*(\lambda_j = 1 | \vec{r})$$

$$= \frac{1}{\sqrt{2\pi}} \int_0^{2\pi} d\phi\, e^{i(M-1)\phi} \times \Sigma_i\, c_i\, \exp\{-a(\frac{R^2}{4} + r^2)\}$$

$$\times \int_0^\pi \sin\theta d\theta [\Theta_{LM}(\cos\theta, \sin\theta) r\sin\theta][\exp(-a_i R\, r\cos\theta) + \exp(a_i R r\cos\theta)], \tag{55}$$

and similarly with other MO. Thus, a typical θ-integral has the form of

$$\int_0^\pi \sin\theta d\theta\, \Theta_{LM}(\cos\theta, \sin\theta)\, f(\cos\theta, \sin\theta)\, \exp(\gamma r\cos\theta), \quad \gamma = \pm aR. \tag{56}$$

In practice the products $\Theta_{LM}(\cos\theta, \sin\theta) x f(\cos\theta, \sin\theta)$ always turn out to be an even function of sine $(\sin^{2n}\theta)$ so that we have to deal only with the following integral.

$$\int_0^\pi \sin\theta d\theta\, \cos^n\theta\, e^{x\cos\theta} = P_n(x) e^{-x} + Q_n(x) e^x, \tag{57}$$

where

$$P_n(x) = (-1)^{n+1} \sum_{m=0}^n \frac{n!}{(n-m)!\, x^{m+1}},$$

and

$$Q_n(x) = (-1)^n P_n(-x). \tag{58}$$

The angular integrations for y_K function in Eq. (45) are performed in a similar manner; the only difference is that there are two MO in the integrand so that the number of terms are increased. However, the form remains the same.

Thus, with the angular integration completed, r-integration is carried out numerically by Simpson's rule for y_K function in Eq. (45). From this V^e are assembled in accordance with Eq. (43), and subsequently by combining V^e and V^N, we obtain $U_{\mu\mu'}(r)$ in Eq. (33) in a tabular form from r=0 to $31a_o$, beyond which $U_{\mu\mu'}(r)$ are fitted to a two term asymptotic form, i.e.,

$$U_{\mu\mu'}(r) = \frac{a}{r^k} + \frac{b}{r^{k+2}} \ . \tag{59}$$

This curve-fitting is based on 50 data points between $r=31$ and $41a_o$ with a maximum error of 0.1% for the worst case. For numerical integration we start with a mesh-size $\delta r=0.0125a_o$ and double it after every 80 quadrature points until $\delta r=0.1a_o$ is reached as shown in Table VI. This quadrature scheme is common to all numerical procedures, i.e., with y_K, Z_K, and the scattered wave F_{ij} of the next subsection, so that the potentials are fed into the scattering equation as they were calculated without further manipulations, except the asymtotic fitting of $U_{\mu\mu'}$, described above.

Similarly, the Z_K functions are tabulated as prescribed by Eq. (48) from $r=0$ to a suitable cut-off value r_{cut}, beyond which the exchange potentials are set to zero. The effective range of exchange is expected to be roughly the extent of the molecular orbitals. In our test calculations we found no appreciable difference (less than 0.2%) in cross sections when we used $r_{cut} = 20, 25,$ and $31a_o$. For the sake of safety, however, we settled on $r_{cut} = 25a_o$, accepting the waste of "overkill."

To ascertain the effect of truncation in the summation over K of Eq. (49), we performed test-calculations with the $b^3\Sigma_u^+$ state at $E = 15$ eV by retaining one, three, and five Z_K terms in Eq. (49). With five Z_K terms, the partial cross sections for $\Lambda = 0$ are .01807, $.1204 \times 10^{-3}$, $.1473 \times 10^{-6}$ a_o^2 respectively for $(\ell,\ell') = (0,1), (2,3),$ and $(4,5)$ as shown in Table VII. The corresponding partial cross sections with three Z_K terms are 0.01810, $.1210 \times 10^{-3}$, and $.1141 \times 10^{-6}$, and with one term, they are .01829, $.1816 \times 10^{-4}$, and $.2725 \times 10^{-10}$. The difference between the three- and five-term results is quite negligible with respect to both the partial cross sections and the total cross section. With regard to the one-term calculation, the larger discrepancy in the (2,3) and (4,5) partial cross sections over the (0,1) may be understood

in the following way. Namely, the last integral of Eq. (48) is nothing but a decomposition of MO ϕ_j by angular momentum, i.e.,

$$\phi_{j,L}(n_j\lambda_j|r) = \int d\hat{r} \, Y_{L,M}(\hat{r}) \phi_j^*(n_j\lambda_j|\vec{r}) \ . \tag{60}$$

For the MO's of H_2 considered here, we find that the largest concentrations are in $\phi_{1\sigma_g},0$ and $\phi_{1\sigma_u},1$ etc. over other higher angular-momentum components. These large components will enter into the summation of Eq. (48) only if $K = \ell, \ell \pm 1$ so that, viewed from this point, $Z_{K=\ell}$ and $Z_{K=\ell\pm1}$ are important terms. In the above example with only $Z_{K=0}$ term, other important terms $Z_{K=2}$ and $Z_{K=4}$ are not taken into account, and this omission may explain the unsatisfactory results for $(\ell,\ell') = (2,3)$ and $(4,5)$. Since these higher partial waves contribute much less to the total cross section than the lower ones, the net effect on the total cross section is merely 0.5% in this case even with only one Z_K term. We expect some minor fluctuations in this discrepancy (0.5%) as we change the incident-electron energy, and consider different electronic states. Therefore, in order to leave ample margin of safety to cover such variations, we decided to retain three leading, non-vanishing Z_K terms in Eq. (49) (e.g., K=0,2,4; 1,3,5; or 2,4,6, etc.) with $K \leq 9$ in all succeeding calculations presented in this report.

B. Scattering equations

For the purpose of discussion here, we re-write the integro-differential equations in Eq. (15) as follows

$$[\frac{d^2}{dr^2} - \frac{\ell_i(\ell_i+1)}{r^2} + k_i^2] \, F_{ij}(r) = 2 \sum_n [U_{in}(r) + W_{in}(r)] F_{nj}(r)$$

$$+ \sum_J(\text{orbital}) \sum_{\ell(J)} \delta_{\ell,\ell_i} \delta_{\lambda_J,(\Lambda-\lambda_i)} \, M_{J\lambda_J,\ell}^{ij} \phi_{J,\ell}(n_J\lambda_J|r), \tag{61}$$

where we used i,j for the scattering and incident channels respectively. The summation J is over the molecular orbitals, and $\ell(J)$ covers even or odd values as dictated by the orbital $(J\lambda_J)$.

Once the $U(r)$, $W(r)$, and $\phi_{J,\ell}(r)$ are made available, the procedure of solution becomes quite analogous to atomic case. We solve this set of integro-differential equations by the noniterative integral equation method (NIEM).[15] Here, we give just a brief description of NIEM as applied to our problem, while the readers are referred to the paper by Smith and Henry[15] for details. We expect two sets of arbitrary constants which are to be determined by the boundary conditions. For the moment we look for the solutions $\psi_{ij}(r)$ of Eq. (61) without regard to boundary conditions, in place of $F_{ij}(r)$ which satisfy the boundary conditions. By means of the Green's-function technique, the solution can be expressed in an integral representation, i.e.,

$$\psi_{ij}(r) = \delta_{ij} G_i^{(1)}(k_i r) + 2 \int_0^r dx\, G_i^{(2,1)}(r|x) \{ \Sigma_n U_{in}(x) \psi_{nj}(x)$$

$$- \Sigma_n \Sigma_{p(in)} g_p \Sigma_K [Z_K(\phi_{p(n)}^* \ell_n \Lambda - \lambda_n | x)$$

$$\times (x^{-K-1} \int_0^x y^K dy - x^K \int_0^x y^{-K-1} dy + x^K \int_0^\infty y^{-K-1} dy)$$

$$\times Z_K(\phi_{p(i)} \ell_i \Lambda - \lambda_i | y)\, \psi_{nj}(y)]$$

$$+ \Sigma_J \Sigma_{\ell(J)}\, \delta_{\ell,\ell_i}\, \delta_{\lambda_J,(\Lambda-\lambda_i)}\, M_{J\lambda_J\ell}^{ij}\, \phi_{J,\ell}(n_J\lambda_J | x) \}, \tag{62}$$

with

$$G_i^{(1)}(k_i r) = k_i^{\frac{1}{2}} r\, j_{\ell_i}(k_i r),$$

$$G_i^{(2)}(k_i r) = k_i^{\frac{1}{2}} r\, y_{\ell_i}(k_i r), \tag{63}$$

$$G_i^{(2,1)}(r|x) = G_i^{(2)}(k_i r) G^{(1)}(k_i x) - G_i^{(1)}(k_i r)\, G_i^{(2)}(k_i x),$$

where j_ℓ and y_ℓ are the spherical Bessel functions of the first and second kind respectively. In Eq. (62) the summation $\Sigma_{p(in)}$ indicates the pair of MO $\phi_{p(n)}$ and $\phi_{p(i)}$ appearing in the two Z_K-functions are dictated by the electronic states to which channels i and n belong. Eq. (62) above corresponds to Eq. (12) of the paper by Smith and Henry. As they point out, the right-side of Eq. (62) are known except the Lagrangian multiplier M and the term,

$$\int_0^\infty y^{-K-1} \, Z_K(\phi_{p(i)} \, \ell_i \, \Lambda-\lambda_i|y)\psi_{nj}(y)dy. \tag{64}$$

Since Eq. (61) is linear in ψ_{ij}, it is possible to treat these unknown terms as inhomogeneity, and seek the complete solutions as appropriate linear combinations of the homogeneous and particular solutions. There is no point in attempting to reproduce their elegant treatment[15] here. We might note in passing that with K and p(in) each taking three distinct values and nine channels, this amounts to in excess of 80 inhomogeneities including the orthogonality terms. However, all particular integrals as well as homogeneous solutions are processed simultaneously in the actual computation.

From the solutions $\psi_{ij}(r)$ the scattering matrix may be determined as follows. For large distance r, we may write

$$\psi_{ij}(r) \sim k_i^{-\frac{1}{2}}[\sin(k_i r-\tfrac{1}{2}\ell_i \pi) \, A_{ij} + \cos(k_i r-\tfrac{1}{2}\ell_i \pi)B_{ij}] \, , \tag{65}$$

where we used the asymtotic form of the spherical Bessel functions j_ℓ and y_ℓ, and $\underline{A}$ and $\underline{B}$ are constant matrices to be determined. On the other hand the required asymtotic form is

$$F_{ij}(r) \sim k_i^{-\frac{1}{2}}[\sin(k_i r-\tfrac{1}{2}\ell_i \pi) \, \delta_{ij} + \cos(k_i r-\tfrac{1}{2}\ell_i \pi)R_{ij}] \, . \tag{66}$$

Therefore,

$$\underline{R} = \underline{B}\underline{A}^{-1}, \tag{67}$$

and

$$\underline{S} = (\underline{1} + i\underline{R})(\underline{1} - i\underline{R})^{-1}. \tag{68}$$

$\underline{A}$ and $\underline{B}$ matrices are determined numerically by matching $\psi_{ij}(r)$ at two adjacent points r_M and $r_M + \delta r$, that is, by setting up two simultaneous matrix equations for the two unknown matrices $\underline{A}$ and $\underline{B}$. In practice we chose $r_M = 31$ and $45a_o$ for the triplet cases, and $r_M = 45$, 55, and $65a_o$ for the $B^1\Sigma_u^+$ state to observe the proper convergence of $\underline{R}$ matrix.

V. RESULTS AND DISCUSSION

We present the cross sections of the triplet states and the $B^1\Sigma_u^+$
state separately, as the two cases differ in treatment as well as in the
energy-range of interest.

A. Excitation to Triplet States

The cross sections of the triplet states have been calculated by including
partial waves $(\ell\ell') \leq 5$, and $\Lambda=0,1,2,3$ at several incident-electron energies.
Typical breakdown of cross sections by $(\ell\ell')$ at two different energies are
shown in Tables VII and VIII. First, we note that the partial cross sections
$Q^\Lambda(\ell,\ell')$ are much larger when $\Delta\ell=(\ell-\ell')=\pm1$ than others. This is reminiscent
of the dipole-selection rule applied to atomic excitation, in which cross
sections are again found to be largest when $\Delta\ell=\pm1$. Next, for a given sequence
of $\Delta\ell$, $Q^\Lambda(\ell,\ell')$ decreases with increasing $(\ell\ell')$, although the effectiveness
of large partial waves lingers on longer at high (40 eV) energy. There is no
surprise here; the present results merely conforms to the long-held view that
only the low partial waves are effective at low incident-electron energies.
In Table IX we show the breakdown of cross sections in terms of Λ, i.e.,

$$Q^\Lambda = \Sigma_{\ell\ell'} \, Q^\Lambda(\ell,\ell'). \tag{69}$$

Since $Q^{\Lambda=\pm n}$ are identical there is no need to repeat calculations with negative
values of Λ. The decreasing trend of Q^Λ with increasing Λ is assured by the
foregoing discussion as the low partial waves $Y_{\ell,\Lambda-\lambda}$ are eliminated with
increasing Λ. Overall, it is evident from these tables that we have included
sufficient number of partial waves even at the highest energy (40 eV) con-
sidered in this report. We found a similar pattern in the partial cross
sections with other triplet states. The total cross sections of the four

triplet states are presented in Table X. We also included in this table
cross sections by other theoretical calculations for comparison. There are
some unexpected features as well as predictable ones in the excitation
functions of these states. We now discuss these points as we compare the
present close-coupling (CC) results with other theoretical calculations.

1. $b^3\Sigma_u^+$ and $e^3\Sigma_u^+$

The lowest excited state $b^3\Sigma_u^+$ is a repulsive state, which dissociates
into two H(1s) atoms. The cross sections of this state are shown in Fig. 3.
We have previously calculated these cross sections by using the Born-Rudge
approximation,[3] they are included in Fig. 3 for comparison. The wave functions
used there[3] are identical to those employed in the present work. These
Born-Rudge (BR) cross sections are in an essential agreement with the earlier
calculation of similar nature by Cartwright and Kuppermann.[4] A difference of
about 20% in magnitude was attributed to the usage of different wave functions.

Comparison of the present CC and the BR calculations shows that the former
gives an appreciably broader excitation function and much smaller ($\sim$30%)
cross sections below 20 eV. However, these two sets are in good agreement
above 20 eV. We will not discuss the Born-type calculations of still earlier
days[7,8] as the works described in Refs. 3 and 4 are representative of the
Born-type calculations. Recently, Rescigno et al.[11] calculated cross sections
of the $b^3\Sigma_u^+$ state by means of the distorted-wave approximation with random-
phase approximation (DW-RPA) to compute the inelastic transition density.
Their results are shown in Table X and also in Fig. 3. (In this figure
the magnitude of their cross sections are reduced by a factor of two). These
authors[11] attempt to account for the distortion of the incident electron by
means of the Coulomb and exchange operators for the molecule in the ground state.

The same operators are used for the distortion of the scattered electron instead of the operators appropriate for the excited state. They justify this procedure based on the previous application of DW-RPA to electron-atom cases.[31] Beside this point, it is difficult to assess to what extent the static distortion in DW-RPA can represent the dynamic process. At any rate, their excitation function is rather similar to the BR calculation cited above, except the magnitude is about twice as large.

In drastic contrast to the $b^3\Sigma_u^+$ state, the excitation function of the $e^3\Sigma_u^+$ state shows an extremely sharp peak as shown in Fig. 4, even though these two states are of same symmetry type. In fact with the threshold energy of 13.22 eV, we found no decreasing trend in cross section as the incident-electron energy is reduced as low as 14 eV. Compared with these CC results, the BR cross sections[3] are much smaller (factor of four) near the threshold, but the difference becomes smaller at high incident energy ($\sim$20% at 40 eV).

The large difference in shape between the excitation functions of $b^3\Sigma_u^+$ and $e^3\Sigma_u^+$ found here, which is not revealed in the Born-Rudge calculation, is somewhat puzzling. One possible explanation is as follows: a singlet-triplet excitation involves an exchange between the colliding electron and a molecular electron. Its cross sections decrease drastically with energy if the colliding electron is found in the vicinity of the target for less than a certain critical time which may be viewed as the range of interaction divided by the velocity of the colliding electron. The $e^3\Sigma_u^+$ state has both electrons in bonding orbitals whereas $b^3\Sigma_u^+$ involves one antibonding orbital. Thus the $b^3\Sigma_u^+$ state has a more diffuse electron density distribution, hence a larger range of interaction. This may account for the fact that the decline in the $b^3\Sigma_u^+$ excitation function sets in at a higher energy. On the other hand when

the Born-Ochkur approximation is used, the $1/k^4$ factor (k being the wave vector) in the scattering-matrix element gives such a steep energy dependence that it obscures the difference in the range of interaction.

2. $a^3\Sigma_g^+$ and $c^3\Pi_u$

Fig. 5 shows the cross sections of $a^3\Sigma_g^+$ computed by the close-coupling, the Born-Rudge approximations,[3] and DW-RPA.[11] The difference in shape of excitation function is not too severe for $a^3\Sigma_g^+$ between CC and BR calculations. Again, we see a large difference in magnitude at low energy ($\sim$40% at 15 eV) but a better agreement at high energy ($\sim$20% at 40 eV). The cross sections by DW-RPA are much larger than CC results ($\sim$50%). However, the shift in the position of peak may well be due to the different values of threshold energy used in the calculations.

The cross sections of $c^3\Pi_u$ presented in this paper are based on the three-state close-coupling calculations technically, as we included the $X^1\Sigma_g^+$ and $c^3\Pi_u(\lambda=\pm1)$ states in the scattering equation. However, at one energy (15 eV) we also performed a two-state calculation, from which we obtained a cross section of 5.95×10^{-17} cm^2 as compared with 5.63×10^{-17} cm^2 from the three-state calculation. The slight difference (6%) indicates that the mutual interactions between channels belonging to the $c^3\Pi_u(\lambda=+1)$ and $c^3\Pi_u(\lambda=-1)$ states have no great effect on the cross sections. The results of $c^3\Pi_u$ cross sections by CC and BR are compared in Fig. 6. Here, the discrepancy is mainly on the magnitude of cross sections. The BR cross sections[3] are much smaller than the CC counterpart. Although the discrepancy diminishes with increasing of incident-electron energy, the BR cross section is only one-half of the CC cross section even at 40 eV. We can offer no particular reason for this discrepancy beyond the inadequacy of the Born-type approximation already discussed.

3. Comparison with Experimental Dissociation Cross Sections

The formation of two H(1s) atoms by electron impact on H_2 arises from direct excitation of $b^3\Sigma_u^+$ and from excitation of other triplet states followed by cascade to $b^3\Sigma_u^+$. It has been shown in Ref. 3 that $a^3\Sigma_g^+$ and $c^3\Pi_u$ are the two major cascading states to $b^3\Sigma_u^+$ and that $e^3\Sigma_u^+$ and $d^3\Pi_u$ play only minor roles. Thus we take the sum of the cross sections of $b^3\Sigma_u^+$, $a^3\Sigma_g^+$, $c^3\Pi_u$, and $e^3\Sigma_u^+$ as the theoretical cross sections for the dissociation process $H_2 \xrightarrow{e} H(1s) + H(1s)$ which are shown in Fig. 7. Experimentally Corrigan[32] has obtained dissociation cross sections (via the excited states of the neutral H_2 molecule) which cover the formation of the excited-state H(nℓ) atoms as well as H(1s). In Ref. 3 efforts were made to subtract from Corrigan's data the experimental cross sections for producing the excited-states atoms. The "corrected" experimental data given in Ref. 3 correspond to the formation of two H(1s) atoms and are reproduced in Fig. 7 for comparison with the theoretical values. The agreement is seen to be quite good. However, it must be cautioned that there is a considerable uncertainty in Corrigan's data (see Fig. 2 of Ref. 32) especially at the high-energy side. The close agreement between theory and experiment, therefore, should not be regarded as having much quantitative significance.

4. Summary

With a limited number of case studies made here, only a tentative conclusion can be drawn on the performance of the Born-type approximations. Nevertheless, we see a pattern emerging. First, at a moderate energy (say 20 eV or above) of incident electron the agreement between CC and BR results is reasonable in most cases. While this comparison reaffirms that the Born-types are basically "high-energy" approximations, it also puts a limit of their applicability on a more quantitative basis as well. The other is much

more serious, that is, at low energy the discrepancy is not only large, neither does it appear to follow any clear trend. We can say neither BR overestimates, nor underestimates cross sections since the details of the exchange-potential, which must reflect the characteristics of electronic states involved, are lost amid the approximate procedures leading to the Born-Rudge or Born-Ochkur method. Indeed, the present close-coupling calculation shows that the shape of excitation functions is not alike for all triplet states whereas a much higher uniformity was seen from the BR results.

B. Excitation to the $B^1\Sigma_u^+$ state

As described in Sec. III-A, our close-coupling calculation for the $X^1\Sigma_g^+ \rightarrow B^1\Sigma_u^+$ excitation has been carried out with the aid of a parallel partial-wave analyses of the Born approximation. The essential assumption made in Sec. III-A was that for large (ℓ,ℓ')

$$Q^{(CC)}(\ell,\ell') \simeq Q^{(Born)}(\ell,\ell') , \tag{70}$$

with

$$Q(\ell,\ell') = \Sigma_\Lambda \ Q^\Lambda(\ell,\ell') . \tag{71}$$

In order to discuss how this assumption may affect the total excitation cross sections, we display in Tables XI and XII the partial cross sections of Eq. (71) summed over $\Lambda = -6$ to $+6$ at the incident-electron energies of 25 and 100 eV. In addition to the Born and CC cross sections, we also included in these tables a set of cross sections calculated by the close-coupling method without the electron-exchange (CCNE). It is evident from these tables that the partial cross sections $Q(\ell,\ell')$ of the singlet state do not decrease with increasing ℓ as rapidly as the triplet counterparts. This is due to the presence of the long-range direct potentials in the singlet-singlet excitation - hence the necessity of a special treatment referred to above. We show in Tables XI and XII

the $Q(\ell,\ell'=\ell-1)$ and $Q(\ell,\ell'=\ell+1)$ sequences only, since their contributions

to the total cross sections are about 90% and 10% respectively. For the

sequence $\ell'=\ell-1$, the three sets of partial cross sections merge to one another;

for example, within 4% at the last entry ($\ell=7$). Furthermore, this error will

affect only the fraction $(\ell,\ell'\geq 7)$ of the total cross section so that the net

effect on the total cross section is expected to be much smaller. As to the

$\ell'=\ell+1$ sequence, the convergence is not as good as $\ell'=\ell-1$ sequence. However,

the entire $Q(\ell,\ell'=\ell+1)$ sequence occupies only 10% of the total, so that any

error there will be scaled down by a factor of 10. Therefore, we estimate that

the total error incurred by our procedure does not exceed 5% or so at 100 eV,

and smaller yet at lower energies of incident electron. The important point

to note here is that the difference between the Born and CC calculations

manifests mainly in the partial cross sections of small ℓ as shown in Tables XI and

XII   so that the partial cross sections of large ℓ may be computed by either

method without incurring much error. Therefore, we replace $Q^{(CC)}(\ell,\ell')$ by

$Q^{(Born)}(\ell,\ell')$ for $(\ell,\ell')>7$ as prescribed by Eq. (29) to obtain the total CC

cross sections. The total cross sections by CCNE are obtained in a similar

manner.

These total cross sections are shown in Table XIII and in Fig. 8. For

comparison we also calculated the cross sections of this state by using the

Born-Ochkur approximation (BO). As expected the Born approximation grossly

overestimates the cross sections at low energy (by 55% at 25 eV), but at high

energy (100 eV) the CC and Born cross sections are within 8% of each other.

The poor performance of CCNE should also have been anticipated, since it makes

no allowance for the electron-exchange. Nevertheless, it is somewhat

disappointing to see a substantial difference between CCNE and CC at energies

as high as 50 eV. The CCNE and Born approximation give essentially the same

cross sections even at 25 eV. It is more difficult to assess the performance

of the Born-Ochkur approximation. While it tends to reduce the cross sections below those given by the Born approximation, such a reduction is assured by the formulation.[33] Therefore, at this time we can view the "success" of the Born-Ochkur approximation only as qualitative and phenomenological.

On the other hand, much better agreement between the Born and CC at high energy is encouraging; even at 75 eV the discrepancy is a mere 10%. With this quantitative assessment, the Born approximation can be now utilized to provide cross sections at still higher incident-electron energies.

VI. CONCLUSION

While the basic formalism governing the collision process is identical in electron-atom and electron-molecule cases, the theoretical advancement of molecular collision lags far behind that of the atomic process. There is no denying that this vast gap between the two is directly attributable to the computational difficulties associated with molecules. In this work we accomplished in devising a computational procedure capable of handling the singlet-singlet and singlet-triplet excitations to the same level of refinement as in the corresponding electron-atom collision theory.

With an application to H_2 molecule, we demonstrated the importance of treating electron-exchange properly, by which certain characteristics of each molecular state involved may be brought out. In contrast, only a qualitative feature can be expected from the short-cut methods hitherto applied to electron-molecule collisions such as the Born-type approximation.

Because of the scarcity of excitation measurements for the low excited states of H_2, we were not able to make a close comparison with experiment. However, with this beginning, extension to homonuclear diatomics of the second row is within our reach where greater abundance of experimental data are available. Finally, in understanding collision processes, we believe theory can offer more to electron-molecule processes than atomic cases as the experimental analyses are more complicated and difficult with the former.

REFERENCES

1. S. Chung and C. C. Lin, Phys. Rev. A $\underline{6}$, 988 (1972).

2. S. Chung and C. C. Lin, Phys. Rev. A $\underline{9}$, 1954 (1974).

3. S. Chung, C. C. Lin, and E. T. P. Lee, Phys. Rev. A $\underline{12}$, 1340 (1975).

4. D. C. Cartwright and A. Kuppermann, Phys. Rev. $\underline{163}$, 86 (1967).

5. D. C. Cartwright, Phys. Rev. A $\underline{2}$, 1331 (1970); idid A $\underline{5}$, 1974 (1972).

6. K. J. Miller and M. Krauss, J. Chem. Phys. $\underline{47}$, 3754 (1967).

7. S. P. Khare and B. L. Moiseiwitsch, Proc. Phys. Soc. Lond. $\underline{88}$, 605 (1966).

8. S. P. Khare, Phys. Rev. $\underline{157}$, 107 (1967).

9. V. I. Ochkur, Zh. Eksp. Teor. Fiz. $\underline{45}$, 734 (1963) [Sov. Phys.-JETP $\underline{48}$, 503 (1964)].

10. M.R.H. Rudge, Proc. Phys. Soc. Lond. $\underline{85}$, 607 (1965).

11. T. N. Rescigno, C. W. McCurdy, Jr., V. McKoy, and C. F. Bender, Phys. Rev. A $\underline{13}$, 216 (1976).

12. J. M. Blatt and L. C. Biedenharn, Rev. Mod. Phys. $\underline{24}$, 258 (1952); I. C. Percival and M. J. Seaton, Proc. Camb. Phil. Soc. $\underline{53}$, 654 (1957); B. H. Bransden and J. S. C. McKee, Proc. Phys. Soc. Lond. $\underline{A69}$, 422 (1956); R. Marriott, Proc. Phys. Soc. Lond. $\underline{A72}$, 121 (1958).

13. B. L. Moisewitsch and S. J. Smith, Rev. Mod. Phys. $\underline{40}$, 238 (1968); this review article contains an extensive bibliography on close-coupling method.

14. K. Smith, R. J. W. Henry, and P. G. Burke, Phys. Rev. $\underline{147}$, 21 (1966).

15. E. R. Smith and R. J. W. Henry, Phys. Rev. A $\underline{7}$, 545 (1973); and references therein.

16. L. L. Barnes, N. F. Lane, and C. C. Lin, Phys. Rev. $\underline{137}$, 388 (1965).

17. D. F. Korff, S. Chung, and C. C. Lin, Phys. Rev. A $\underline{7}$, 545 (1973).

18. F. E. Fajen, Ph.D. Dissertation (The University of Oklahoma, 1968) (un-published); F. E. Fajen and C. C. Lin, Bull. Am. Phys. Soc. 14, 225 (1969).

19. K. F. Black and N. F. Lane, in Abstracts of Papers, Sixth International Conference on the Physics of Electronic and Atomic Collisions, Cambridge, Mass., 1969 (The MIT Press, 1969), p. 107.

20. K. F. Black and N. F. Lane, in Abstracts of Papers, Seventh International Conference on the Physics of Electronic and Atomic Collisions, Amsterdam, The Netherlands, 1971 (North-Holland, 1971), p. 332.

21. U. Fano and D. Dill, Phys. Rev. A 6, 185 (1972).

22. E. S. Chang and U. Fano, Phys. Rev. A 6, 173 (1972).

23. For the sake of clarity, we suppress the spin s in the channel index, no confusion arising from this omission.

24. See, for example, Ref. 14 and K. Smith and L. A. Morgan, Phys. Rev. 165, 110 (1968).

25. Incident channel index μ is omitted here; however, it is understood that the orthogonality condition applies to scattered waves initiated by all incident channels.

26. This is a statement that the integrals of Eq. (16) and (17) vanish unless integrand are an even function with respect to inversion.

27. For the range of incident-electron energy considered in this paper, it is realistic to use the representation in which Λ is diagonal. See, for example, Ref. 22 for details.

28. E. U. Condon and G. H. Shortley. The Theory of Atomic Spectra (Cambridge University Press, Cambridge, England, 1963).

29. S. Huzinaga, J. Chem. Phys. 42, 1293 (1965), Tables V and VI.

30. C. C. J. Roothaan, Rev. Mod. Phys. 23, 69 (1951); ibid 32, 179 (1960); W. M. Huo, J. Chem. Phys. 45, 1554 (1966).

31. D. H. Madison and W. N. Shelton, Phys. Rev. A $\underline{7}$, 499 (1973); M. S. Pindzola and H. P. Kelly, Phys. Rev. A $\underline{11}$, 221 (1975).

32. S. J. B. Corrigan, J. Chem. Phys. $\underline{43}$, 4381 (1965).

33. See, for example, Eq. (9) of Ref. 1.

Table I. Threshold (vertical excitation) energies in eV.

$X^1\Sigma_g^+$	$B^1\Sigma_u^+$	$b^3\Sigma_u^+$	$a^3\Sigma_g^+$	$c^3\Pi_u$	$e^3\Sigma_u^+$
0.0	11.37	10.50	11.80	11.96	13.22

Table II. Coupling potentials for $(X^1\Sigma_g^+, B^1\Sigma_u^+)$ system.

	$X^1\Sigma_g^+$	$B^1\Sigma_u^+$
$X^1\Sigma_g^+$	$2(1\sigma_g,1\sigma_g) + \{1\sigma_g,1\sigma_g\}$	$\sqrt{2}(1\sigma_u,1\sigma_g) + \frac{1}{\sqrt{2}}\{1\sigma_u,1\sigma_g\}$
$B^1\Sigma_u^+$	$\sqrt{2}(1\sigma_g,1\sigma_u) + \frac{1}{\sqrt{2}}\{1\sigma_g,1\sigma_u\}$	$(1\sigma_g,1\sigma_g) + (1\sigma_u,1\sigma_u)$ $\frac{1}{2}\{1\sigma_g,1\sigma_g\} + \frac{1}{2}\{1\sigma_u,1\sigma_u\}$

Table III. Coupling potentials for $(X^1\Sigma_g^+, a^3\Sigma_g^+)$ system.[a]

	$X^1\Sigma_g^+$	$a^3\Sigma_g^+$
$X^1\Sigma_g^+$	$2(1\sigma_g,1\sigma_g) + \{1\sigma_g,1\sigma_g\}$	$\sqrt{\tfrac{3}{2}}\{2\sigma_g,1\sigma_g\}$
$a^3\Sigma_g^+$	$\sqrt{\tfrac{3}{2}}\{1\sigma_g,2\sigma_g\}$	$(1\sigma_g,1\sigma_g) + (2\sigma_g,2\sigma_g)$ $-\tfrac{1}{2}\{1\sigma_g,1\sigma_g\} -\tfrac{1}{2}\{2\sigma_g,2\sigma_g\}$

[a]Tables for $(X^1\Sigma_g^+, b^3\Sigma_u^+)$ and $(X^1\Sigma_g^+, e^3\Sigma_u^+)$ systems are similarly obtained by substituting $1\sigma_u$ and $2\sigma_u$ orbitals respectively for $2\sigma_g$ orbital.

Table IV. Coupling potentials for $(X^1\Sigma_g^+, c^3\Pi_u)$ system.[a]

	$X^1\Sigma_g^+$	$c^3\Pi_u(\lambda=+1)$	$c^3\Pi_u(\lambda=-1)$
$X^1\Sigma_g^+$	$2(1\sigma_g,1\sigma_g) + \{1\sigma_g,1\sigma_g\}$	$\sqrt{\tfrac{3}{2}}\{1\pi_u^+,1\sigma_g\}$	$\sqrt{\tfrac{3}{2}}\{1\pi_u^+,1\sigma_g\}$
$c^3\Pi_u(\lambda=+1)$	$\sqrt{\tfrac{3}{2}}\{1\sigma_g,1\pi_u^+\}$	$(1\sigma_g,1\sigma_g) + (1\pi_u^+,1\pi_u^+)$ $-\tfrac{1}{2}\{1\sigma_g,1\sigma_g\} - \tfrac{1}{2}\{1\pi_u^+,1\pi_u^+\}$	$(1\pi_u^-,1\pi_u^+) - \tfrac{1}{2}\{1\pi_u^-,1\pi_u^+\}$
$c^3\Pi_u(\lambda=-1)$	$\sqrt{\tfrac{3}{2}}\{1\sigma_g,1\pi_u^-\}$	$(1\pi_u^+,1\pi_u^-) - \tfrac{1}{2}\{1\pi_u^+,1\pi_u^-\}$	$(1\sigma_g,1\sigma_g) + (1\pi_u^-,1\pi_u^-)$ $-\tfrac{1}{2}\{1\sigma_g,1\sigma_g\} - \tfrac{1}{2}\{1\pi_u^-,1\pi_u^-\}$

[a] One-electron orbitals π^+ and π^- refer to $\pi(\lambda=+1)$ and $\pi(\lambda=-1)$ respectively.

Table V. Expansion coefficients of molecular orbitals as defined in Eqs. (53) and (54).

Exponents	$1\sigma_g(X^1\Sigma_g^+)$	$1\sigma_u(B^1\Sigma_u^+)$	$1\sigma_u(b^3\Sigma_u^+)$	$2\sigma_u(e^3\Sigma_u^+)$	$2\sigma_g(a^3\Sigma_g^+)$	$1\pi_u(c^3\Pi_u)$
s-type						
1 0.082217	.008161	.014707	.072015	.085134	-.079538	
2 0.224660	.056787	.012820	.114357	-.041434	.097826	
3 0.673320	.109047	.013728	.097461	-.047528	.023497	
4 2.34648	.099505	.017342	.065106	-.029563	.047893	
5 10.2465	.065448	.012806	.040253	-.018133	.017078	
6 68.1600	.035669	.006979	.021938	-.009883	.009308	
p-type						
7 0.020185	.000047	.002002	.000336	.007021	.013628	.001276
8 0.055713	-.000204	.010115	.004223	-.013251	-.032689	.007440
9 0.174211	-.001571	.014515	.009789	-.019582	.012642	.014973
10 0.733825	-.021730	.016108	.025107	-.006282	-.032281	.022637

Table VI. Step-size of integration regions[a] in a_o.

r_A	δr	r_B
0.0125	0.0125	1.0
1.0125	0.025	3.0
3.05	0.05	7.0
7.1	0.1	--

[a]r_A and r_B are the starting and final points of a region.

Table VII. Partial cross sections[a] $Q^{\Lambda=0}(\ell,\ell')$ in a_o^2 defined as in Eq.(25) for the $b^3\Sigma_u^+$ state at E = 15 eV.

ℓ' ℓ	0	1	2	3	4	5
0		.181(-1)		.779(-4)		.181(-7)
1	.413(0)		.129(-1)		.913(-5)	
2		.583(-2)		.120(-3)		.180(-7)
3	.319(-2)		.735(-3)		.317(-5)	
4		.138(-4)		.368(-4)		.147(-6)
5	.768(-4)		.597(-5)		.305(-5)	

[a]Numbers in the parentheses indicate the power of 10.

Table VIII. Partial cross sections[a] $Q^{\Lambda=1}(\ell,\ell')$ in a_0^2 defined as in Eq.(25) for the $b^3\Sigma_u^+$ state at $E = 40$ eV.

ℓ \ ℓ'	1	2	3	4	5
1		.250(-2)		.448(-5)	
2	.475(-1)		.244(-2)		.308(-5)
3		.102(-1)		.481(-3)	
4	.278(-4)		.145(-2)		.675(-4)
5		.372(-5)		.192(-3)	

[a]Numbers in the parentheses indicate the power of 10.

Table IX. Partial cross sections $Q^\Lambda(b^3\Sigma_u^+)$ in a_o^2 defined as in Eq.(69) at E = 15 and 40 eV.

Λ	Q^Λ E = 15 eV	E = 40 eV
0	.454019	.077405
1	.271013	.064906
2	.002737	.006672
3	.000038	.000721
sum[a]	1.001595	0.222003

[a] $Q^{-\Lambda} = Q^{+\Lambda}(\Lambda \neq 0)$ are included in the sum.

Table X. Total cross sections of triplet states in units of 10^{-17} cm².

Energy (eV)	$b^3\Sigma_u^+$			$e^3\Sigma_u^+$		$a^3\Sigma_g^+$			$c^3\Pi_u$	
	CC[a]	BR[b]	DW-RPA[c]	CC	BR	CC	BR	DW-RPA	CC	BR
13	2.19	4.47	8.24			.269	1.07	.571	4.63	1.96
14	2.56	4.41	9.23	1.285	.330					
15	2.80	4.18	8.89	.914	.417	.889	1.22	1.18	5.63	1.98
16	2.84	3.88	8.44					1.35		
17.5	2.81	3.41		.620	.421	.715	1.06			
20	2.53	2.69	5.49	.500	.357	.552	.854	1.31	3.44	1.19
25	1.82	1.70		.301	.234	.364	.534		1.95	.702
30	1.26	1.10		.192	.152	.268	.342		1.10	.433
40	.622	.525		.0902	.0717	.135	.160		.410	.196

[a] Close-coupling of this work.

[b] Born-Rudge approximation of Ref. 3.

[c] Distorted-wave with random-phase approximation of Ref. 11.

Table XI. Partial cross sections[a] $Q(\ell,\ell')$ defined as in Eq.(71) for the $B^1\Sigma_u^+$ state at $E = 25$ eV in a_o^2.

ℓ	$Q(\ell,\ell'=\ell-1)$			$Q(\ell,\ell'=\ell+1)$		
	CC	CCNE	Born	CC	CCNE	Born
0				.355(-2)	.671(-3)	.887(-2)
1	.287(-1)	.943(-1)	.370(0)	.329(-1)	.161(-1)	.159(-3)
2	.184(0)	.468(0)	.605(0)	.248(-1)	.169(-1)	.320(-2)
3	.378(0)	.674(0)	.533(0)	.213(-1)	.162(-1)	.341(-2)
4	.351(0)	.432(0)	.360(0)	.639(-2)	.738(-2)	.239(-2)
5	.234(0)	.238(0)	.217(0)	.416(-2)	.295(-2)	.124(-2)
6	.114(0)	.126(0)	.122(0)	.912(-3)	.107(-2)	.687(-3)
7	.685(-1)	.660(-1)	.676(-1)		.384(-3)	.344(-3)
8		.347(-1)	.364(-1)			

[a] Numbers in the parentheses indicate the power of 10.

Table XII. Partial cross sections[a] $Q(\ell,\ell')$ defined as in Eq. (71) for the $B^1\Sigma_u^+$ state at E = 100 eV in a_o^2.

ℓ	$Q(\ell,\ell'=\ell-1)$			$Q(\ell,\ell'=\ell+1)$		
	CC	CCNE	Born	CC	CCNE	Born
0				.948(-3)	.111(-2)	.127(-2)
1	.763(-2)	.102(-1)	.113(-1)	.441(-2)	.113(-2)	.987(-4)
2	.197(-1)	.146(-1)	.334(-1)	.625(-2)	.192(-2)	.405(-3)
3	.223(-1)	.349(-1)	.583(-1)	.574(-2)	.498(-2)	.198(-2)
4	.437(-1)	.616(-1)	.791(-1)	.576(-2)	.758(-2)	.368(-2)
5	.667(-1)	.863(-1)	.920(-1)	.118(-1)	.870(-2)	.488(-2)
6	.887(-1)	.911(-1)	.975(-1)	.795(-2)	.858(-2)	.536(-2)
7	.943(-1)	.935(-1)	.967(-1)		.733(-2)	.532(-2)
8		.890(-1)	.920(-1)			

[a]Numbers in the parentheses indicate the power of 10.

Table XIII. Total cross sections of the $B^1\Sigma_u^+$ state in units of 10^{-17} cm^2.

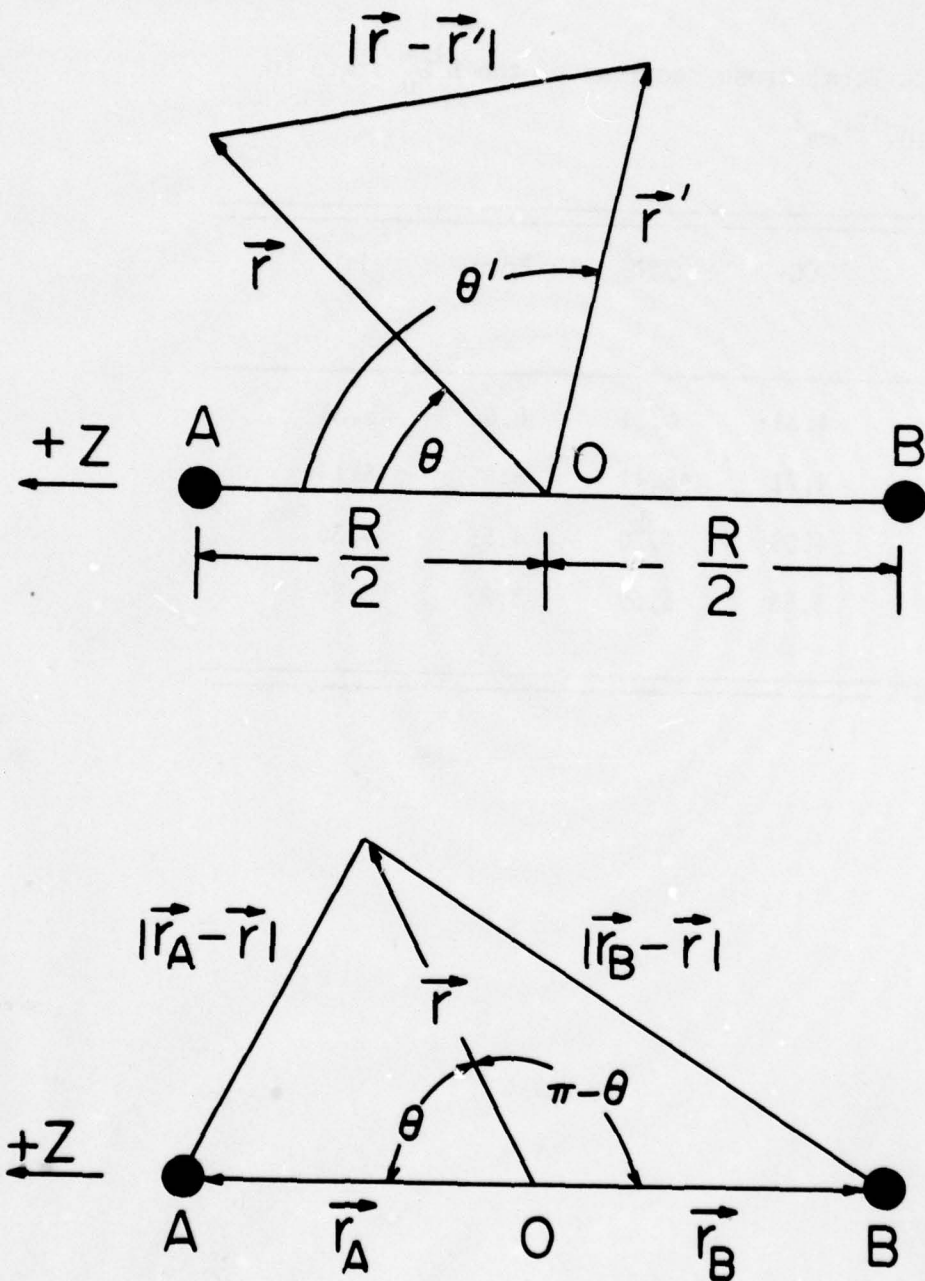| Energy (eV)	CC	CCNE	Born	BO
25	4.31	6.31	6.66	5.31
50	4.71	5.41	5.55	5.14
75	4.09	4.30	4.55	4.36
100	3.58	3.69	3.87	3.76

Fig. 1. Coordinate system showing the expansions of $|\vec{r}-\vec{r}'|^{-1}$, $|\vec{r}_A-\vec{r}|^{-1}$, and $|\vec{r}_B-\vec{r}|^{-1}$.
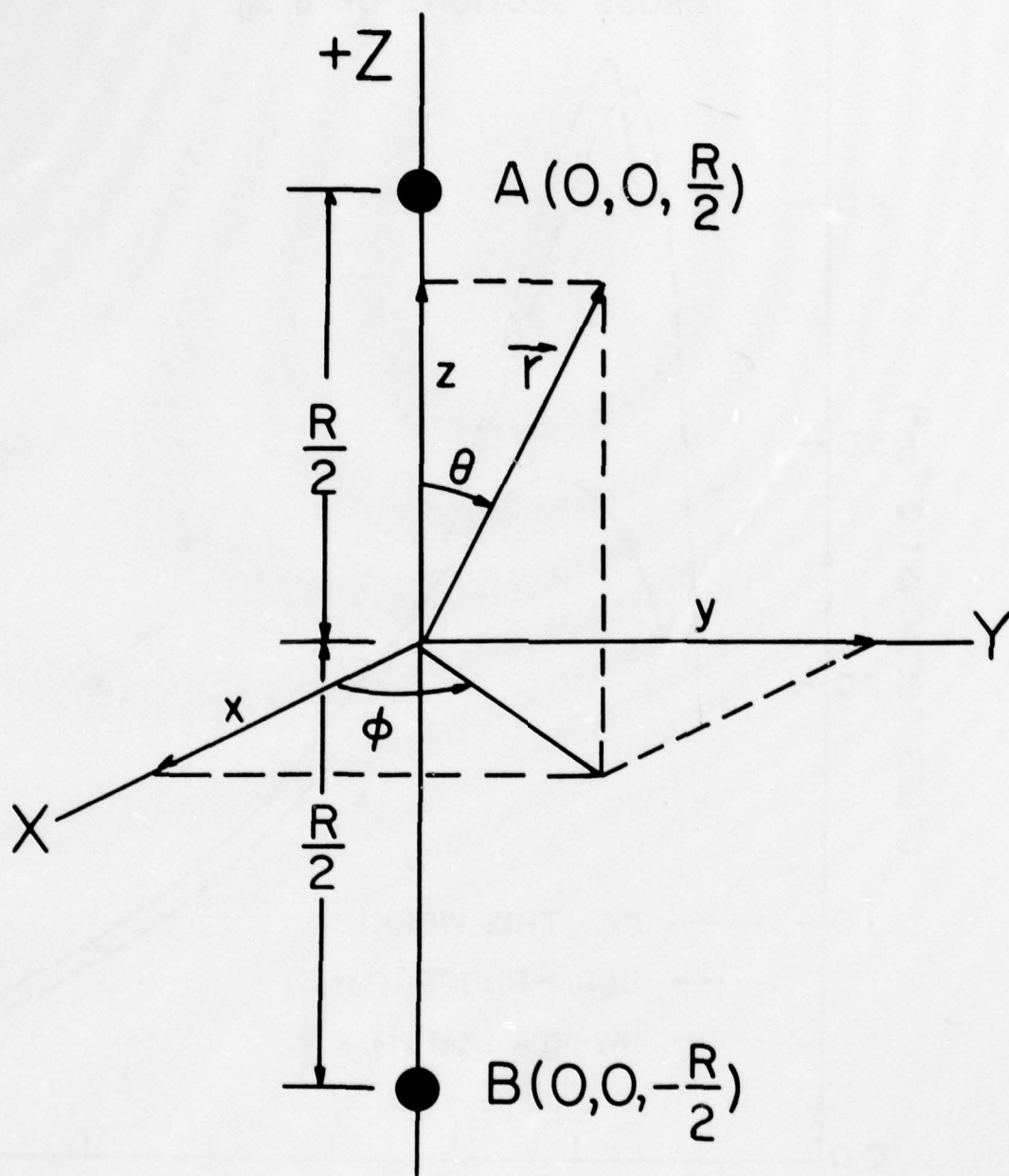
Fig. 2. Gaussian-type orbitals in the Cartesian and spherical coordinate systems.

Fig. 3. Excitation cross sections of the $b^3\Sigma_u^+$ state calculated by means of (i) the close-coupling (solid line) of this work; (ii) the Born-Rudge approximation (uniform dashed line) in Ref. 3; (iii) DW RPA reduced to one-half (long-short dashed line) in Ref. 11.

Fig. 4. Excitation cross sections of the $e^3\Sigma_u^+$ state calculated by means of (i) close-coupling (solid line) of this work; (ii) the Born-Rudge approximation (dashed line) in Ref. 3.

Fig. 5. Excitation cross sections of the $a^3\Sigma_g^+$ state calculated by means of (i) close-coupling (solid line) of this work; (ii) the Born-Rudge approximation (uniform dashed line) in Ref. 3; (iii) DW-RPA (long-short dashed line) in Ref. 11.
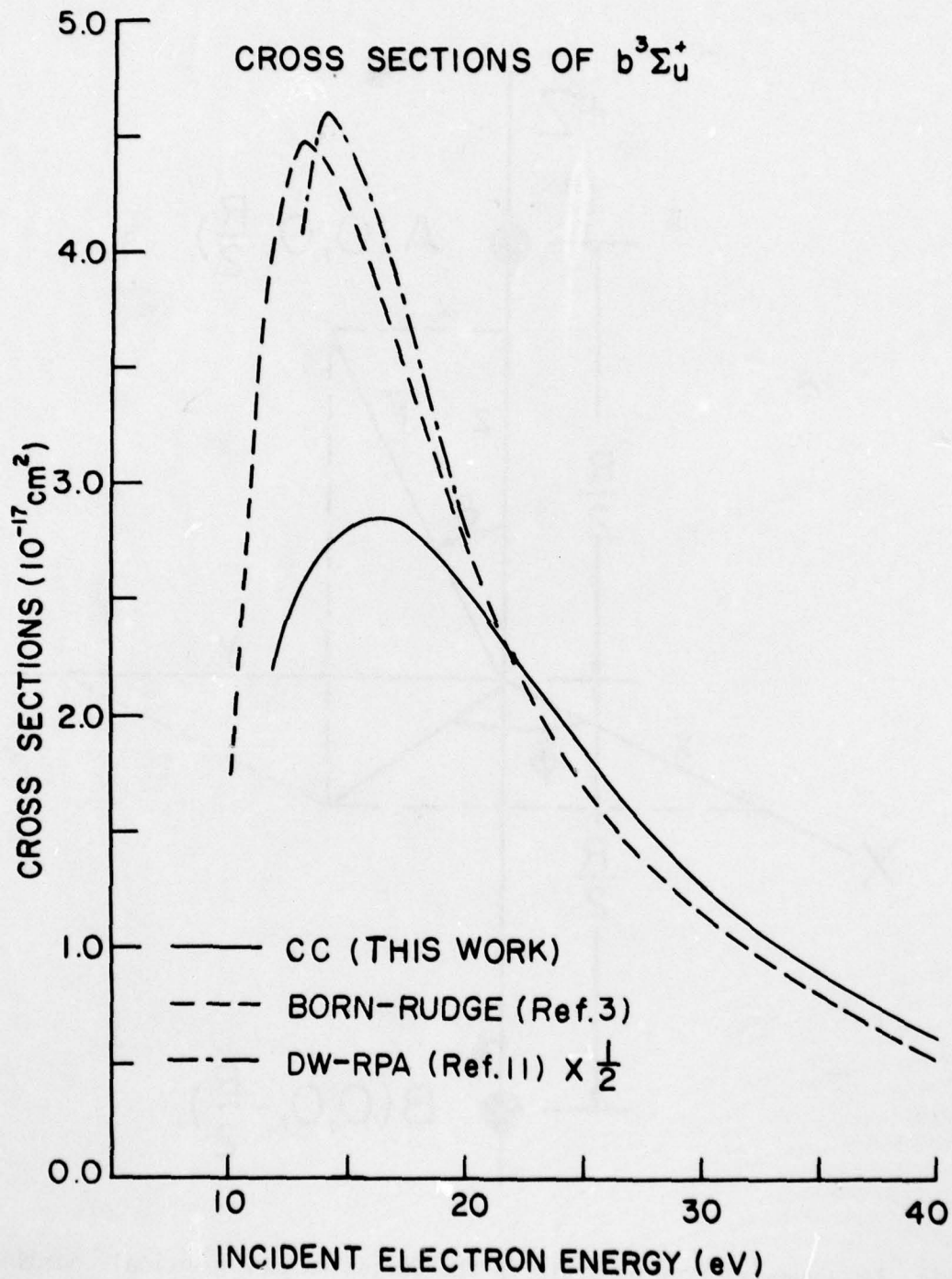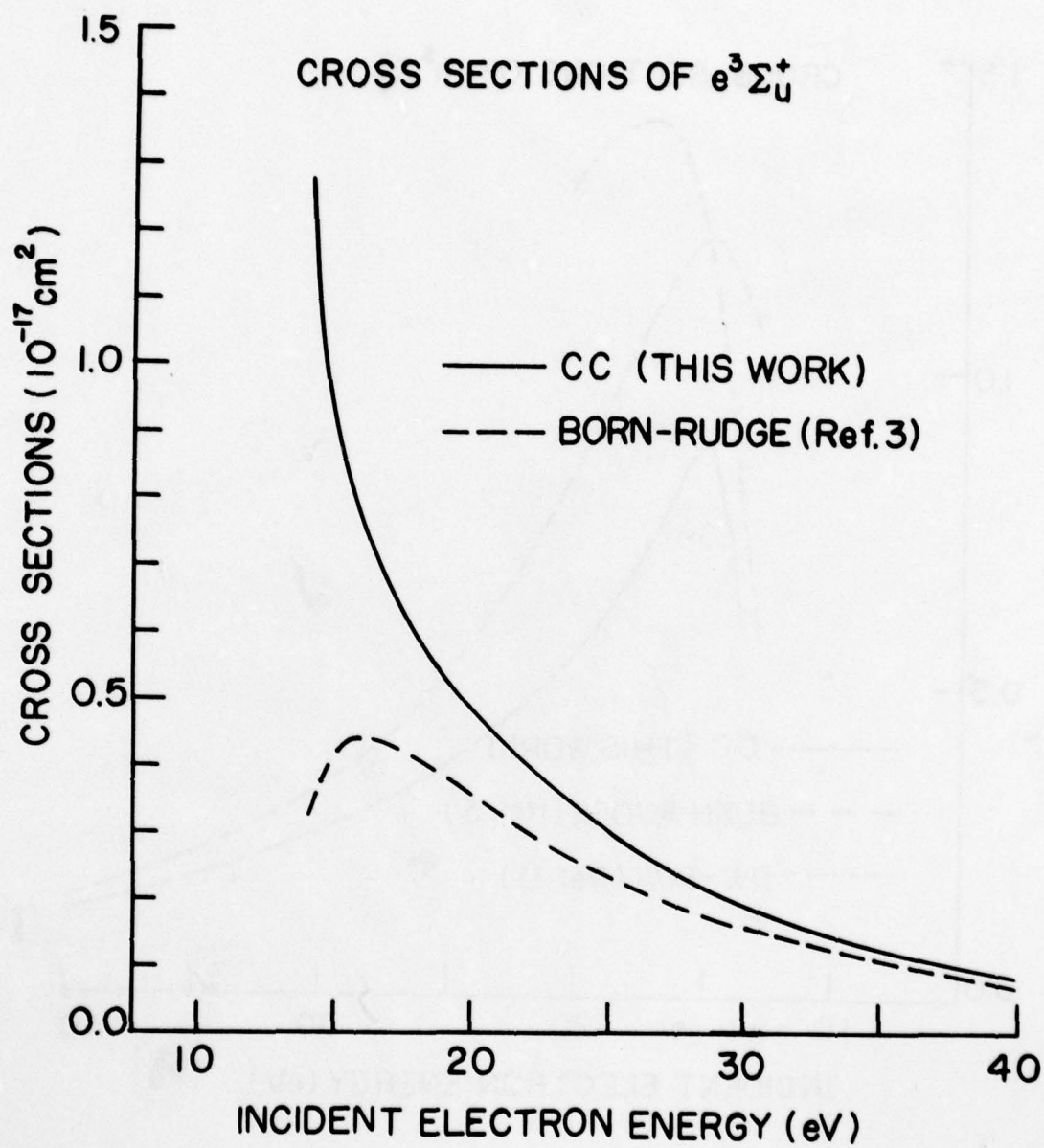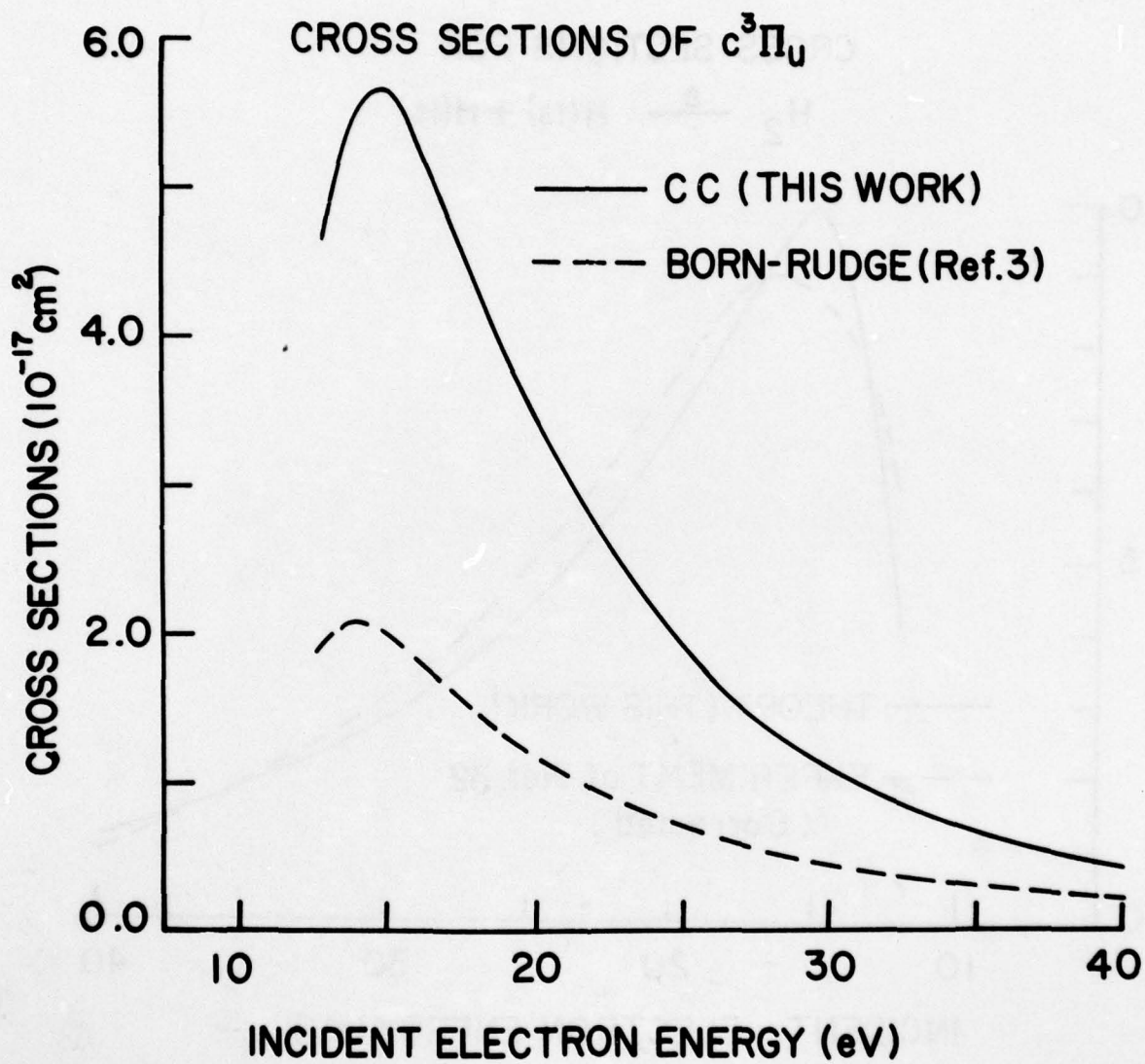
Fig. 6. Excitation cross sections of the $c^3\Pi_u$ state calculated by means of (i) the close-coupling (solid line) of this work; (ii) the Born-Rudge approximation (dashed line) in Ref. 3.

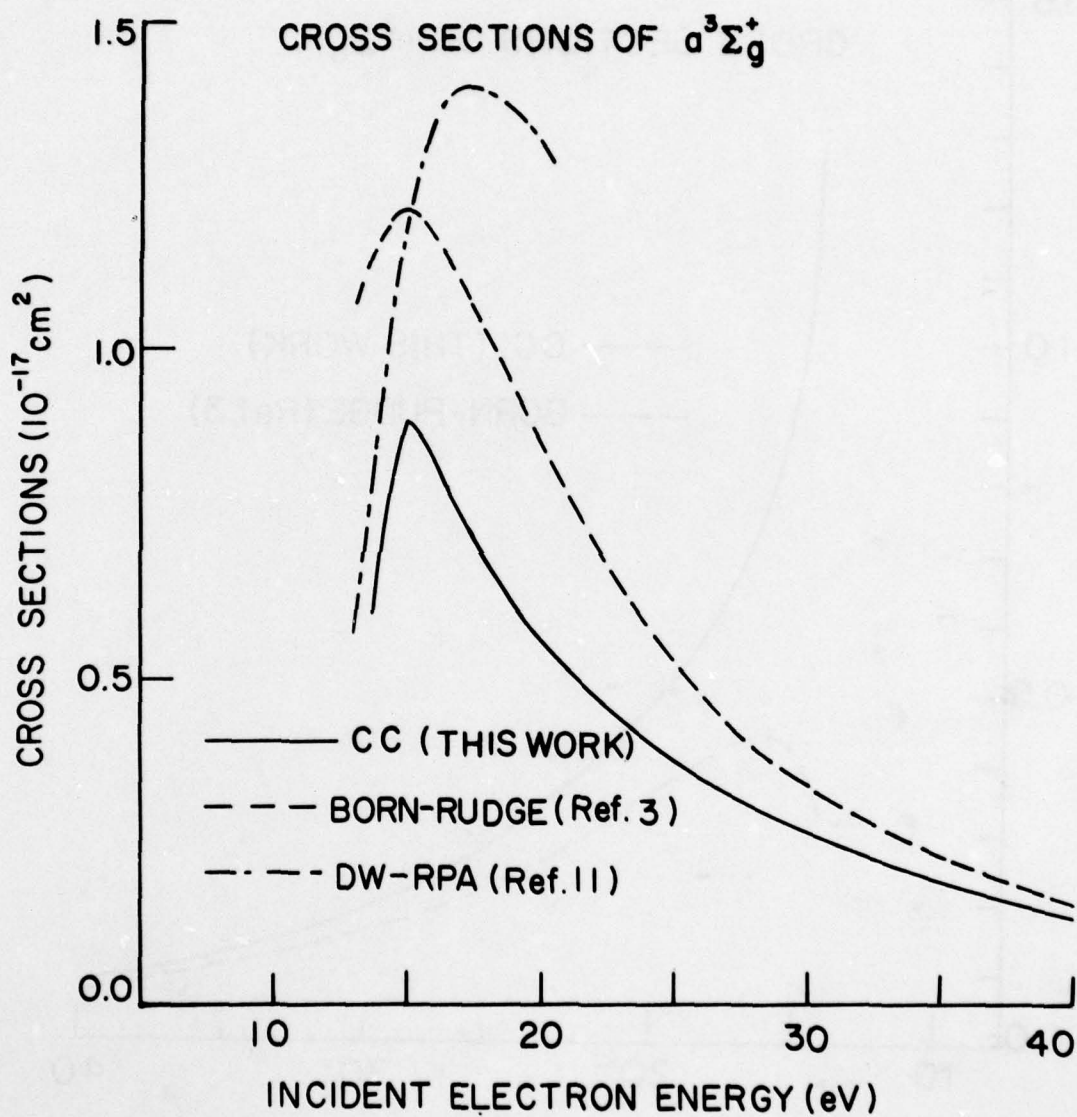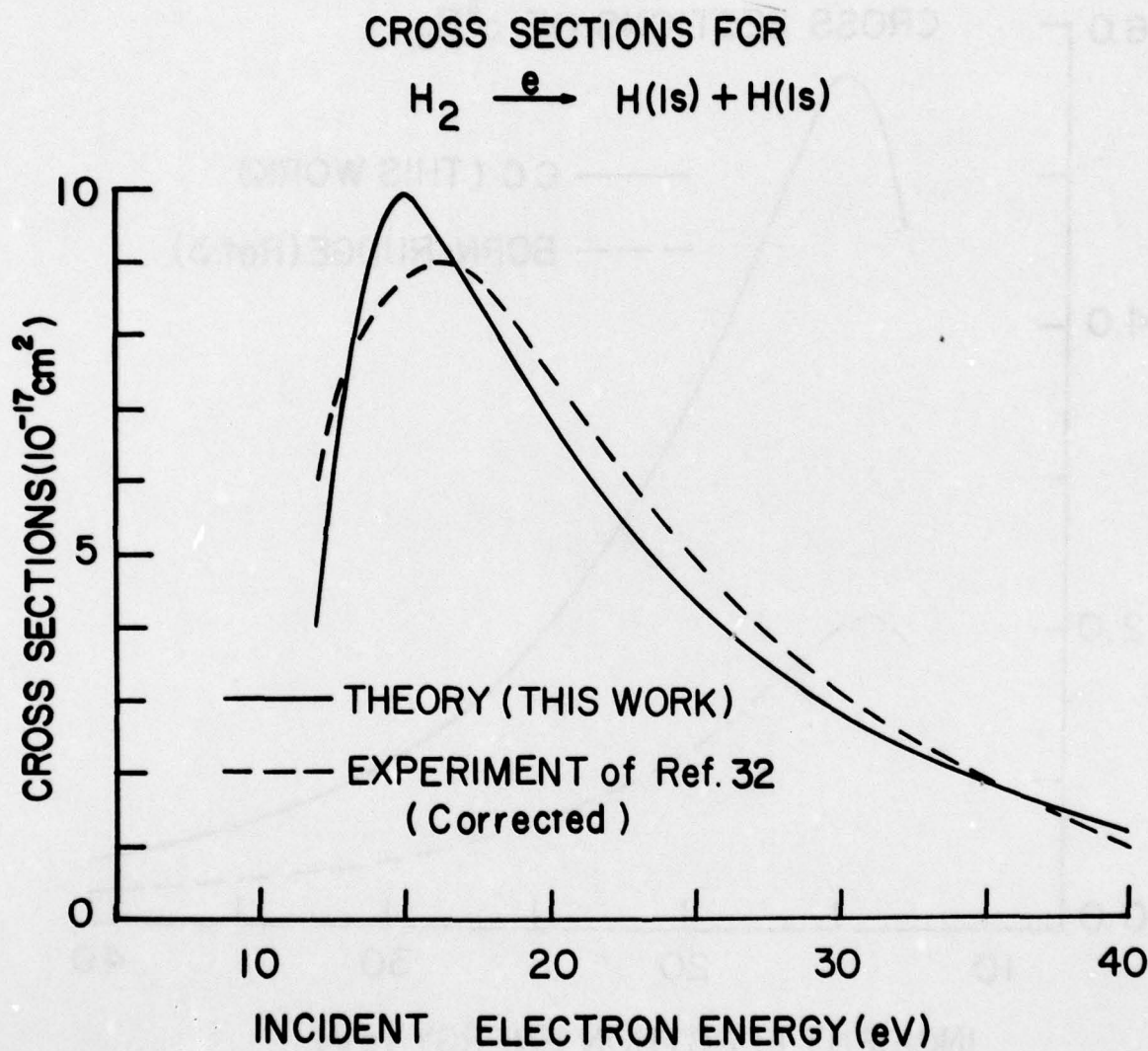Fig. 7. Theoretical cross sections of this work (solid line) for the dissociation process $H_2 \xrightarrow{e} H(1s) + H(1s)$ as compared with experimental values (dashed line) of Ref. 32 corrected to represent the production of H(1s) atoms only as described in Ref. 3.

CROSS SECTIONS OF B$^1\Sigma_u^+$
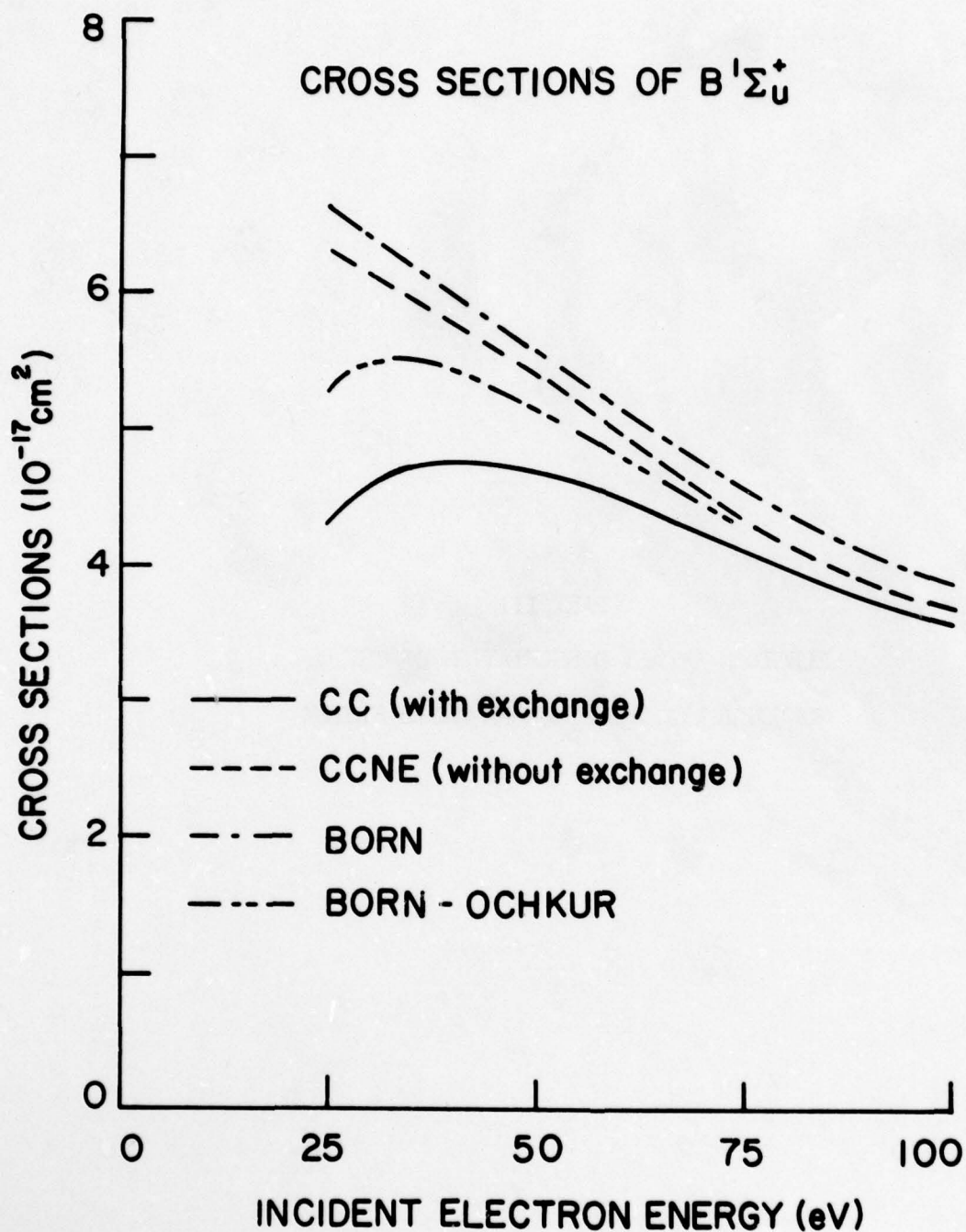
Fig. 8. Excitation cross sections of the B$^1\Sigma_u^+$ state calculated by means of (i) the close-coupling <u>with exchange</u> (solid line): (ii) the close-coupling <u>without exchange</u> (uniform dashed line); (iii) the Born approximation (long-short dashed line); (iv) the Born-Ochkur approximation (long-short-short dashed line).

PART III

ELECTRON IMPACT DISSOCIATION OF THE O_2
MOLECULE VIA THE SCHUMANN-RUNGE SYSTEM

I. INTRODUCTION

Inelastic collisions of electrons and molecules with resulting excitation and dissociation of molecules constitute a very basic kind of processes in many different phenomena. The importance of the O_2 molecules in the atmospheric physics has long been recognized.[1] More specifically, the Schumann-Runge system of O_2, to which this part of the report is directed, has been extensively studied experimentally, both by the optical[2-4] and electron-energy loss spectroscopy.[5,6] The upper state of the Schumann-Runge system is the lowest dipole-allowed excited state, and it is a repulsive state which dissociates into $O(^3P)$ and $O(^1D)$ atoms (see Fig. 1). Thus, the continua of this system is responsible for dissociation of O_2 in the earth's upper atmosphere by UV absorption of the solar radiation. The O_2 molecule may also be dissociated by electron-impact. In spite of the importance of such processes, systematic theoretical studies based on the first principle calculations are sparse in the literature, and do not exceed the stages of the optical oscillator strength.[7] The very complicated numerical procedures required to evaluate the multicenter integrals had been the major source of difficulty. However, with the introduction of the Gaussian type orbitals (GTO) to the molecular wave functions, the evaluation of the multicenter integrals has become a rather simple task, and the advantage of using GTO for calculating excitation cross sections has been amply demonstrated by the cases of H_2, N_2, and CO molecules.[8-10]

An additional complication arises in the theoretical studies of O_2 molecule in contrast with other atmospheric molecules cited above. That is, the ground state of O_2 has an incompletely filled shell. Therefore, a single-configuration wave function is not adequate in describing the molecular wave

function, and one must employ multiconfiguration (MC) wave functions. We shall examine in some detail the effect of the configuration-mixing on the cross sections. Because of this additional complexity, our report will be confined to the level of the Born-type calculation. As with the N_2 and CO molecules,[8,9] we shall rely on the Ochkur's[11] modified version of the Born approximation, and present the dissociation cross sections of the O_2 molecule from the threshold to 1000 eV of the incident-electron energy.

II. THEORY

A theoretical formulation for the problem of electron excitation/
dissociation of diatomic molecules by electron impact has been presented in
Ref. 10 and Part I of this report. In this section the key steps will be
sketched only. We are concerned with calculation of excitation cross
sections to an excited state characterized by electronic and vibrational
quantum numbers (nW) from the ground electronics-vibrational state (00).
It should be noted that the upper state of the Schumann-Runge system
$B^3\Sigma_u^-$ state is a repulsive state, so that the "vibrational states" are in
fact continua. Molecular rotation will not be included explicitly in the
formulation, but its effect will be taken into account by averaging the cross
sections over the relative orientation between the molecular axis and the
direction of incident electron. The total wave functions of molecule are
written as a product of the vibrational part $\chi(R)$ and the electronic part
$\Psi(\vec{r}_1,\vec{r}_2,\ldots,\vec{R})$. It is convenient to couple the molecular wave functions with
the spin of the colliding electrons to form a set of basis functions, from
which the direct-excitation (Born approximation) and the exchange-excitation
(Ochkur's version[11]) collision amplitudes can be calculated. We assume
this has been done. Then the transition amplitude is[8]

$$\varepsilon_{on}(K,R, ,\phi) = -\int \Psi_n^*(\vec{r}_1,\vec{r}_2,\ldots\vec{r}_N,\vec{R}) \sum_{i=1}^{N} \exp(i\vec{K}\cdot\vec{r}_i)$$

$$\Psi_o(\vec{r}_1,\vec{r}_2,\ldots\vec{r}_N,\vec{R}) \, d\vec{r}_1 d\vec{r}_2\ldots.d\vec{r}_N. \tag{1}$$

The differential cross sections in $(\theta\phi)$ direction for excitation from the
ground (00) to the upper (nW) state are

$$I_{nW}(\theta,\phi) = (\omega_n k_{nW}/4\pi k_{oo}) \int |\chi_{nW}^*(R)\chi_{oo}(R)$$

$$(2K^{-2}-k_{oo}^{-2})\epsilon_{on}(K,R,\theta,\phi)|^2 \, R^2 dR \, \sin\theta d\theta d\phi \, , \qquad (2)$$

where ω_n is the degeneracy of the excited state. Integration of the differential cross sections over $(\theta\phi)$ gives the cross section for excitation to a unit energy range about W of the repulsive state, viz.,

$$Q(00 \to nW) = \int I_{nW}(\theta,\phi) \, \sin\theta d\theta d\phi \, . \qquad (3)$$

It follows that the cross sections of the entire repulsive state, irrespective of the continuum levels are

$$Q(0 \to n) = \int_0^\infty Q(00 \to nW) \, dW. \qquad (4)$$

Another quantity of physical significance is the generalized oscillator strengths, which are related to the transition amplitude of Eq. (1) as

$$F_{on}(K,R) = (2W_m \Delta E/4\pi K^2) \int |\epsilon_{on}(K,R,\theta,\phi)|^2 \times \sin\theta d\theta d\phi, \qquad (5)$$

where ΔE is the vertical excitation energy in a.u. (1 a.u. = 27.2 eV). In particular, the optical oscillator strengths,

$$f_{on}(R) = F_{on}(K=0,R) \qquad (6)$$

are closely related to the photodissociation processes of the O_2 molecule via the Schumann-Runge $(X^3\Sigma_g^- \to B^3\Sigma_u^-)$ system. From the foregoing discussion, it is clear that the transition amplitude ϵ_{on} in Eq. (1) governs the accuracy of the theoretical calculation that follows, be it the excitation cross section or photodissociation cross section.

In the usual approach of writing wave functions as an antisymmeterized products of one-electron functions ϕ, if the wave functions in Eq. (1) are

considered to be single-configuration functions, Eq.(1) reduced to

$$\epsilon_{on}(K,R,\Theta,\phi) = - \int \phi_j^*(\vec{r},\vec{R})\exp(i\vec{K}\cdot\vec{r})\phi_i(\vec{r},\vec{R})d\vec{r}, \tag{7}$$

where ϕ_i and ϕ_j are the pair of "active" electron-functions. As we mentioned in Sec. I, a single-configuration functions are not sufficient in the case of the O_2 molecule; therefore, we adopt the wave functions in Eq. (1) in the form of multi-configuration (MC) functions, viz.,

$$\Psi_o(\vec{r}_1,\vec{r}_2,\ldots,R) = \Sigma_i \, a_i(R) \, \psi_i(\vec{r}_1,\vec{r}_2,\ldots,R) \tag{8}$$

$$\Psi_n(\vec{r}_1,\vec{r}_2,\ldots,R) = \Sigma_j \, b_j(R) \, \psi_j(\vec{r}_1,\vec{r}_2,\ldots,R) \tag{9}$$

where ψ_i, ψ_j are the single-configuration wave functions, and a_i, b_j are the configuration-mixing coefficients. The details of computing these MC wave functions will be presented in Sec. III. In this scheme of using MC wave functions, the transition amplitude becomes

$$\epsilon_{on}(K,R,\Theta,\phi) = -\Sigma_{i,j}\Delta_{i,j}a_i(R)b_j(R)\int\phi_j^*(\vec{r},\vec{R})\exp(i\vec{K}\cdot\vec{r}) \, \phi_i(\vec{r},\vec{R})d\vec{r} \, , \tag{10}$$

where $\Delta_{ij} = 1$, if the antisymmeterized product ψ_i differ by one one-electron orbital from that of ψ_j, i.e., ϕ_i and ϕ_j respectively; otherwise $\Delta_{ij} = 0$. Corresponding to this, the optical oscillator strength may be computed by substituting Eq. (10) into (5), and taking the limiting value as $K\rightarrow 0$, with the result,

$$f_{on}(R) = (2\omega_n\Delta E/3) \mid \Sigma_{i,j} \, \Delta_{ij} \, a_i(R)b_j(R)$$

$$\int \phi_j^*(\vec{r},\vec{R}) \, z \, \phi_i(\vec{r},\vec{R}) \, d\vec{r}\mid^2. \tag{11}$$

For the purpose of studying the effects of configuration mixing, it is sufficient to examine the dipole transition amplitude, i.e.,

$$\bar{z} = \Sigma_{ij} \, \Delta_{ij} a_i(R) b_j(R) \int \phi_j^*(\vec{r}, \vec{R}) z \, \phi_i(\vec{r}, \vec{R}) d\vec{r}. \tag{12}$$

In Sec. IV we shall examine in detail how $\bar{z}$ varies and converges as we include more and more configurations.

As shown in Eqs. (6) and (11), the optical oscillator strength varies with the internuclear separation R. Therefore, in order to obtain the optical oscillator strength of the entire Schumann-Runge system, we must integrate $f_{on}(R)$ with the vibrational functions $\chi(R)$, i.e.

$$f_{SR} = \int_{R_1}^{R_2} R^2 dr \, \chi(X|R) f_{on}(R) \chi(B|R) \ . \tag{13}$$

In principle R_1 and R_2 should be 0 and ∞, but since χ's are localized so that finite limits may be used.

1.0

2.8   2.5

3.2   2.2

3.6

4.0   2.0

1.1

18

1.25   1.4   1.6
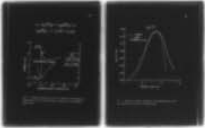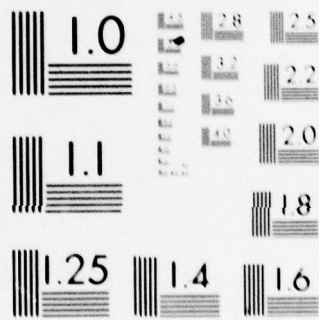
MICROCOPY RESOLUTION TEST CHART
NATIONAL BUREAU OF STANDARDS-1963-A

III. Multi-configuration (MC) wave functions

The dominant configurations of the ground $X^3\Sigma_g^-$ and the upper $B^3\Sigma_u^-$ states are[12]

$$X: \ (1\sigma_g)^2(1\sigma_u)^2(2\sigma_g)^2(2\sigma_u)^2(3\sigma_g)^2(1\pi_u)^4(1\pi_g)^2 , \tag{14}$$

$$B: \ (1\sigma_g)^2(1\sigma_u)^2(2\sigma_g)^2(2\sigma_u)^2(3\sigma_g)^2(1\pi_u)^2(1\pi_g)^3 . \tag{15}$$

within the single-configuration approximation, each of the molecular orbitals. (MO) may be expanded in a suitable GTO basis set, and the expansion coefficients are determined by the standard self-consistent-field (SCF) method.[13] However, as these configurations have partially filled shells, they are subject to severe configuration mixing. Therefore, the refined wave functions must be taken as linear combinations of different single-configuration functions as shown in Eqs. (8) and (9).

In our investigation we adopted the multiconfiguration self-consistent-field method (MCSCF) to determine the configuration-mixing coefficients. The MCSCF method offers greater flexibility than the more restricted configuration-interaction (CI) method in that the configuration-mixing coefficients as well as the orbital expansion coefficients are optimized simultaneously. Therefore, at the present MCSCF is considered to be the best theoretical means of obtaining accurate wave functions for the molecules. We have developed a computer program to handle the MCSCF procedures for diatomic molecules, and applied it to the O_2 molecule.

Although, in principle, there are an infinite number of configurations that may be included for a given symmetry of electronic state, as a practical matter this number must be restricted to a manageable size. In constructing different configurations, we have considered the following shells

$$(2\sigma_g)(2\sigma_u)(3\sigma_g)(3\sigma_u)(1\pi_u)(1\pi_g) \ . \tag{16}$$

We restricted $(1\sigma_g)$ and $(1\sigma_u)$ shells to be always doubly occupied, since the electrons in these shells are very tightly bound to the nuclei, and are relatively immune to perturbation. However, in order to gain greater flexibility we included $(3\sigma_u)$ shell, although it does not appear in the dominant configurations shown in (14) and (15). By permuting the assignment of 12 electrons in the shells shown in (16), there arise 30 configurations consistent with $^3\Sigma_g^-$ symmetry (ground state) and 28 configurations for $^3\Sigma_u^-$ symmetry (upper state of the Schumann-Runge system). In Table I and II, we present these configurations along with the mixing coefficients at the equilibrium internuclear separation for the ground $X^3\Sigma_g^-$ state, and for the $B^3\Sigma_u^-$ state respectively. Configurations are specified by the occupation number of electrons in each shell. It is noted that, when three or more shells are partially occupied, we have more than one configuration from such occupancy. This is due to the different way three spin functions may be coupled to yield a triplet function. It is possible and probably necessary to include more configurations than shown in Tables I and II, if our goal is to construct the potential-energy curves of the O_2 molecule. However, with the present objective of studying electron-impact excitation and dissociation, we believe we have considered sufficient number of configurations.

IV. RESULTS AND DISCUSSION

A. Optical Oscillator Strength

With the multiconfiguration functions for both the ground $X^3\Sigma_g^-$ and the upper $B^3\Sigma_u^-$ states as shown in Tables I and II, the dipole transition amplitude $\bar{z}$ of Eq. (12) is reduced as follows

$$\bar{z} = \Sigma_{ij} \, \Delta_{ij} \, a_i(R) \, b_j(R) \, \{<1\pi_u|z|1\pi_g>$$

$$+ \, <3\sigma_g|z|3\sigma_u> + \, <3\sigma_g|z| \, \sigma_u> + \, <2\sigma_g|z|3\sigma_u>$$

$$+ \, <2\sigma_g|z|2\sigma_u>\}, \tag{17}$$

with

$$<1\pi_u|z|1\pi g> = \int \phi^*(1\pi_g|\vec{r},\vec{R}) \, z \, \phi(1\pi_u|\vec{r},\vec{R})d\vec{r}, \text{ etc.} \tag{18}$$

In Table III we list these five matrix elements computed at the equilibrium separation of the ground state (R=1.2Å). In Eq. (17) for a given pair of configuration (i,j), at most one of the five elements is nonvanishing. In Tables IV we present some of the significant contributions, i.e., the products $f \, a_i(R)b_j(R)$, R = 1.2Å from various pairs of configurations (i,j). The factor f covers the normalization of determinantal functions and ±1 sign coming from the interchange of columns in the determinantal function. It is readily apparent from these tables that only a few configurations are important as far as the studies of electron-excitation or photoabsorption processes are concerned. In fact a few (less than five) well-chosen configurations give a sufficiently accurate oscillator strength as shown in Table IV. Considering the large amount of numerical work yet to be processes before the final goal of the cross sections, we decided to limit the number of configurations to five (configurations 1,2,3,7,13) for the ground state and to five (1,4,8,12,10) for the upper state. By using these five-configuration

wave functions we have computed the transition amplitude, oscillator strength, etc. at R = 0.9, 1.0, 1.1, 1.2, 1.3, 1.4, and 1.5 Å. Finally, since the Schumann-Runge system is a continuum, by integrating the transition amplitude with the continuum "vibrational" functions as shown in Eq. (13), we obtained the oscillator strength of the entire system. The continuum vibrational functions are constructed from the potential curve[12], and the integration in Eq. (13) was carried out numerically R_1, R_2, and ΔR corresponding to W = 7.0, W = 10.0, and W = 0.1 eV, respectively. In this manner we obtained the theoretical optical oscillator strength of 0.131. This value is somewhat smaller than experimental data[2-5] ranging from 0.142 to 0.162 by the optical method, and 0.161 by the electron-energy loss method. Recently, Julienne, Neumann, and Krauss[7] reported the oscillator strength of this system as 0.18 at the equilibrium separation of the ground state. These authors included in their calculations 2π orbitals as well as d-type orbitals in the basis set. On the other hand, they did not go through the averaging process of Eq. (13). Beside the optical oscillator strength, Huebner, et. al. measured the oscillator strengths as a function of vertical excitation energy from their electron-energy loss experiment. Since the veritcal excitation energy ΔE is a function of internuclear separation R, we convert our theoretical oscillator strengths in terms of ΔE, and compare them with the experiment in Fig. 2. We see a very good agreement between theory and experiment up to $\Delta E \simeq 9$ eV. Beyond $\Delta E = 9$ eV the experimental values may contain contribution from another repulsive $^3\Pi_u$ state.[14] This may cause the experimental values to appear larger, since, in the electron-energy loss experiment,[5] the distinction of different electronic states was not made. On the theoretical side, the potential curve of the $B^3\Sigma_u^-$ state rises very rapidly as R decreases in this region so that the continuum function becomes less reliable. Those

factors could explain the discrepancy between theory and experiment above $\Delta E = 9.0$ eV.

B. Dissociation Cross Sections

In order to obtain the dissociation cross sections, the transition amplitude in Eq. (1) must be computed at a number of values of K as well as R. Our numerical procedure consists of computing the transition amplitude at 32 distinct K-values for each of the seven internuclear separations ranging from 0.9 to 1.5 $\overset{o}{A}$. Next, the differential cross sections are computed by the angular averaging procedure as shown in Eq. (2). Finally, the total cross sections are obtained by means of the Born-Ochkur method, indicated in Eqs. (2)-(4). In evaluating Eq. (4) the limits are taken to be $W = 7.0$ to 10.0 eV as before (See Sec. IV-B). The total cross sections are presented in Table VI. We find the peak cross section of 7.3×10^{-17} cm^2 at 20 eV. There are no extensive experimental measurements for excitation (dissociation) of this state. By extrapolating the differential cross section data, Trajma et al.[15] reports a cross section of 8.6×10^{-17} cm^2 at 20 eV, which is in fair agreement with our calculation. But their cross section (11.5×10^{-17} cm^2) at one other energy (45 eV) is much larger than the present result.

V. CONCLUSION

In spite of the importance of the O_2 molecule in aeronomical studies, laboratory measurements of electron-impact cross sections of excitation (dissociation) of O_2 have been very meager. As with other molecules, overlaping of molecular spectra due to different states makes the experiment a difficult task.

In this report we have presented the Born-Ochkur cross sections of the electron-impact dissociation of O_2 via the Schumann-Runge system. As with other diatomic molecules the computing procedures have been facilitated by the GTO technique we have developed past several years. However, for this particular dissociation process, two additional obstacles are encountered. One is the continua of the vibrational states as opposed to discrete states. We treated this problem by generating numerically a tabular function for the continuum functions from the potential-energy curves. The other has to do with strong configuration mixing of the electronic wave functions peculiar to O_2 molecule. Although as many as 30 configurations have been examined, by a careful analysis, we have been able to these configurations to mere five so as to keep the computation practical, while still maintaining the over-all accuracy of theoretical calculations.

In view of the experimental difficulty of direct measurements of cross sections, we believe our theoretical cross sections are valuable in understanding the aeronomical phenomena.

REFERENCES

1. See, for example, J. W. Chamberlain, Physics of the Aurora and Airglow (Academic Press, New York, 1961); B. M. McCormac and A. Omholt, Atmospheric Emissions (Van Nostrand Reinhold Company, New York, 1969).

2. K. Watanabe, E. C. Y. Inn, and M. Zelikoff, J. Chem. Phys. $\underline{21}$, 1026 (1953).

3. P. H. Metzger and G. R. Cook, J. Quant. Spectrosc. Radiat. Transfer $\underline{4}$, 107 (1964).

4. R. Golstein and F. N. Mostrup, J. Opt. Soc. Am. $\underline{56}$, 765 (1966).

5. R. H. Huebner, R. J. Cellotta, S. R. Mielczarek, and C. E. Kuyatt, J. Chem. Phys. $\underline{63}$, 241 (1975).

6. E. N. Lassettre, S. M. Silverman, and M. E. Krasnow, J. Chem. Phys. $\underline{40}$, 1261 (1964); S. M. Silverman and E. N. Lassettre, J. Chem. Phys. $\underline{40}$, 2922 (1964).

7. P. S. Julienne, D. Neumann, and M. Krauss, J. Chem. Phys. $\underline{64}$, 2990 (1976).

8. S. Chung and C. C. Lin, Phys. Rev. A $\underline{6}$, 988 (1972).

9. S. Chung and C. C. Lin, Phys. Rev. A $\underline{9}$, 1954 (1974).

10. S. Chung, C. C. Lin, and E. T. P. Lee, Phys. Rev. A $\underline{12}$, 1340 (1975); S. Chung and C. C. Lin, Phys. Rev. A $\underline{17}$, 1874 (1978).

11. V. I. Ochkur, Zh. Eksp. Teor. Fiz. $\underline{45}$, 734 (1963) [Sov. Phys.-JETP $\underline{18}$, 503 (1964)].

12. P. H. Krupenie, J. Phys. and Chem. Ref. Data, $\underline{1}$, 423 (1972).

13. C. C. J. Roothaan, Rev. Mod. Phys. $\underline{23}$, 69 (1951); $\underline{32}$, 179 (1960).

14. T. M. Fang, S. C. Wofsy, and A. Dalgarno, Planet. Space Sci. $\underline{22}$, 413 (1974).

15. S. Trajmar, W. Williams, and A. Kuppermann, J. Chem. Phys. $\underline{56}$, 3759 (1972).

Table I. Configurations for the $X^3\Sigma_g^-$ State[a]

	$2\sigma_g$	$2\sigma_u$	$3\sigma_g$	$3\sigma_u$	$1\pi_u^+$	$1\pi_u^-$	$1\pi_g^+$	$1\pi_g^-$	Coefficients[b]
1.	2	2	2	0	2	2	1	1	.956082
2.	2	2	0	2	2	2	1	1	-.072058
3.	2	2	2	0	1	1	2	2	-.199331
4.	2	2	0	2	1	1	2	2	.039208
5.	0	2	2	2	2	2	1	1	-.029427
6.	2	0	2	2	2	2	1	1	-.014419
7.	2	1	2	1	2	2	1	1	.122624
8.	2	1	2	1	2	2	1	1	-.037672
9.	2	2	2	2	1	1	1	1	.021566
10.	2	2	2	2	1	1	1	1	-.000094
11.	1	2	1	2	2	2	1	1	-.041254
12.	1	2	1	2	2	2	1	1	.000191
13.	2	2	1	1	1	2	2	1	-.127933
14.	2	2	1	1	1	2	2	1	.008548
15.	2	2	1	1	1	2	2	1	-.009622
16.	1	2	2	1	1	2	2	1	.055217
17.	1	2	2	1	1	2	2	1	-.008658
18.	1	2	2	1	1	2	2	1	.002904
19.	0	2	2	2	1	1	2	2	.008228
20.	2	0	2	2	1	1	2	2	.003764
21.	1	2	1	2	1	1	2	2	.022654
22.	1	2	1	2	1	1	2	2	-.000504
23.	2	1	2	1	1	1	2	2	-.031174
24.	2	1	2	1	1	1	2	2	.006808
25.	2	1	1	2	1	2	2	1	.025786
26.	2	1	1	2	1	2	2	1	-.000533
27.	2	1	1	2	1	2	2	1	.005620
28.	1	1	2	2	1	2	2	1	.002310
29.	1	1	2	2	1	2	2	1	.001286
30.	1	1	2	2	1	2	2	1	-.002463

[a]Configurations are specified by the occupation numbers.

[b]Mixing coefficient at R = 1.2Å.

Table II. Configuration for the $B^3\Sigma_u^-$ States[a]

	$2\sigma_g$	$2\sigma_u$	$3\sigma_g$	$3\sigma_u$	$1\pi_u^+$	$1\pi_u^-$	$1\pi_g^+$	$1\pi_g^-$	Coefficients[b]
1.	2	2	2	0	2	1	1	2	.903183
2.	2	2	0	2	2	1	1	2	-.012380
3.	2	0	2	2	2	1	1	2	-.027354
4.	2	1	2	1	2	1	1	2	.079494
5.	2	1	2	1	2	1	1	2	-.000534
6.	2	1	2	1	2	1	1	2	-.036249
7.	0	2	2	2	2	1	1	2	-.021400
8.	2	2	1	1	2	2	1	1	.374944
9.	2	2	1	1	2	2	1	1	.049311
10.	2	2	1	1	1	1	2	2	.109441
11.	2	2	1	1	1	1	2	2	.003832
12.	1	2	2	1	2	2	1	1	-.077988
13.	1	2	2	1	2	2	1	1	-.025139
14.	1	2	2	1	1	1	2	2	-.066132
15.	1	2	2	1	1	1	2	2	-.000042
16.	2	1	1	2	2	2	1	1	-.079394
17.	2	1	1	2	2	2	1	1	-.015914
18.	2	1	1	2	1	1	2	2	-.015732
19.	2	1	1	2	1	1	2	2	-.004150
20.	2	2	2	2	2	1	0	1	-.042689
21.	2	2	2	2	0	1	2	1	.022660
22.	1	2	1	2	2	1	1	2	-.003645
23.	1	2	1	2	2	1	1	2	-.000996
24.	1	2	1	2	2	1	1	2	.001298
25.	1	1	2	2	1	1	2	2	-.004650
26.	1	1	2	2	1	1	2	2	.002139
27.	1	1	2	2	2	2	1	1	-.013389
28.	1	1	2	2	2	2	1	1	.004883

[a] Configurations are specified by the occupation numbers.

[b] Mixing coefficients at $R = 1.2$ Å.

Table III. Dipole Matrix Elements[a]

1.	$\langle 1\pi_u | z | 1\pi_g \rangle$	1.182825
2.	$\langle 3\sigma_g | z | 3\sigma_u \rangle$	-1.117884
3.	$\langle 3\sigma_g | z | 2\sigma_u \rangle$	-1.253562
4.	$\langle 2\sigma_g | z | 3\sigma_u \rangle$	0.141830
5.	$\langle 2\sigma_g | z | 2\sigma_u \rangle$	-0.887668

[a]Defined in Eq. (18); $R = 1.2$Å.

Table IV. Contributions to Dipole Matrix Element

Configurations		Type[a]	Contribution
X	B		
1	1	1	1.444464
1	8	2	-.566726
3	1	1	-.301152
13	1	2	.182671
13	8	1	-.080239
7	8	3	.057635
2	8	2	.042713
3	10	2	.034488
13	10	1	.023421
7	4	1	.016306
1	12	4	-.014956
13	4	3	.012749
7	16	2	.010883
2	16	3	.010142
16	1	4	-.010003
7	12	5	-.008489
16	12	1	.007203
4	10	2	-.006784
16	14	1	.006108
16	4	5	-.003896
11	12	2	.003597
11	16	5	-.002907
3	14	4	.002644
13	2	2	.002504
8	9	3	-.002329
8	6	1	.002284
11	8	4	.002194
2	2	1	.001492
4	18	3	.001094
9	20	1	.001089
5	7	1	.001053
others			.001998
total			.873282

[a]Types are as listed in Table III.

Table V. Excitation (Dissociation) Cross Sections
O_2 $(X^3\Sigma_g^- \rightarrow B^3\Sigma_u^-)$ in 10^{-17} cm^2.

eV	Cross Section
10	3.13
15	6.57
20	7.29
25	7.21
30	6.91
40	6.20
50	5.56
75	4.40
100	3.64
150	2.74
200	2.21
300	1.62
500	1.08
1000	0.93

$$e + O_2(X^3\Sigma_g^-) \longrightarrow O_2(B^3\Sigma_u^-) + e$$

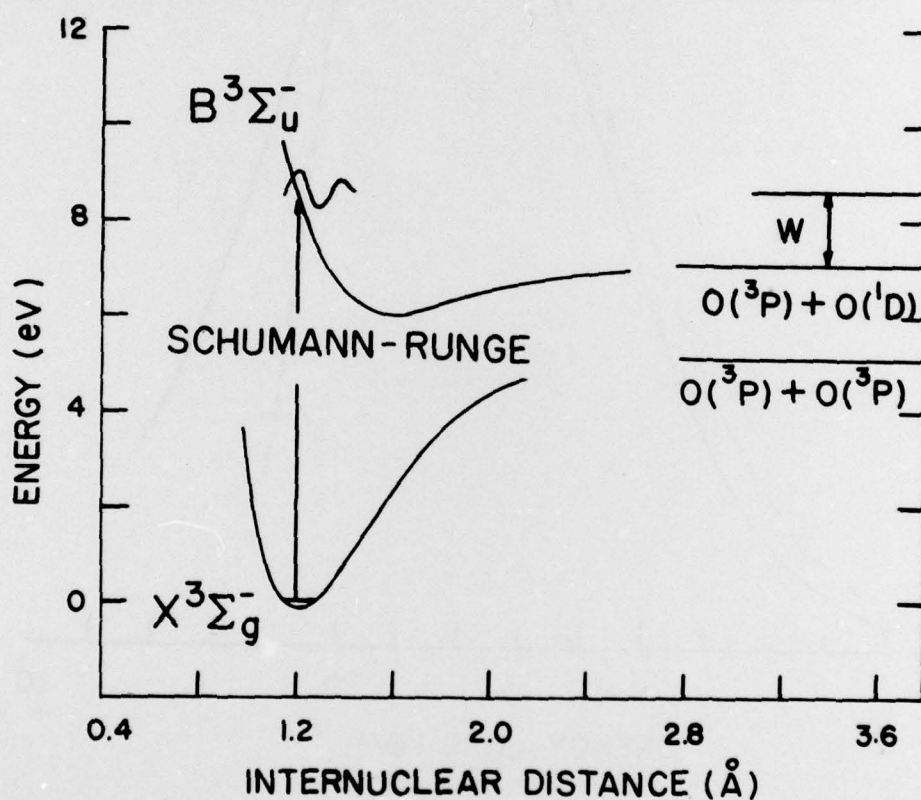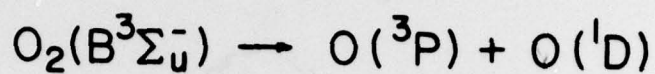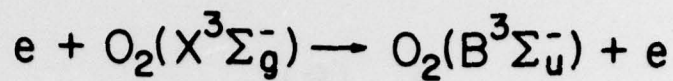$$O_2(B^3\Sigma_u^-) \longrightarrow O(^3P) + O(^1D)$$

Fig. 1. Potential-energy curves of the O_2 molecule illustrating the dissociation of O_2 via electron-impact excitation of the Schumann-Runge system.
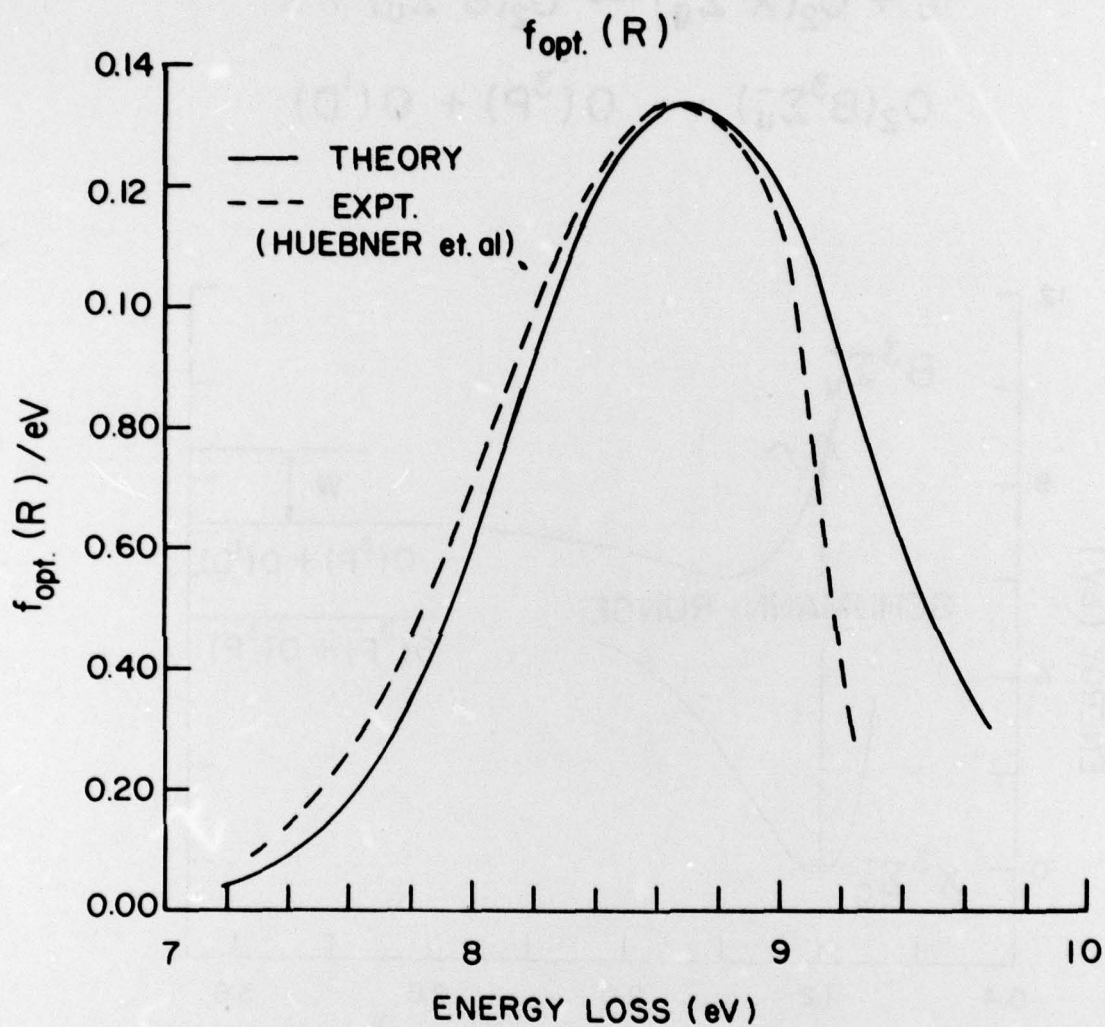
Fig. 2. Optical oscillator strength of the Schumann-Runge system as a function of vertical excitation-energy.

Publications

The following papers have been published under the sponsorship of this contract.

1. Sunggi Chung, Chun C. Lin, and Edward E. T. P. Lee, Phys. Rev. A $\underline{12}$, 1340 (1975).

2. Sunggi Chung and Chun C. Lin, Phys. Rev. A $\underline{17}$, 1874 (1978).

DISTRIBUTION LIST

DEPARTMENT OF DEFENSE

Director
Defense Advanced Rsch. Proj. Agency
    Attn: LTC W.A. Whitaker

Defense Documentation Center
    Attn: TC (2 Copies)

Director
Defense Nuclear Agency
    Attn: TITL Tech. Library (3 Copies)
    Attn: TISI Archives
    Attn: RAEV Harold C. Fitz, Jr.
    Attn: RAAE Maj. J. Mayo
    Attn: RAAE G. Soper
    Attn: RAAE Maj. R. Bigoni

Dir. of Defense Rsch. & Engineering
Department of Defense
    Attn: DD/S&SS(OS) Daniel Brockway

Commander
Field Command
Defense Nuclear Agency
    Attn: FCPR

Chief Livermore Division
FLD Command DNA
    Attn: FCPRL

DEPARTMENT OF THE ARMY

Commander/Director
Atmospheric Sciences Laboratory
U.S. Army Electronics Command
    Attn: DRSEL-BL-SY-A.F. Niles
    Attn: H. Ballard

Commander
Harry Diamond Laboratories
    Attn: DRXDO-NP, F.H. ..iminetz (2 Copies)

Director
BMD Advanced Technical Center
    Attn: ATC-T, M. Capps
    Attn: ATC-O, W. Davies

Dep. Chief of Staff for Rsch,Dev & Acout.
Department of the Army
    Attn: MCB Division
    Attn: DAMA-CSZ-C
    Attn: DAMA-WSZC

Director
U.S. Army Ballistic Rsch Labs.
    Attn: John Mester
    Attn: Tech. Library

Commander
U.S. Army Electronics Command
    Attn: Inst. for Expl. Research
    Attn: Weapons Effects Section

Commander
CORADCOM
    Attn: PP-Library

DEPARTMENT OF THE NAVY

Commander
Naval Oceans Systems Center
    Attn: Code 2200 William Moler

Director
Naval Research Laboratory
    Attn: Code 7712 D.P. McNut
    Attn: Code 6701 J.D. Brown
    Attn: Code 2600 Tech. Library
    Attn: Code 7175J C.Y. Johnson
    Attn: Code 6700 T.P. Coffey
    Attn: Code 7709 Wahab Ali
    Attn: Code 6780 D.F. Strobel
    Attn: Code 6780 P. Juluenne
    Attn: Code 67800 J. Fedder
    Attn: Code 6780 S. Ossakow
    Attn: Code 6707 J. Davis

Commander
Naval Surface Weapons Center
    Attn: Code WA 501 Navy NUC Prgms. Off.
    Attn: Technical Library

Superintendent
Naval Post Graduate School
    Attn: Rech Rpts Librarian

Commander
Naval Intelligence Support Ctr
    Attn: Document Control

DEPARTMENT OF THE AIR FORCE

AF Geophysics Laboratory, AFSC
    Attn: LKB,K.S.W. Champion
    Attn: OPR, A.T. Stair, Jr.
    Attn: OPR ,P.G. Doyle
    Attn: OPR, R. Murphy
    Attn: LKO, R. Huffman

AF Weapons Laboratory, AFSC
    Attn: Maj. Gary Ganong, DES

Commander
ASD
    Attn: ASD-YH-EX-LTC R. Leverette

SAMSO/AW
    Attn: SZJ Lt. Col. Doan

SAMSO/YN
    Attn: Maj. P. Sivgals

AFTAC
    Attn: Tech Library
    Attn: TD

HQ
Air Force Systems Command
    Attn: DLS
    Attn: Tech Library
    Attn: DLCAL
    Attn: DLTW
    Attn: DLXP
    Attn: SDR
    Attn: RDQ

US ENERGY RSCH. and DEV. ADMIN.

Division of Military Application
U.S. Energy Rsch & Dev Admin
    Attn: Doc. Con.

Los Alamos Scientific Laboratory
    Attn: DOC CON for H.V. Argo
    Attn: DOC CON for M.B. Pongratz
    Attn: DOC CON for R. Brownlee
    Attn: Group AP-4,MS 567
    Attn: DOC CON for J. Zinn

University of California
Los Alamos Scientific Laboratory
    Attn: Librarian MS 362

Sandia Laboratories
    Attn: DOC CON for W.B. Brown,Org.1353
    Attn: Tech. Library, Org. 3141

Argonne National Laboratory
Records Control
    Attn: Doc. Con. for D.W. Green
    Attn: Doc. Con. for LIR SVCS Rpts Sec
    Attn: Doc. Con. for G.T. Reedy

Unviersity of California
Lawrence Livermore Laboratory
    Attn: W.H. Duewer,L-262
    Attn: J. Chang, L-71

U.S. Energy Rsch & Dev. Admin
Division of Headquarters Services,
Library Bracnh
    Attn: Doc. Con. for Class.Tech. Lib.

OTHER GOVERNMENT

Department of Transportation
Office of the Secretary
    Attn: S.C. Coroniti

NASA
Goddard Space Flight Center
    Attn: Code 6801 A. Temkin
    Attn: Tech. Library
    Attn: Code 900 J. Siry

NASA
Langley Station
    Attn: Tech. Library

NASA
Ames Research Center
    Attn: N-245-3 R. Whitten

Department of the Army
Bal. Miss. Def. Adv. Tech. Ctr.
    Attn: W.O. Davies

Federal Aviation Administration
    Attn: HAPP/AEC-10/James W. Rogers

Central Intelligence Agency
    Attn: ED/SI RM 5G48 HQ Bldg.
    Attn: NED/CS I-2G4R HQS

Department of Commerce
National Bureau of Standards
    Attn: Sec. Officer for M. Krauss
    Attn: Sec. Officer for L.H. Gevantman

National Oceanic & Atmospheric Admin.
Environmental Research Laboratories
Department of Commerce

        Attn: G. Reid
        Attn: E. Ferguson
        Attn: F. Fehsenfeld

DEPARTMENT OF DEFENSE
    CONTRACTORS

Science Applications Inc.
    Attn: D.G. Hopper

Aero-Chem Research Laboratories, Inc.
    Attn: A. Fontijn
    Attn: H. Pergament

Aerodyne Research, Inc.
    Attn: F. Bien
    Attn: M. Camac

Aerospace Corporation
    Attn: N. Cohen
    Attn: R. Mayer
    Attn: R.J. McNeal
    Attn: T.D. Taylor
    Attn: J. Reinheimer
    Attn: R.D. Rawcliffe

AVCO-Everett Research Laboratory Inc.
    Attn: Tech. Library
    Attn: C.W. Von Rosenberg, Jr.

Battelle Memorial Institute
    Attn: H.L LaMuth
    Attn: STOIAC

Brown Engineering Company, Inc.
    Attn: N. Passino

General Research Corporation
    Attn: D. Jones

California At Riverside,University of
    Attn: J.N. Pitts, Jr

California at San Diego, University of
    Attn: S.C. Lin

California University of Berkeley
    Attn: Sec. Officer for H. Johnston
    Attn: Sec. Officer for Dept of Chem.,
        H.L. Strauss

Calspan Corporation
    Attn: C.E. Treanor
    Attn: J.M. Grace
    Attn: M.G. Dunn
    Attn: W. Wurster

University of Colorado
Astro-Geophysics
    Attn: J.B. Pearce

Colorado, University of
Office of Contracts and Grants
    Attn: G.M. Lawrence, LASP

Concord Sciences
    Attn: E.A. Sutton

University of Denver
Space Science Laboratory
    Attn: B. Van Zyl

University of Denver
Denver Research Laboratory
    Attn: Sec. Officer for D. Murcray

General Electric Company
Tempo-Center for Advanced Studies
    Attn: DASAIC
    Attn: W.S. Knapp
    Attn: T. Stephens
    Attn: D. Chandler
    Attn: V.R. Strull

General Electric Company
Space Division
    Attn: M.H.Bortner,Space Science Lab.
    Attn: J. Burns
    Attn: F. Alyea
    Attn: P. Zavitsands
    Attn: R.H. Edsall
    Attn: T. Baurer

General Research Corporation
    Attn: J. Ise, Jr.

Geophysical Institute
University of Alaska
    Attn: J.S. Wagner
    Attn: N. Brown

Lowell University of
Center for Atmospheric Research
    Attn: G.T. Best

Lockheed Missiles and Space Company
    Attn: J. Kumer, Dept. 52-54
    Attn: J.B. Cladis, Dept 52-12,B202
    Attn: B.M. McCormac, Dept. 52-54
    Attn: T. James, Dept. 52-54
    Attn: M. Walt, Dept. 52-10
    Attn: R.D. Sears, Dept. 52-54

Institute for Defense Analysis
    Attn: E. Bauer
    Attn: H. Wolfhard

Mission Research Corporation
    Attn: D. Archer
    Attn: D. Fischer
    Attn: M. Scheibe
    Attn: D. Sappenfield
    Attn: D. Sowle

Photometrics, Inc.
    Attn: I.L. Kofsky

Berkeley Research Associates
    Attn: J.B. Workman

Physical Dynamics Inc.
    Attn: A. Thompson

Physical Sciences, Inc.
    Attn: K. Wray
    Attn: R.L Taylor
    Attn: G. Caledonia

Physics International Company
    Attn: Doc Con for Tech Library

Pittsburgh, University of the Comwlth
System of Higher Education
    Attn: W.L. Fite
    Attn: M.A. Biondi
    Attn: F. Kaufman

R & D Associates
    Attn: R. Latter
    Attn: R.G. Lindgren
    Attn: B. Gabbard
    Attn: R. Lelevier
    Attn: A.L. Latter
    Attn: F. Gilmore

Rand Corporation
    Attn: C. Crain

Science Applications, Inc.
    Attn: D.A. Hamlin
    Attn: D. Sachs

Stanford Research Institute International
    Attn: M. Baron
    Attn: W.G. Chesnut

Technology International Corporation
    Attn: W.P. Boquist

United Technologies Corporation
    Attn: H. Michels
    Attn: R.H. Bullis

Utah State University
    Attn: D. Baker
    Attn: K. Baker
    Attn: C. Wyatt
    Attn: A. Steed

Visidyne, Inc.
    Attn: H. Smith
    Attn: J.W. Carpenter
    Attn: T.C. Degges
    Attn: C. Humphrey

Wayne State University
    Attn: R.H. Kummler
    Attn: W.E. Kaupplia

Commander
Rome Air Development Center
    Attn: OSCA, J.J. Simons

Stewart Radiance Laboratory
    Attn: R. Huppi

Boston College
Space Data Analysis Laboratory
    Attn: E.R. Hegblom
    Attn: W.F. Grieder

Forrestial Campus Library
Princeton Univeristy
    Attn: Librarian